An Investigation of the Longwall Mining Subsidence Impacts on Pennsylvania Highway I-70: A Case Study

by

Emily Adelsohn

B.S. in Civil Engineering, University of Pittsburgh, 2018

Submitted to the Graduate Faculty of the

Swanson School of Engineering in partial fulfillment

of the requirements for the degree of

Master of Science in Civil Engeineering

University of Pittsburgh

2020

UNIVERSITY OF PITTSBURGH

SWANSON SCHOOL OF ENGINEERING

This thesis was presented

by

Emily Adelsohn

It was defended on

March 6, 2020

and approved by

Luis Vallejo, Ph.D., Professor, Department of Civil and Environmental Engineering

Julie Vandenbossche, Ph.D., P.E., William Kepler Whiteford Professor, Department of Civil and Environmental Engineering

Thesis Advisor: Anthony T. Iannacchione, Ph.D. P.E. P.G., Associate Professor, Department of Civil and Environmental Engineering

An Investigation of the Longwall Mining Subsidence Impacts on Pennsylvania Highway I-70: A Case Study

Emily Adelsohn, M.S.

University of Pittsburgh, 2020

Over the last 50 years, longwall mining has become the most efficient and effective way to remove coal from underground deposits, like the Pittsburgh Coalbed. Longwall mining is a form of full extraction mining that allows large areas of coal to be removed. In Southwest Pennsylvania, longwall panels are typically approximately 15,000-feet long, 1,200-feet wide, and 7-feet thick. As these large areas of coal are removed, a subsidence basin is formed on the surface, causing the ground to drop several feet and inducing damaging horizontal strains and deformations. Although over 600 longwall panels have been mined in Pennsylvania's Pittsburgh Coalbed, much is still unknown about how the formation of subsidence basins impact highway alignments and how these impacts can be mitigated.

In the winter of 2019, a 2,650-foot section of I-70 was undermined by a longwall panel in the Tunnel Ridge Mining district. This panel was monitored extensively by the Pennsylvania Department of Transportation, its contractors, and the University of Pittsburgh to provide a greater understanding of the impacts of subsidence on an interstate. Throughout the undermining process, surveys of the road and adjacent slopes were conducted regularly, and tiltmeters and inclinometers recorded data regarding the behavior of the deforming ground surface. The survey and instrumentation data were supplemented by weekly field observations made throughout the undermining process.

Extracting Tunnel Ridge Panel 15 caused as much as 5-feet of vertical subsidence and 1.5-feet of horizontal movement on the highway surface as the subsidence basin formed. These large movements caused measurable damage on the surface of the highway in the form of tensile cracks, open pavement joints, shear failures, and compression bumps. The reinforced concrete pavement structure and mitigation techniques, including full depth asphalt sections and contraction joints, caused the observations and survey data to deviate from the predictive models. The highway was additionally influenced by the presence of a large embankment which consolidated approximately 0.7-feet over 80-feet and spread laterally when undermined. As a result, this study determined that these factors have a significant impact on the behavior of a highway subjected to longwall mining subsidence and the mitigation thereof.

Table of Contents

List of Tables

List of Figures

Preface

Acknowledgements

First and foremost, my sincerest gratitude is due to my advisor Dr. Anthony Iannacchione. His guidance, patience, and motivation throughout this process has been invaluable. There could not have been a better advisor and mentor for my master's study. I would also like to thank the rest of my thesis committee, Dr. Luis Vallejo and Dr. Julie Vandenbossche, for their encouragement, insight, and guidance.

None of this could have been possible without PennDOT's support of the University's research efforts, especially the support provided by Roy Painter, Eric Wanson, and Joe Szczur. At the University of Pittsburgh, PennDOT supported research is managed by Mark Magalotti and Kieth Johnson through its Center for Sustainable Transportation Infrastructure (CSTI). Their commitment to our work allowed us to perform a study of subsidence unlike any that came before. I would also like to acknowledge SPK Engineering, Earth Inc, and T3 Global for collecting and providing the data for this study.

Thanks is also due to Dr. Zach Agioutantis at the University of Kentucky for his assistance during the modeling phase of this study. As he maintains the SDPS software, Dr. Agioutantis was able to provide unparalleled support and guide me through the more complicated stages of modeling the subsidence basin.

Additionally, I would like to thank my research team, Robert Winn, Taylor DaCanal, Mingzhou Li, and Ethan Fisher. Their excellent work and assistance when collecting and analyzing the data was crucial and I could not have completed this study without them.

Finally, I must express my profound gratitude to my family and friends for providing me with unfailing support and continuous encouragement in every aspect of my life including my education and the process of researching and writing this thesis. This accomplishment could not have been possible without them.

Nomenclature and Definitions

- Act 54 – Bituminous Min Subsidence and Land Conservation Act as amended in 1994
- ArcGIS – Geographic Information System software developed by ESRI
- Asphalt Relief Section – Areas of pavement in which the concrete base was removed and replaced with full-depth asphalt to absorb strains during mining
- Blow-ups – localized upward movement (buckling) of the pavement surface caused by large in-plane pressure buildups in the concrete slab
- Compression bumps – large transverse bumps in the asphalt created by high in-plane pressure buildup in regions with full-depth asphalt
- Consolidation – process by which the soil changes volume gradually in response to changes in pressure
- Contraction joint – joints cut into the asphalt overlay to accommodate movement in the pavement surface
- Gateroads – room and pillar mine developments that outline a longwall panel, used primarily for ventilation and coal haulage
- Gob – zone of broken rock rubble that forms due to roof rock strata collapse behind an active longwall face

- Guiderail deformations – shear or compression failure of guiderail due to movement of pavement surface
- Ground strain – strain on the ground as caused by mining modeled using surface points around a point of interest to determine the overall relative movement of the surface terrain
- Horizontal strain – change in horizontal length between two points divided by the original length between two points
- I-70 – Interstate 70
- Inflection line – a line comprised of individual inflection points on the subsidence basin where the surface transitions from tension to compression; represents the idealized location of highest slope and greatest horizontal deformation
- LiDAR – light detection and ranging; a remote sensing method that uses light using pulsed lasers to measure the ranges of distances to points
- Longitudinal cracks – cracks that are predominately parallel to the pavement centerline that tended to occur above the lane-shoulder joint
- Longwall face – location of active longwall mining, where the shearer is cutting the coal and the gob is being formed
- Longwall mining – form of full extraction underground mining in which a large area of coal is removed causing subsidence on the ground surface
- Overburden (h) – strata above a mine
- PA – Commonwealth of Pennsylvania
- PA DEP – Pennsylvania Department of Environmental Protection
- PASDA – Pennsylvania Spatial Data Access
- PennDOT – Pennsylvania Department of Transportation

- Rigidity – measure of elasticity that represents a material's resistance to bending and permanent deformation
- SDPS – Subsidence Deformation Prediction Software developed by Michael Karmis at the Virginia Polytechnic Institute and State University and funded by the Office of Surface Mining
- Separations – the widening between the edge of the slab and the soil adjacent to the structure
- Shear failures – cracks that formed along the lane-shoulder longitudinal joint that are caused by shear forced generated with the mainline expanded/contracted at a different rate than the shoulder
- Strain – the response of a system to an applied stress, measured by the change in length divided by the original length
- Stress – the force or load applied distributed over the original cross-sectional area of the specimen
- Subsidence – the gradual caving in or sinking of areas of land
- The University – The University of Pittsburgh
- Tiltmeters – instruments to examine the change in tilt that occurred at different points along the highway
- Transverse cracks – cracks that predominately perpendicular to the pavement centerline
- Widened contraction joints – the opening of transverse contraction joints
- WV – West Virginia

1.0 Introduction

1.1 Underground Bituminous Coal Mining in Western Pennsylvania

Coal has been an integral part of the history of Western Pennsylvania. Bituminous coal was first mined in Pennsylvania on Mount Washington, or "Coal Hill" in Pittsburgh in the late 1700s. By the 1830s, Pittsburgh alone consumed more than 400 tons of bituminous coal per day for domestic and industrial use (*PA Mining History*, n.d.). This coal production allowed Pittsburgh to flourish into an industrial center and earned it the name the "Steel City". Though reliance on coal as an energy source in Western Pennsylvania has decreased to about 21% over the years, Pennsylvanian coal is still a major contributor to the national and global energy scene (*Pennsylvania – State Energy Profile Overview*, 2019). The amount of coal produced in Pennsylvania has skyrocketed since 1830; over 40,769,000 tons of coal were produced from underground mining in 2015 (*PA Mining History*, n.d.), making Pennsylvania the third-largest coal producing state in the United States and the second largest coal exporter to foreign markets in 2017 (*Pennsylvania – State Energy Profile Overview*, 2019).

Throughout the years of underground bituminous coal mining in Pennsylvania, several techniques were developed and utilized. The two primary mining techniques utilized in Western Pennsylvania are room-and-pillar mining and longwall mining. Though very different in application, each of these underground mining techniques has its own advantages and disadvantages.

1.1.1 Room-and-Pillar Mining

The first mines that were developed in Western Pennsylvania were room-and-pillar mines. This mining technique is utilized in moderate to thick coalbeds with low to moderate inclines. Room-and-pillar mining developments involve the advancement of tunnel-like openings, known as entries or rooms, between rectangular blocks of coal, known as pillars, as can be seen in Figure 1. The pillars are left behind to hold up the strata above the coal mine and prevent collapses of the extracted areas. The overall mining development is designed to maximize the amount of coal recovery; the pillars are sized to provide the necessary support to prevent the collapse of the overburden and the rooms are sized to hold the equipment needed underground. Typically, the coal recovery using the room-and-pillar method is low, ranging between 35% and 70% (*PA Mining History*, n.d.).

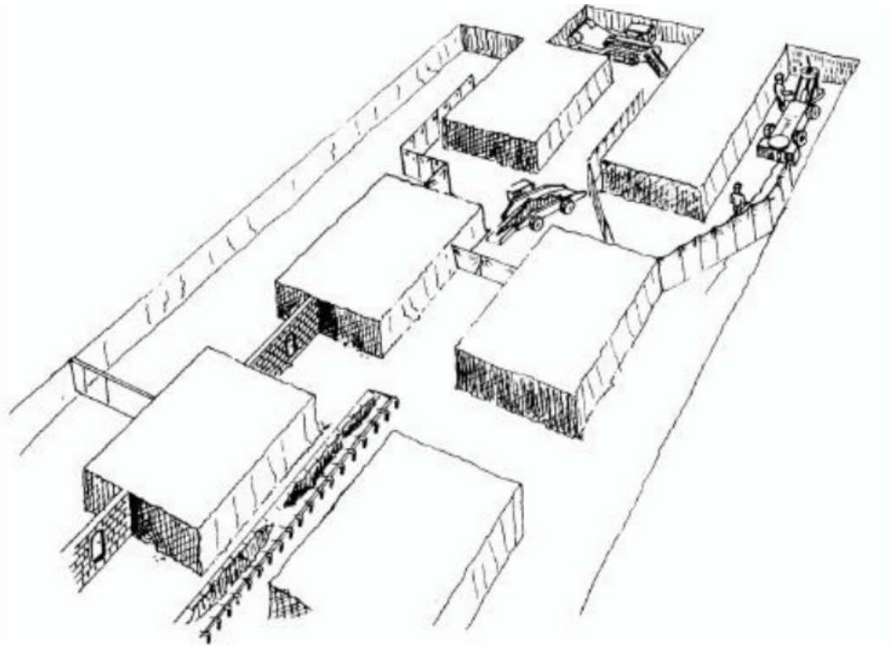

Figure 1 Room-and-pillar mining method

(Bayer and Nienhaus, 2000)

The original room-and-pillar mines in Western Pennsylvania utilized the coal outcrops on Mount Washington and manual pick mining and haulage techniques for coal extraction. With the rapid development of technology, mechanical alternatives were developed to optimize room-and-pillar mining, causing continuous miners to become the dominate room-and-mining technique. A continuous miner was an electrically powered machine with sharp tungsten carbide teeth attached to a steel drum that rotated, cutting coal from the face. The miner could remove coal much faster than any previous techniques; it could remove as much as five tons of coal in a minute, which previously would have taken a coal miner in the 1920s an entire day to achieve (*Continuous Miners*, n.d.). This system was improved through the development of the place change continuous mining method, in which a continuous miner would make a cut and then be moved ahead, while a roof bolter installed roof supports in the recently mined area, to improve the stability of the entries (Bayer and Nienhaus, 2000). In both of these methods, the mines would utilize a system of conveyors to transport the coal to the surface.

In recent years, the place-change continuous mining method was improved with the implementation of continuous haulage room-and-pillar mining. Through this method, the coal removed by a continuous miner is loaded directly into a haulage system that moves with the miner. This haulage system transports the coal out to the surface using conveyor belts. Like the place-change method, the continuous haulage method also consists of a roof bolter to install roof supports immediately after the coal is extracted (Bartels et al., n.d.). In the last five years at more than 66% of Pennsylvania room-and-pillar mines used the continuous haulage mining technique (DaCanal, 2019).

A small number of room-and-pillar mines implement retreat mining. During retreat mining, select pillars are extracted after the initial room-and-pillar mining process has taken place,

as can be seen in Figure 2. The removal of these pillars allows for additional coal to be removed, meaning a potential for higher profits. However, the removal of pillars decreases the support for the roof, which can cause subsidence on the surface (Mark and Guanna, 2017). In the late 1970s, only about 26% of room-and-pillar mines implemented pillar recovery; in the last five years, that number decreased even further, with only about 11% of mines using pillar recovery (DaCanal, 2019).

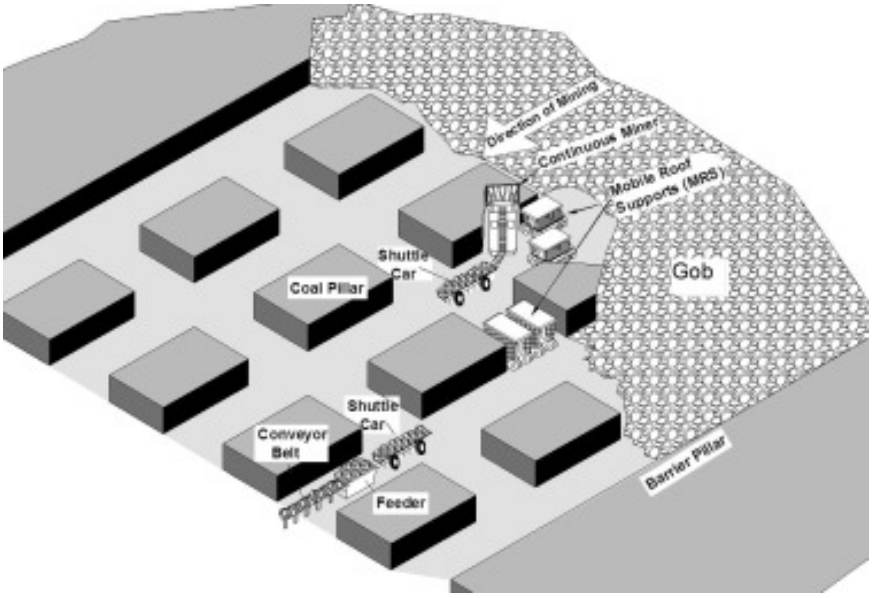

Figure 2 Pillar recovery in room-and-pillar mining

(Mark and Guanna, 2017)

1.1.2 Longwall Mining

In the late 1960s, a form of coal extraction, known as longwall mining, revolutionized the mining industry in the United States. Longwall mining is a form of full extraction mining, in which a large area of coal is completely removed. Due to the methodology employed for this

mining technique, longwall mining can only be performed in coalbeds that have a consistent minable thickness and large horizontal extents.

Before longwall mining can occur, a large rectangular area of coal, known as a panel, is outlined using a multi-entry system of room-and-pillar mining, known as gateroads, for ventilation and haulage. A longwall machine consisting of mechanical shearers, a conveyor system, and a series of self-advancing hydraulic roof supports, known as shields, is positioned in setup entries to begin extraction along the longwall face. Once set up, the entire longwall mining operation is automated. Modern longwall mining machines can support a face length of up to about 1400-feet and an extraction thickness of 5 to 10-feet (*Longwall Mining*, n.d.).

The shearer moves horizontally across the long longwall face, removing coal with each pass and allowing it to fall onto the conveyor belt to be transported out of the mine. The shields temporarily support the roof directly above and behind the active longwall development; however, as the longwall miner advances along a panel, the shields move forward and roof behind the active face is allowed to collapse into the void forming a broken rock material, known as gob, and producing subsidence that can propagate to the ground surface. Figure 3 shows a rendering of the longwall mining operation.

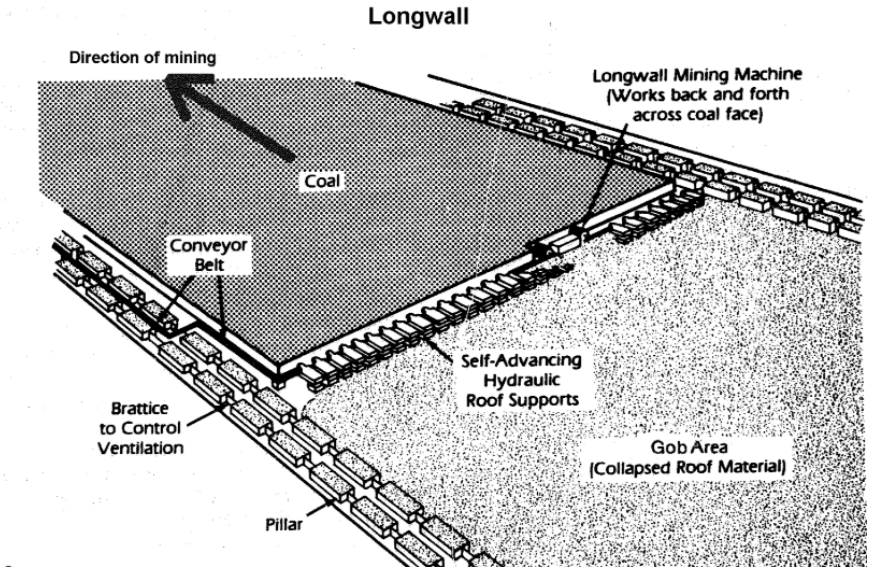

Figure 3 Longwall mining method

(figure sourced from U.S. Engergy Information Administration)

Since the 1960s, almost 800 longwall panels have extracted huge reserves of coal in Western Pennsylvania. Over 600 of those panels were extracted from the Pittsburgh coalbed, a consistent and moderately thick coal seam that extends from Western Pennsylvania into Ohio, West Virginia, and Maryland. As longwall mining allows for as much as 80% coal extraction, its efficiency has made it an increasingly popular modern technique. In recent years, almost half of the coal acreage extracted in Pennsylvania was removed using the longwall mining method.

1.2 Background and Motivation for Study

Since longwall mining in the Pittsburgh Coalbed first occurred in the 1960s, a great deal has been learned about how the formation of a subsidence basin impacts surface features, such as buildings, water supplies, and streams. However, of the hundreds of longwall panels that have

been mined in Pennsylvania, only 25 of them have undermined interstates, resulting in significantly less knowledge about the impact of subsidence on these highways, supporting embankments, and cut slopes.

1.2.1 Tunnel Ridge's Panel 15

Alliance Coal's Tunnel Ridge Mine has plans to undermine Interstate 70 (I-70) utilizing the longwall mining method in both Pennsylvania and West Virginia over the coming years. The first panel to impact the highway was scheduled to be mined from late 2018 into 2019 and would impact a section of highway between the West Virginia border and the West Alexander interchange that is maintained by the Pennsylvania Department of Transportation's (PennDOT) District 12 offices. The interstate has a one-way average daily traffic (ADT) of about 19,000 vehicles and a one-way average daily truck traffic (ADTT) of about 6,100 vehicles. Due to the soil properties and geology that is common in this area of Pennsylvania, PennDOT was particularly concerned that the impact of subsidence caused by this and future panels on I-70 could cause failures on the road and embankments. Rerouting traffic around this route in case of a catastrophic failure would require diverting vehicles onto a long detour consisting of local roads that are not designed to accommodate these traffic loads. As a result, PennDOT contracted the University of Pittsburgh (the University) to monitor the initial undermining of I-70, complete an independent analysis of the subsidence impacts to the interstate, and make predictions of potential impacts to be caused by future undermining.

The first of Tunnel Ridge's panels to undermine I-70, Panel 15, crossed beneath the interstate in early 2019. This panel had a minimum and maximum overburden of 526-feet and 771-feet respectively, with an average of 675-feet of overburden around the interstate. It extracted

7.25-feet of coal at the longwall face. With a width of approximately 1,200-feet, the panel crossed the interstate at an angle, causing it to pass beneath approximately 2,130-feet of I-70.

1.2.2 Panel 15 Study Area

The section of I-70 influenced by the undermining of Panel 15 which makes up the initial study area extends from about one-mile south of the West Alexander I-70 interchange to approximately 700-feet beyond the West Virginia border. The study area was considered to be 3,300-feet of highway consisting of a concrete pavement with an asphalt overlay, including the 2,130-feet of underlying panel, 520-feet of underlying gateroads, and 650-feet of buffer zone over unmined adjacent coal, as can be seen in Figure 4.

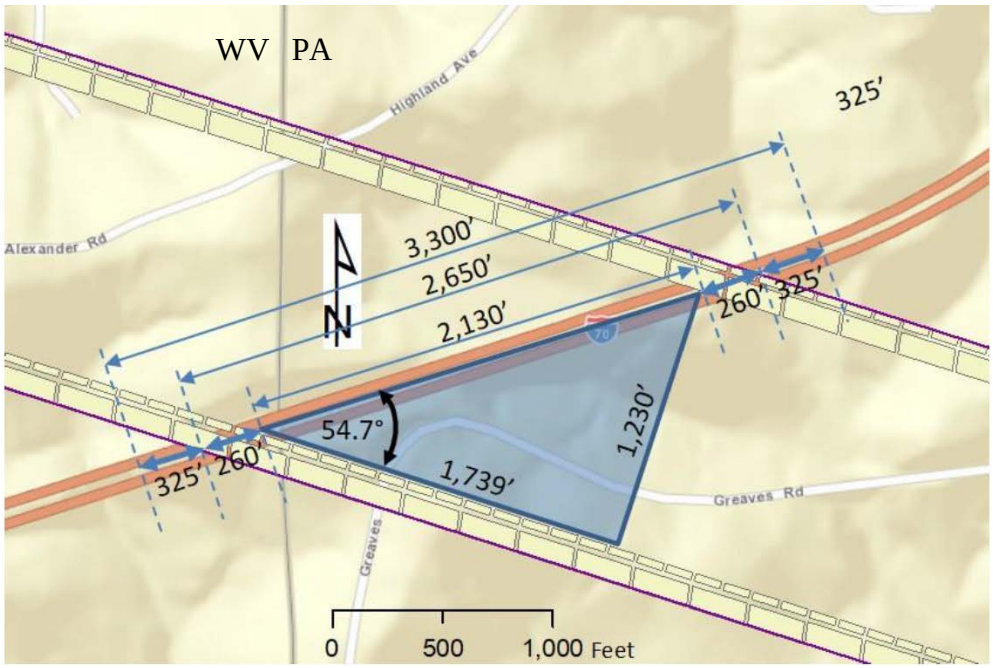

Figure 4 Location and dimensions of the initial I-70 study area

This initial study area included two large embankments, one in the center of the panel and one over the panel's gateroads. Due to the age of I-70 and the landslide prone soils common in this area of Pennsylvania, a large emphasis was placed on determining the stability of these embankments before and after the undermining event. Two substantial cut slopes were also located within the study area and were monitored for the project's duration. The location of the embankments and the slopes can be seen in Figure 5.

Also located within the study area were four man-made asphalt relief sections. As I-70 consisted of an asphalt surface on top of a concrete base, in the areas where the highest strains from subsidence were expected to occur according to predictive models, a 60-foot section of the concrete base was removed and refilled with a full-depth asphalt material. This was done so that these areas would then be better suited to adapt to the strain conditions caused by subsidence, as asphalt is more flexible than concrete. As a result, special attention was paid to the performance of these asphalt relief sections during the project's duration. The location of the asphalt relief sections can be seen in Figure 5.

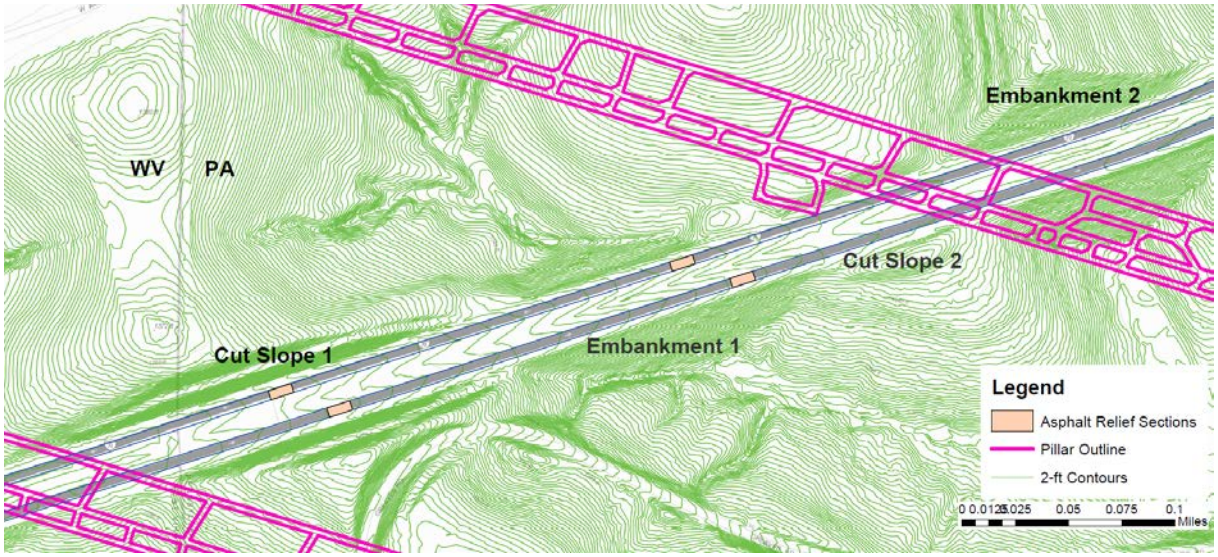

Figure 5 Location of embankments, cut slopes, and asphalt relief sections within the initial I-70 study area

1.3 Study Objectives

Upon contracting the University, PennDOT set forth a series of project objectives to guide the investigation into the behavior of the roadway. The objectives for the project were adopted and modified to guide this study. The study objectives are as follows:

- Investigate the influence of longwall mining on highway alignments and associated slopes/embankments
- Evaluate how the highway deforms during the undermining with a focus on determining its transient characteristics
- Utilize models to better understand subsidence impacts to the highway alignment
- Characterize the behavior of the pavement structure during undermining
- Suggest alternate mitigation techniques for future undermining activities

1.4 Purpose of Study

The impact of the Tunnel Ridge Mine on I-70 is likely to be significant over the coming years. The goal of this study is to collect information regarding the initial undermining of this section of roadway to better characterize the response of the interstate, slopes, and asphalt relief sections after they are subjected to longwall mining subsidence. This study assessed the behavior of the I-70 highway alignment when subjected to undermining by a longwall mining operation. The subsidence basin formed over a 3-month period and resulted in both large and small impact features to the highway alignment. This research produced a better understanding of important factors influencing subsidence-related damage to the highway alignment. This was accomplished

by comparing subsidence impacted features to observations and measurements taken during longwall undermining with both empirical and analytical predictive models.

2.0 Literature Review

2.1 Background on Longwall Mining Subsidence Theory

Longwall mining generates subsidence basins that propagate to the surface causing horizontal and vertical deformations, stresses, and strains. The characteristics of the longwall panel, including width (W), length (L), extraction thickness (M) and overburden (h), influence the formation of the subsidence basin. A visualization of some of the properties affecting the formation of a subsidence basin can be seen in Figure 6. Subsidence basins are characterized by the panel width to overburden depth ratio. Typically, a subsidence basin will form whenever the width to overburden ratio is greater than 0.25. Based on the nature of the coalbeds in Pennsylvania, the formation of subsidence basins can be expected for all Pennsylvania longwall panels.

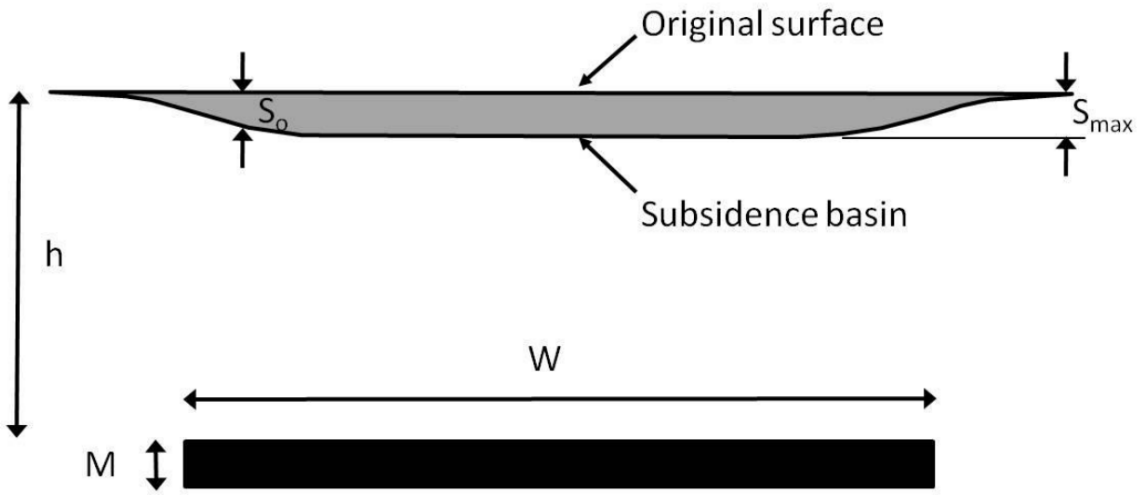

Figure 6 Properties that impact the formation of a subsidence basin

(Iannacchione et. al, 2008)

Subsidence basins initiate at the coalbed and propagate upward. As a subsidence basin propagates to the surface, subsidence effects the strata differently throughout the overburden. There are four zones of movement within the overburden: the caved zone, fractured zone, continuous bending (deformation) zone, and soil zone (Figure 7). The caved zone is the area immediately above the roof of the extraction area that breaks up and fills the void left by mining. This zone is typically 2 to 8 times the extraction thickness of the mine. The fractured zone is immediately above the caved zone that is characterized by strata breakage, loss of continuity, and increased permeability and porosity. The density of fracturing in this zone decreases from bottom to top. The combined thickness of the caved zone and the fractured zone is generally 20 to 30 times the extraction thickness of the mine. Above the fractured zone is the deformation zone, which is characterized by bending in the strata; the strata bends downwards without breaking. Continuity is not lost within this layer meaning that original features of the layer remain intact. The surface layer is known as the soil layer and consists of soil and weathered rocks. Depending on the physical properties of the soil, cracks may open, especially near the edges of the panel (Peng et al., 1992).

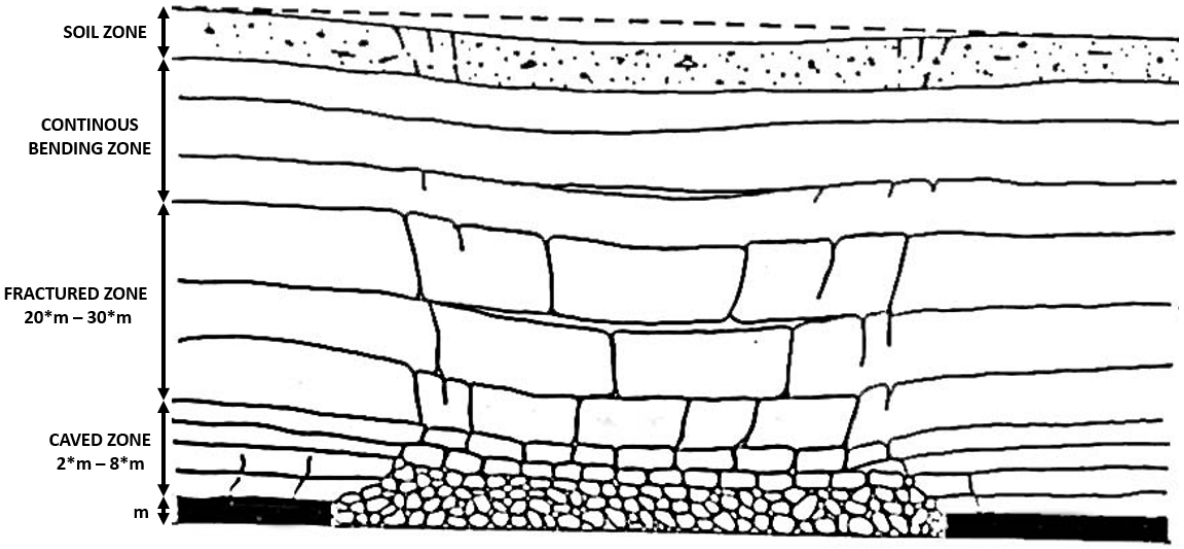

Figure 7 Four zones of strata movement above longwall mining

(Peng et al., 1992)

As mentioned previously, subsidence basins are characterized by the ratio of panel width to overburden depth; this ratio is used to characterize basins as supercritical, critical, or subcritical. A width to overburden ratio greater than 1.2 typically produces a supercritical basin, while a ratio less than 1.2 typically produces a subcritical basin (Karmis et al., 1981). A supercritical basin is bathtub shaped with a flat bottom that reaches the maximum vertical subsidence predicted for the given characteristics; contrarily, a subcritical basin slopes to a point with a peak subsidence less than the maximum vertical subsidence predicted. Most longwall panels mined in the Pittsburgh Coalbed fall into the supercritical category. The longwall panel being considered in this study has a width to overburden ratio of 1.78, classifying it too as a supercritical basin.

2.1.1 Final Subsidence Basin Formation

Every point of a subsidence basin being mined from a horizontal coal seam moves towards the center of the basin. As a result, the movements caused by longwall mining include both vertical

subsidence and horizontal deformation. The subsidence basin can also be characterized by slope, curvature, horizontal strain, twisting, and shear strain (Peng et al., 1992).

There are a variety of factors that influence the magnitude and shape of the final deformations caused by a subsidence basin. Surface subsidence and strata movements are results of both mining activities and geologic conditions. The following factors can have an influence on the final subsidence basin (Peng et al., 1992): strength and hardness of overburden strata, width of mining opening, overburden depth, extraction height, proximity of nearest longwall panel, and topography.

There is an inverse relationship between overburden strength and hardness and the amount of vertical subsidence; this means that the maximum subsidence observed will be smaller when the strata is strong and hard than if it was soft and weak. The maximum subsidence will also be smaller when the extraction height is lower. In the Pittsburgh Coalbed, the extraction height is relatively consistent, averaging about 7-feet in height.

The surface topography in the area can also impact the movement of the surface due to subsidence. The stability of steep slopes within a subsidence basin may be impacted by subsidence causing landslides in slip-prone areas (Peng et al., 1992). In 2000, a group of Australian engineers and geologists noted that severe topographic changes in mining areas in Australia could cause unexpected subsidence behavior. These behaviors include closure of gorges and large horizontal displacements. These effects could be seen up to 5000-feet from mining in the direction of the gob. The distance of these effects from the longwall face could only be explained by the steep topography (Hebblewhite et al., 2000).

The overburden and panel width also have a significant impact on the subsidence basin characteristics. The influence of overburden and panel width can be seen in Figure 8. As can be

seen in this figure, overburden and panel width impact the amount of vertical subsidence, the width of the subsidence basin, and the slope of the basin sides. Typically, shallower panels produce more vertical subsidence, while deeper panels cause less vertical subsidence. The width of the panel is directly proportional to the width of the final subsidence basin and the radius of influence, r. The figure also shows that shallow panels tend to produce larger slopes than deep panels and supercritical panels tend to cause larger slopes than their subcritical equivalents. The slope parameter is important, as it, along with strain, can be used as a surrogate to horizontal deformation.

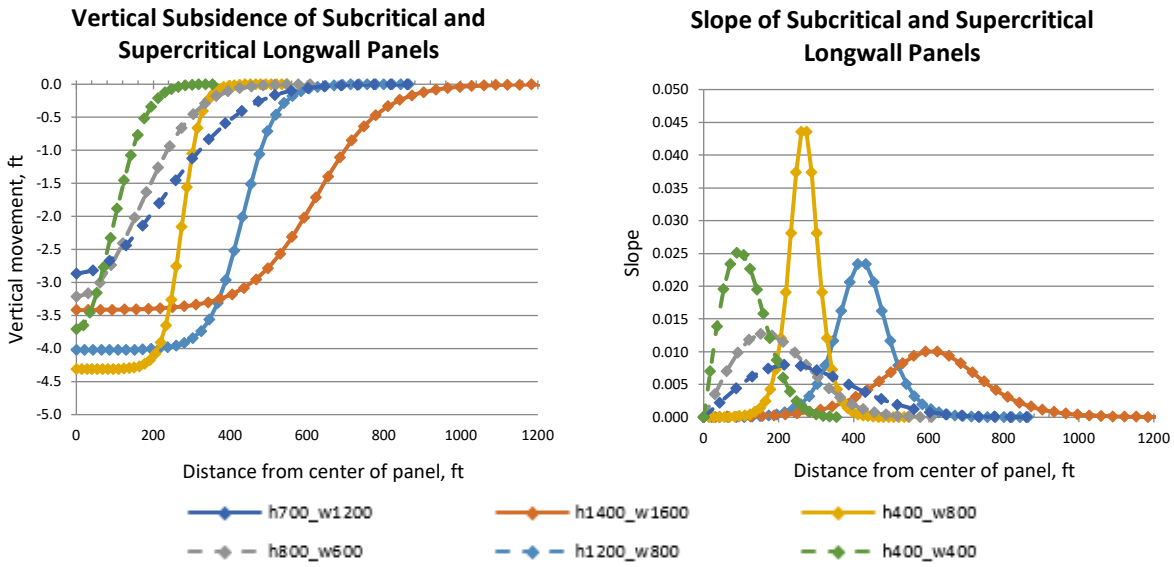

Figure 8 Profile function models of longwall panels vertical subsidence (left) and slope (right) for supercritical (solid lines) and subcritical (dashed lines) panels

(Adelsohn et al., 2019)

2.1.2 Dynamic Subsidence Basin Formation

As the longwall face progresses over time, the subsidence effects impact the surface gradually, creating a dynamic subsidence wave. Dynamic subsidence occurs when the longwall face is still active and subjects the surface to changing forces as the face advances. The dynamic subsidence wave subjects the ground first to tensile forces and then to compression forces, as can be seen in Figure 9 and Figure 10. Figure 9 shows the proximity of the inflection point, where the forces switch from tension to compression, to the longwall face. Figure 10 shows that the features in front of the longwall face are subjected to tension as the ground starts to move into the gob, but once the longwall face has passed the area is subjected to compression (Peng et al., 1992). This gradual change causes the surface to experience horizontal stresses and strains within the radius of influence, r, before and after the inflection point. These stresses and strains occur at different magnitudes and locations than represented in the final subsidence event.

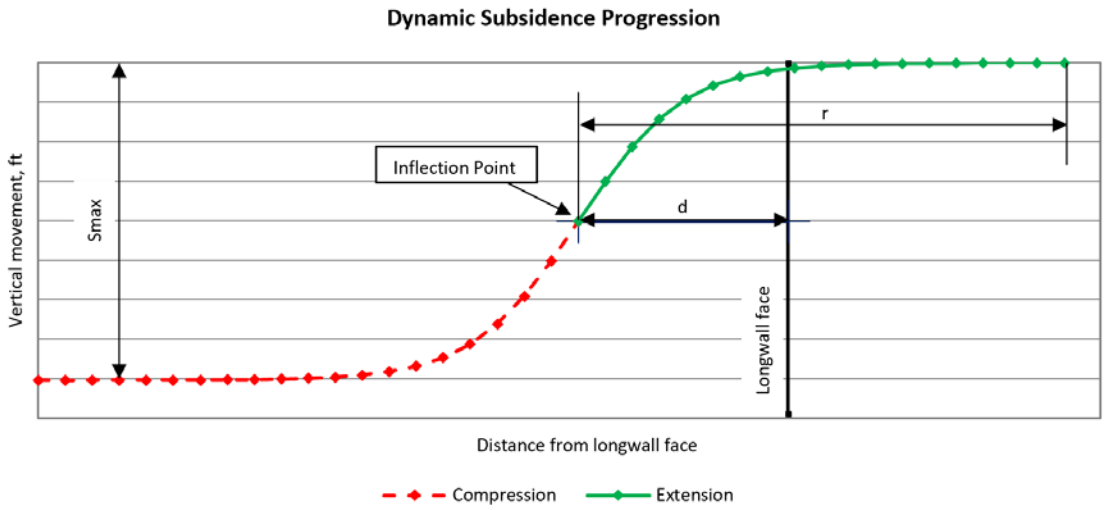

Figure 9 Relationship between vertical subsidence and tension/compression deformations caused by a dynamic subsidence wave

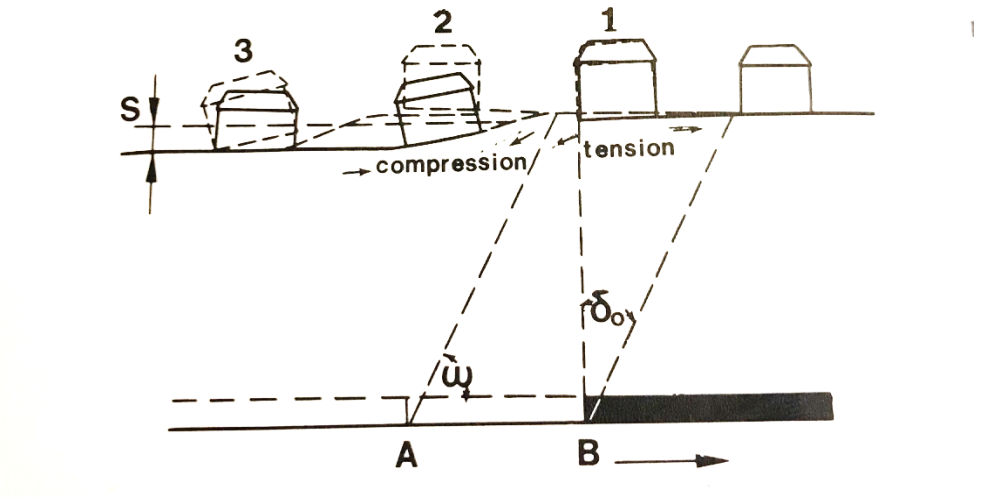

Figure 10 Zones of tension and compression during dynamic subsidence

(Peng et al., 1992)

When the longwall face is a sufficient distance away from the set-up entry, the center of the basin reaches the maximum subsidence values. The sufficient distance that the longwall face must move to reach maximum subsidence has been determined to be between 0.9 and 2.2 times the overburden height (Peng et al., 1992). The subsidence profile continues to progress forward at a regular rate until the face reaches the end of the panel. When the face stops, the profile continues to subside and stabilize until it reaches the final subsidence profile (Peng et al., 1992). The dynamic progression of the longwall face with the associated subsidence basins can be seen in Figure 11.

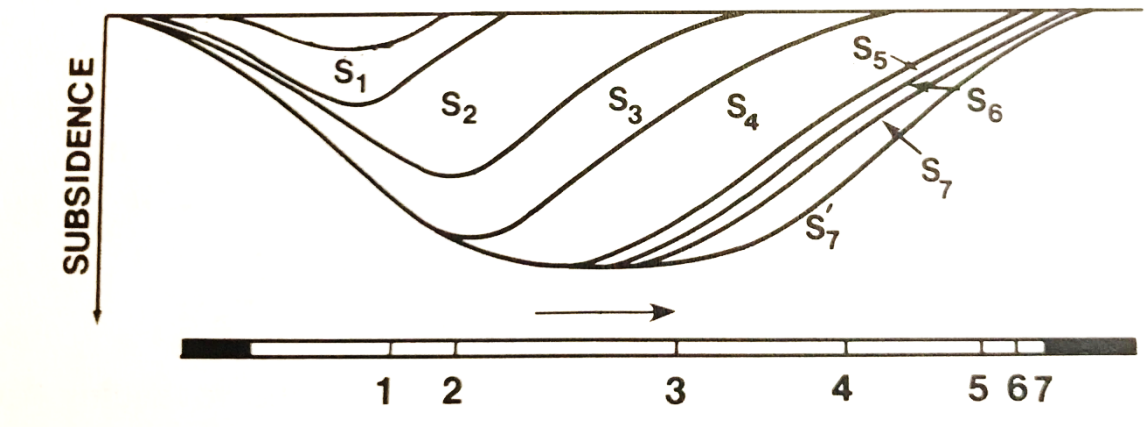

Figure 11 Advancing of the dynamic subsidence basins to the final subsidence basin (Peng et al., 1992)

The rate of face advance has a large role in the impact of dynamic subsidence. A study performed in West Virginia shows that as the mining rate increases, the rate of subsidence, or subsidence velocity, also increases. In addition, the study determined that as the gob size increases, the subsidence velocity increases. A point experiences the maximum subsidence velocity when the longwall face is a fixed distance past that point. Based on a study performed by Peng and Geng in 1984, the maximum subsidence velocity is typically between 0.02-feet/day to 1.00-feet/day in the Appalachian Coalfield, depending on seam depth and it increases as the rate of face advance increases. The dynamic movement has concluded and stabilized to the final subsidence basin when the accumulated subsidence does not exceed 1.2-inches in a six-month period (Peng et al., 1992).

2.1.3 Subsidence Prediction Methods

There are several different methods that can be used to predict subsidence caused by longwall mining. These methods can be classified into empirical, semi-empirical, and numerical methods. The empirical and semi-empirical methods are widely used in the mining industry due to ease of calculations. These methods include the empirical relationships, profile function methods, and influence function methods.

Empirical relationships were derived from extensive field data. These databases have been collected over many years of mining in each location. Formulas for various parameters were developed based on the data collected in these regions, which can be applied to future mining. Unfortunately, since this data is developed in a specific context (range of overburdens, geologies, mine dimension, extraction thicknesses, etc.) the formulas cannot be accurately applied to other contexts (Saeidi et al., 2013). In 1984, Peng was instrumental in the development of these equations for the Pittsburgh Coalbed. They can be used to predict the values for a variety of factors influencing the size and shape of the subsidence basin including the maximum subsidence, the location of the inflection point, and the radius of influence (Peng and Chiang, 1984).

The profile function methods are analytical models that use mathematical equations to model the subsidence profile. These mathematical functions have been obtained by fitting curves to previously observed conditions. These functions can only be used for rectangular shaped extraction geometries (Saeidi et al., 2013). The two most common profiles are the negative exponential function and the hyperbolic tangent function, as can be seen below in Equation 2-1 and Equation 2-2 respectively (Peng and Chen, 1981). Typically, the negative exponential function is used to predict the subsidence basin of subcritical panels and the hyperbolic tangent function is used to predict the subsidence basin of critical and supercritical panels.

$$S(x) = S_0 * e^{-c*(\frac{x}{R})^e} \quad \textbf{[2-1]}$$

where: So = maximum subsidence
x = the distance from the panel center
R = half the width of the subsidence basin

$$S(x) = \frac{S_o}{2} * (1 - \tanh\left(\frac{c * x}{h}\right)) \quad \textbf{[2-2]}$$

where: So = maximum subsidence
x = the distance from the inflection point (pointing outward)
c = coefficient, typically around 8.3
h = overburden

The influence function methods are based on the superposition principle and consider the displacements induced by subsidence at a given point as a function of the sum of all the surface subsidence due to the extraction of an infinite number of elements in the seam horizon. This method has advantages over the other empirical and profile methods because it can be applied to any type of mine geometry and can analyze both vertical and horizontal ground movements induced by subsidence simultaneously (Saeidi et al., 2013). As the influence function is complex and requires the analysis of many points simultaneously, it is typically performed using a computer program.

In this area of Southwest Pennsylvania, the Surface Deformation Prediction Software (SDPS) is generally used for an influence function analysis. SDPS can also be used to model the profile function but, as this is a simpler prediction method, it can be calculated in any graphing software, such as Excel. The subsidence prediction software SDPS was developed by Michael

Karmis of Virginia Polytechnic Institute and State University and is currently being maintained by Zach Agioutantis of the University of Kentucky. SDPS models output graphs of the surface impacts caused by mining including vertical subsidence, horizontal movement, horizontal strain, and ground strain.

2.2 Surface Impacts Caused by Longwall Mining

When a longwall panel subsides the ground, it not only drops the ground surface in elevation, but also causes movement within the horizontal plane. Through these movements, the subsidence event induces forces on the surface. Considering the final subsidence profile, it is evident that the ground on the sides of the basin will be subjected to tensile forces near the gateroads and compression forces approaching the flat basin bottom. However, the subsidence basin causes additional stresses as it forms. As described previously, the ground is subjected to tensile forces as the longwall face approaches and passes a point and then transitions into a zone of compression once the inflection point passes before settling into its final subsidence location. These stresses impact and cause damage to the surface including structures, roads, water sources, and the land.

2.2.1 Structural Impacts

Though much of longwall mines located in Southwest Pennsylvania undermine less populated areas, there are a variety of structure types that have been undermined by longwall panels including, houses, churches, schools, cellular towers, bridges, dams, and roads. Structural

features within 200-feet of active mining are generally tracked by the Pennsylvania Department of Environmental Protection (PA DEP) to consider the impact of mining (Iannacchione et al., 2008).

There are several types of surface disturbances that can be transferred to structures and cause damage. Both continuous and discontinuous ground disturbances cause damage to the surface structures. Structural damages caused by discontinuous ground disturbances are generally represented by fissures or cracks and bumps. The types of damage observed vary depending on the location of the structure in the subsidence basin (Peng et al., 1992).

Fissures and cracks can open to be a variety of widths, which cause varying impacts to structures. Open cracks can dislocate the surface structure and affect its structural stability if the gaps are sufficiently large so that the structural element cannot resist failure. Contrarily, minor cracks may only affect the appearance of a structure and may not compromise the structural integrity. As the longwall face continues to move, these cracks can open and then may gradually close again over time or may remain open permanently. Cracks that remain open tend to occur near the panel edges, where the ground is permanently subjected to tensile forces (Peng et al., 1992).

Bumps, or compression ridges, result from ground compression. These features are triggered by compressive forces and can disrupt roadways or a building floor. If located under a supporting member of the structure, a compression bump can damage the structural integrity. Bumps most commonly occur near the panel center some time after the longwall face has passed (Peng et al., 1992).

Continuous ground damage becomes more prominent for longwall mines deeper than 600-feet. This means that the subsidence basin becomes more of a zone of continuous non-destructive ground deformations. These ground deformations contain subsidence, slope, curvature,

displacement, horizontal strain, twisting, and shearing and can predicted using subsidence prediction modeling software (Peng et al., 1992).

2.2.2 Structural Impacts to Roads

There are a series of standardly defined distresses that occur commonly on jointed cement concrete pavements. These methods were developed by the Federal Highway Administration (Miller and Bellinger, 2003). As can be seen in Table 1, there are four general categories of distresses with 16 subcategories.

Table 1 Distress types for jointed concrete pavements

(Iannachione et al., 2008; Miller and Bellinger, 2003)

Category	Distress Type/ Photograph
Cracking	*Corner Breaks* – A portion of the slab separated by a crack, which intersects with the adjacent transverse and longitudinal joints, describing approximately a 45-degree angle with the direction of traffic. The length of sides is from 1 ft to ½ the width of the slab on each side of the corner
	Durability Cracking – Closely spaced, crescent-shaped hairline cracking pattern, occurring adjacent to joints, cracks, or free edges. Initiates in slab corners with dark coloring of the cracking pattern and surrounding area
	Longitudinal Cracking – Cracks that are predominately parallel to the pavement centerline
	Transverse Cracking – Cracks that are predominately perpendicular to the pavement centerline
Joint Deficiencies	*Joint Seal Damage* – Conditions which enable incompressible materials or water to infiltrate the joint from the surface. Typical types of joint seal damage are: extrusion, hardening, adhesive failure (bonding), cohesive failure (splitting), or complete loss of sealant; intrusion of foreign material in the joint; and weed growth in the joint
	Spalling of Longitudinal Joint – Cracking, breaking, chipping or fraying of slab edge within 0.3 m from the face of the longitudinal joint
	Spalling of Transverse Joint – Cracking, breaking, chipping, or fraying of slab edges within 0.3 m from the face of the transverse joint
Surface Defects	*Map Cracking and Scaling* – Map cracking is a series of cracks that extend only into the upper surface of the slab. Larger cracks frequently are oriented in the longitudinal direction of the pavement and are interconnected by finer transverse or random crack. Scaling is the deterioration of the upper concrete surface, normally 3mm to 13mm, and may occur anywhere over the pavement
	Polished Aggregate – Surface mortar and texturing worn away to expose coarse aggregate
	Popouts – Small pieces of pavement broken loose from the surface, normally ranging in diameter from 25mm to 100mm, and depth from 13mm to 50mm
Miscellaneous Distress	*Blow-ups* – Localized upward movement of the pavement surface at transverse joints or cracks, often accompanied by shattering of the concrete in the area
	Faulting of Transverse Joints and Cracks – Difference in elevation across a joint or crack
	Lane-to-Shoulder Dropoff – Differences in elevation between the edges of slab and outside shoulder; typically occurs when the outside shoulder settles
	Lane-to-Shoulder Separation – Widening of the joint between the edge of the slab and the shoulder
	Patch/Patch Deterioration – A portion, greater than 0.1 m^2, or all of the original concrete slab that has been removed and replaced, or additional material applied to the pavement after original construction
	Water Bleeding and Pumping – Seeping or ejection of water from beneath the pavement through cracks. In some cases, detectable by deposits of fine material left on the pavement surface, which were eroded (pumped) from the support layers and have stained the surface

These methods of distress can be utilized to characterize the damage that occurs on a pavement structure during undermining. As previously described, longwall mining induces both tension and compression stresses on the ground surface. The damage that occurs on roadways as a result of longwall mining has primarily been in the form of longitudinal and transverse cracks, transverse compression bumps, and lane-to-shoulder separations. The longitudinal and transverse cracks and lane-to-shoulder separations occur in areas of tension, while compression bumps form in areas of compression.

2.2.3 Water source and Stream Impacts

There are several types of water sources both below the ground and on the surface that can be impacted by longwall mining, including water wells, aquifers, lakes, and streams. There are a number of factors that may play a role in the hydrogeologic response of watersources. These factors may include the topographic location, the overburden depth, the proximity of source to mining, the average seasonal precipitation rates, and the seasonal infiltration rates (Iannacchione et al., 2008).

Water loss to these types of water sources are more likely in areas above and adjacent to active mining. A study performed at West Virginia University considered a number of case studies of mines where water loss occurred. This study determined that most of the damage to watersources occurred within a 27-degree to 38-degree angle from the edge of active mining. As a result of this study, the PA DEP issued a technical guidance document defining a Rebuttable Presumption Zone (RPZ) as any area within a 35-degree angle from the edge of active mining (Figure 12). Due to this document, any damaged water source that falls within the RPZ is the responsibility of the mining company to repair and restore (Iannacchione et al., 2008).

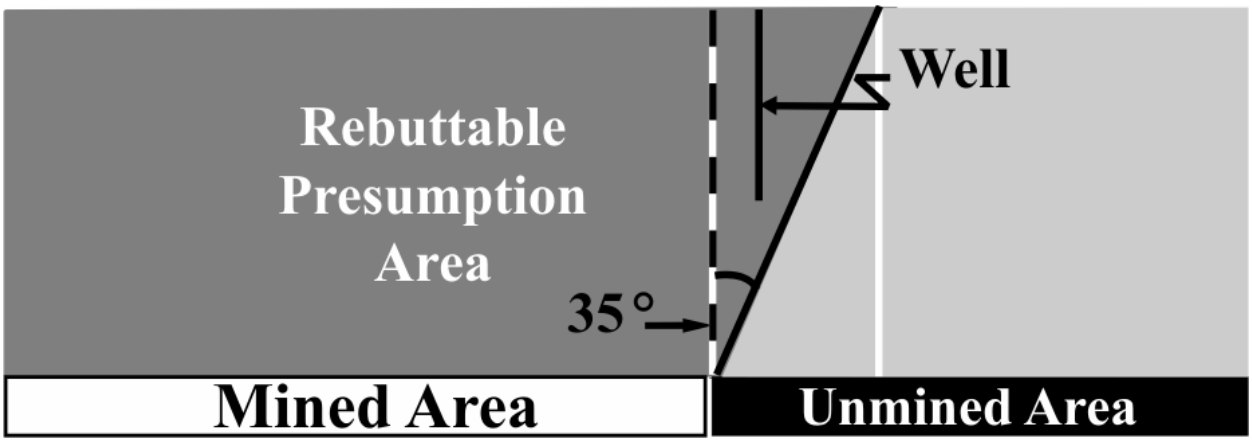

Figure 12 Depiction of Rebuttable Presumption Zone showing area where mining is responsible for water source damage

(Iannacchione, 2018)

In addition to water loss, streams and other surface water features can also be impacted through changes to the biologic diversity. A healthy water source has certain biological make up, which can be damaged by changes to water flow caused by longwall mining. Additionally, mine discharge can cause pollution of waterways and damage the stream biology and overall stream health (Iannacchione et al., 2008).

2.2.4 Land Impacts

Like with the formation of damage on roadways, the ground surface is also subjected to tension and compression stresses during longwall mining. The impacts to the ground surface from longwall mining have been less documented over time, but generally consist of tension cracks, settlement, ponding, scarps, and mass wasting. Like on the road surface, tension cracks occur in areas of tension. Scarps and mass wasting occur on slopes and can be triggered by either tension or compression stresses. These instabilities to slopes can also cause other damage to structures,

roadways, and streams. The settlement and ponding damages are common and caused by the subsidence and changes in slope on the surface.

Cave-in-pits, or sinkholes, can also be caused by longwall mining. Sinkholes result from the local collapse of the ground from the mine level to the surface. These typically only occur when the overburden is very shallow, less than 150-feet, and above abandoned mines. If the caved-in-pit is larger than the surface structure, the structure may drop into the pit and become unstable. On the other hand, if the pit is smaller than the structure, the structure may become overhung or lose support in some portions (Peng et al., 1992). However, since most modern longwall panels are not mined at an overburden of less than 150-feet, cave-in-pits do not occur frequently in Southwest Pennsylvania.

2.3 History of Longwall Mining beneath Interstates

Over the last four decades, two of Pennsylvania's interstates in Greene and Washington Counties have been undermined by longwall mines. Interstate 70 (I-70) has been undermined twice and Interstate 79 (I-79) has been undermined thrice. Through these five undermining episodes, a total of 25 panels that have undermined or influenced the interstates, as can be seen in Figure 13.

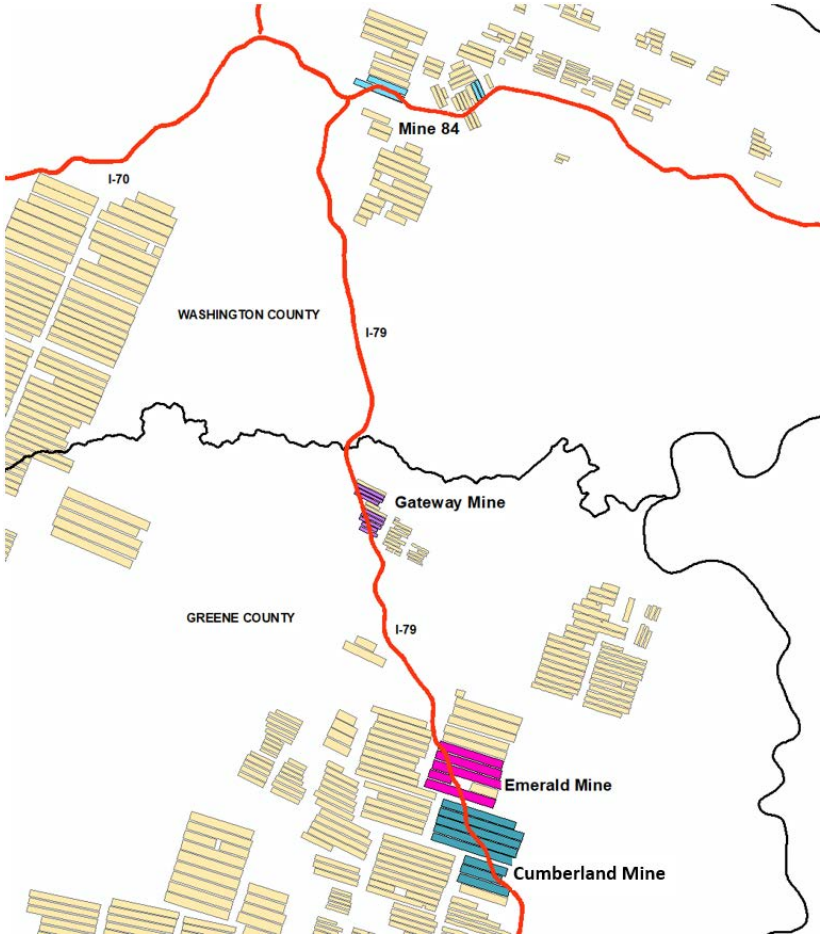

Figure 13 Longwall panels that have undermined Pennsylvania Interstates

2.3.1 Gateway Mine

In the 1980's, the Gateway Mine extracted eight longwall panels that crossed I-79 just north of the Ruff Creek Interchange at Exit 19. These panels were mined from south to north and there were two panels in the middle of the block that did not cross the interstate (Figure 14). These panels crossed the roadway at an average angle of 41-degrees. The Gateway panels were smaller than modern panels, with an average width of 511-feet (Table 2).

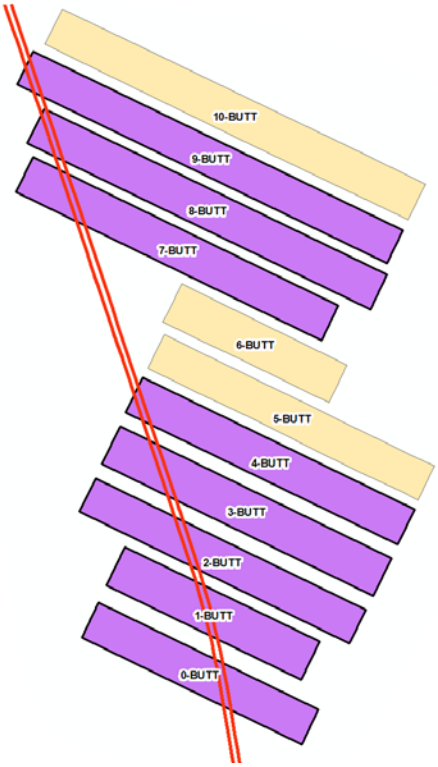

Figure 14 Gateway mine longwall panels that undermined section of I-79

Though the Gateway panels were small, they were some of the deepest panels to undermine an interstate in Pennsylvania. These panels had an average overburden of 788-feet with minimum and maximum overburdens of 648-feet and 945-feet respectively (Table 2). Due to the small panel width and large overburdens, the width to overburden ratios for all these panels averaged 0.70, which classified the resulting subsidence basins as subcritical.

Table 2 Characteristics of Gateway Mine panels that undermined I-79

Panel ID	Days to Mine	Acres	Dates Mined		Days to Mine 1 acre	Panel Dimensions		Overburden, ft			Width to height Ratio
			Start	Finish		Width ft	Length ft	Min	Max	Avg	
0-Butt	336	38	6/16/1982	5/18/1983	8.8	522	3218	648	863	770	0.68
1-Butt	235	37	6/18/1983	2/8/1984	6.4	567	2842	657	934	742	0.76
2-Butt	258	45	9/15/1984	5/31/1985	5.7	504	3957	655	915	759	0.66
3-Butt	344	45	9/13/1985	8/23/1986	7.6	534	3969	648	909	786	0.68
4-Butt	179	46	9/15/1986	3/13/1987	3.9	503	3967	667	945	820	0.61
7-Butt	158	51	2/15/1988	7/22/1988	3.1	499	4468	696	902	780	0.64
7-Butt	170	56	8/15/1988	2/1/1989	3.0	489	4995	701	918	831	0.59
9-Butt	227	58	2/15/1989	9/30/1989	4.0	470	5386	716	890	813	0.58
Average	238	47			5.3	511	4100	673	910	788	0.70

A study performed by Yancich at West Virginia University (1986) analyzed the subsidence characteristics of the first three of the Gateway panels (0-Butt, 1-Butt, and 2-Butt) to impact the interstate. This study included the regular monitoring of fixed survey monuments along the northbound lanes of I-79 and ultimately compiled a final subsidence profile for the three panels (Figure 15).

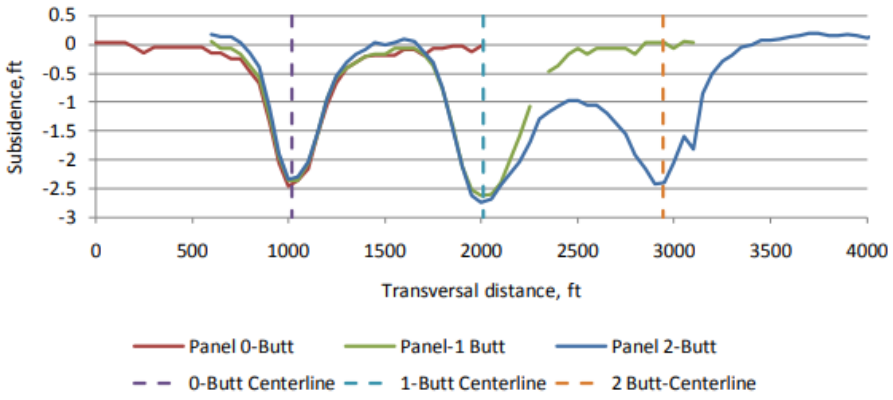

Figure 15 Final subsidence profiles for three Gateway panels undermining northbound I-79 (Yancich, 1986)

The surveys clearly depict three separate subsidence basins, that all come to a point around a maximum vertical subsidence of 2.5-feet to 2.7-feet. It is also noteworthy that, after the completion of all three panels, there was about a foot of vertical subsidence over the gateroads between Panel 1-Butt and Panel 2-Butt; this amount of vertical subsidence indicates yielding pillars in the gateroads between these two panels.

The study went on to examine the slope and curvature of these panels derived from the final subsidence basins (Figure 16). The maximum slope ranged from +1.9% to -1.56% and the points of zero slopes were located at the approximate location of the center of the panels and the gateroad entries. The maximum curvature ranged between $+2x10^{-4}$/ft and $-2x10^{-4}$/ft, with the areas of highest curvature between the edges and centers of the panels (Yancich, 1986). Most impacts on I-79 were expected to occur in these areas of highest slope and curvature.

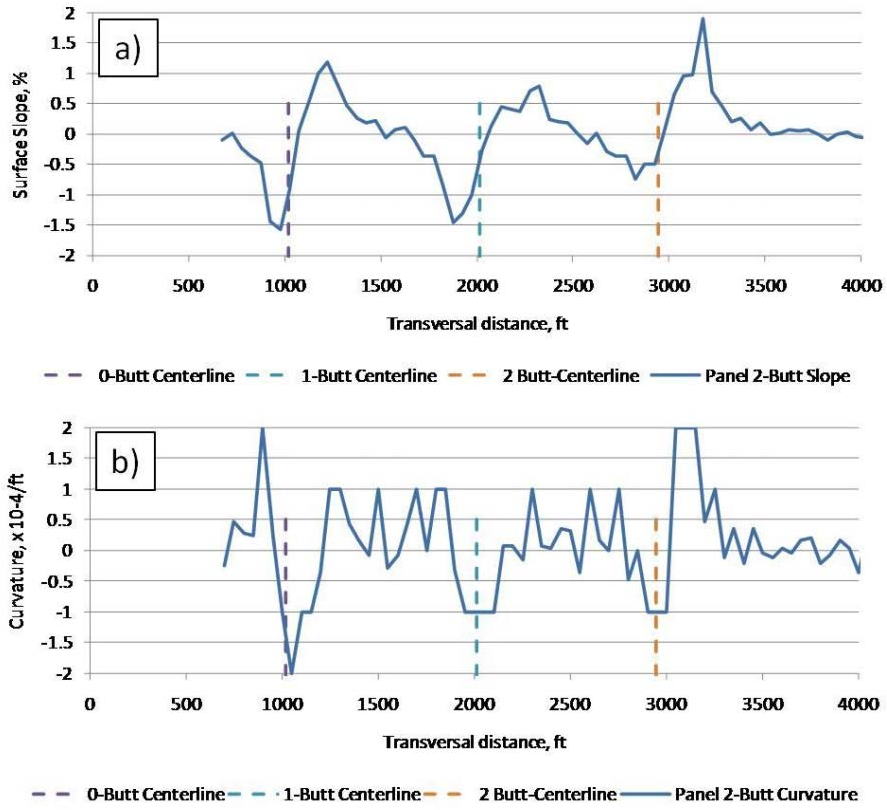

Figure 16 Profiles of a) surface slope and b) curvature from three Gateway panels undermining I-79 northbound

(Yancich, 1986)

Despite these higher slopes and curvatures, only minor damage was reported on the northbound lanes of I-79 as a result of undermining. Figure 17 depicts repaired damage to I-79 a) between the centerline and southern edge of panel 0-Butt, b) near the southern edge of panel 1-Butt, and c) near the northern edge of panel 2-Butt. However, the Yancich study only described a subset of the impacts, making it difficult to determine the overall magnitude of damage and repairs associated with this undermining event.

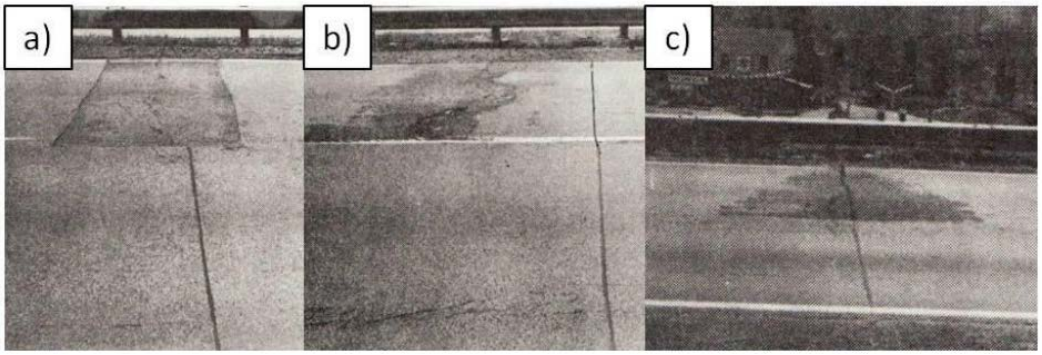

Figure 17 Photographs of impacts to northbound lanes of I-79 over a) 0-Butt, b)1-Butt, and c) 2-Butt panels of the Gateway Mine

(Yancich, 1986)

2.3.2 Mine 84

I-70 was first undermined by Mine 84. There were four panels that influenced I-70 that were mined in two episodes (Figure 18).

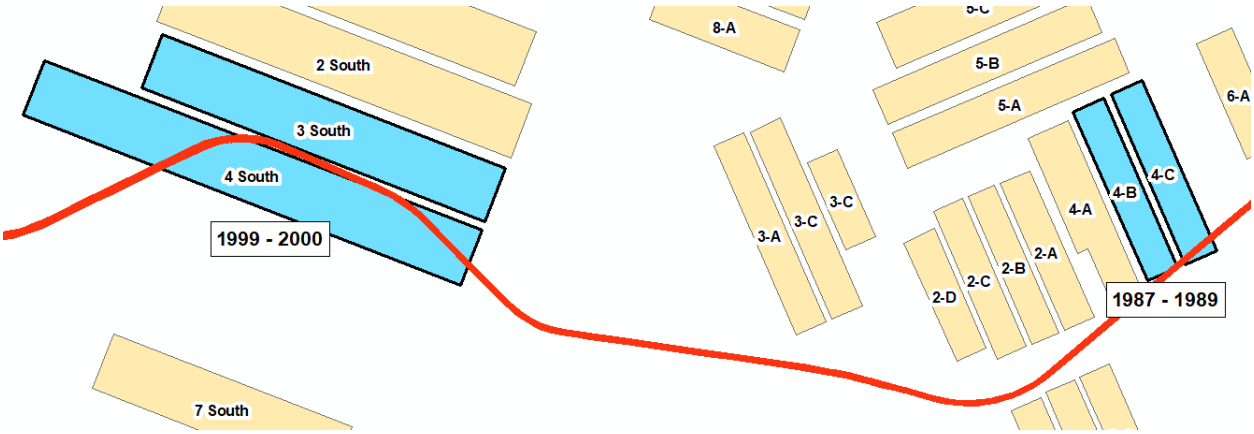

Figure 18 Mine 84 longwall panels that undermined I-70

The first of these panels were extracted between 1987 and 1989 with the mining of two longwall panels, panels 4B and 4C, whose extreme southern tips intersected a small portion of the road at an angle of 17-degrees. Like the panels from the Gateway mine, these two panels were small, with an average width of 622-feet. Like the previously described Gateway panels, these panels formed subcritical basins. They were located in a shallower section of the Pittsburgh Coalbed with an average overburden of 579-feet and minimum and maximum overburdens of 451-feet and 692-feet respectively (Table 3). The lower overburden and slightly wider panel combined for an average width to overburden ratio of 1.08. No information on the impacts of this initial episode of mining under I-70 was found.

Table 3 Characteristics of Mine 84 panels that undermined I-70, 1987 to 1988

Panel ID	Acres	Dates Mined		Panel Dimensions		Overburden, ft			Width to height Ratio
		Start	Finish	Width, ft	Length, ft	Min	Max	Avg	
4-B	48	n/a	1987	612	3428	451	635	556	1.10
4-C	49	n/a	1988	632	3445	459	692	602	1.05
Average	49			622	3436	455	664	579	1.08

The second episode of undermining I-70 occurred between 1999 and 2000, with the mining of longwall panels 3-South and 4-South. These panels were oriented to minimize the impacts to the interstate; as a result, there was approximately 0.75-miles of interstate that ran over the gateroads between the two panels (Figure 18). Due to new technology, these panels were significantly larger than any panels than had previously undermined interstates with an average width of 1,071-feet. They were in a similar area of the Pittsburgh Coalbed placing them at a similar overburden as the previous Mine 84 panels. These panels had an average overburden of 597-feet and minimum and maximum overburdens of 498-feet and 775-feet respectively (Table 4). The larger widths of these panels generated an average width to height ratio of 1.79, causing the resulting subsidence basins to be classified as supercritical.

Table 4 Characteristics of Mine 84 panels that undermined I-70, 1999 to 2000

Panel ID	Days to Mine	Acres	Dates Mined		Days to Mine 1 acre	Panel Dimensions		Overburden, ft			Width to height Ratio
			Start	Finish		Width ft	Length ft	Min	Max	Avg	
3-South	258	166	11/22/1999	3/2/2000	0.61	1061	6843	465	788	587	1.81
4-South	344	215	3/9/2000	10/16/2000	1.03	1081	8715	498	775	607	1.78
Average	301	191			0.82	1071	7779	481	782	597	1.79

A study completed by O'Connor in 2001 analyzed the second undermining of I-70. For this study, a series of 32 tiltmeters were installed along the highway to detect hazardous

deformations during undermining. These tiltmeters were outfitted with real-time data acquisition systems and triggered an alarm if levels of tilt exceeded 0.002 ft/ft. To minimize the damage to the road during undermining, PennDOT implemented a plan to temporarily support the Zediker Station Road overpass, dismantle some of the overhead signs, decrease the speed-limit to 40-miles-per-hour, provide for lane closures and detours, and visually monitor highway conditions (O'Connor, 2001). As a result of these mitigation techniques, there were no accidents caused by the undermining of this section of I-70.

After reviewing the data, between 3-feet and 5-feet of maximum vertical subsidence was observed on the highway. O'Connor (2001) reported that the vertical subsidence measured was significantly different than that predicted. The tiltmeters showed the surface tilting primarily around the trough margins and that larger ground surface curvature and strains were observed than were originally anticipated. The report stated that –

> …The ground surface ultimately deformed into a trough with a maximum subsidence of three to five feet with surface tilting occurring around the margins of the trough. Precursor movement occurred ahead of the mine face, and outside the edges of the panel being mined. Predicted subsidence profiles, however, differed from the actual measured subsidence. As a consequence of differential tilt, (the) ground surface, pavement, and structures were subjected to greater curvature and larger curvature strain than anticipated. Buried culverts and an overpass along the undermined section of I70 were not damaged, but longitudinal cracks developed between lanes, as did transverse bumps. This led to temporary lane closures as cracks were filled and bumps were milled down. Along the secondary roads, some transverse cracking occurred and the wall blocks in a railroad bridge abutment cracked and shifted… (O'Connor, 2001)

Some damage occurred to I-70 as a result of this undermining event. Movement was seen both inside and outside of the panels mined. The damage observed included small compression bumps, longitudinal cracks, and transverse cracks. These cracks needed to be filled and the transverse compression bumps needed to be milled during the undermining process. Temporary lane closures needed to be implemented to make repairs to the roadway. It was reported that this damage occurred in areas with high residual strains and that some of the cracking occurred on joints between lanes (O'Connor, 2001).

2.3.3 Emerald and Cumberland Mines

Between 2003 and 2010, 13 longwall panels operated by Alpha Resources undermined I-79. These panels were part of the Emerald and Cumberland Mines and will be further characterized by mine.

2.3.3.1 Characterization of the Cumberland Panels

The Cumberland Mine extracted eight panels that crossed beneath I-79 (Figure 19). The panels were mined from north to south and crossed the road at a 39-degree angle. The distance between panels LW53 and LW 54 is greater than that between other panels due to the presence of main entries between these two panels.

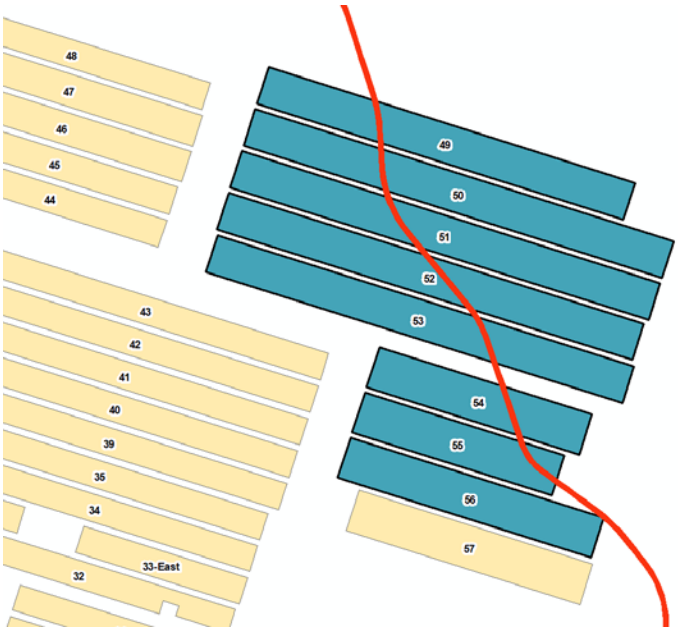

Figure 19 Cumberland longwall panels that undermined I-79

The Cumberland panels were the largest to undermine an interstate, with an average size of 349-acres and an average width of 1,317-feet. The average overburden for these panels is 717-feet with minimum and maximum overburdens of 543-feet and 960-feet respectively (Table 5). The average width to overburden ratio for these panels is 1.84, characterizing the subsidence basins for these panels as supercritical.

Table 5 Characteristics of Cumberland Mine panels that undermined I-79

Panel ID	Days to Mine	Acres	Dates Mined		Days to Mine 1 acre	Panel Dimensions		Overburden, ft			Width to height Ratio
			Start	Finish		Width ft	Length ft	Min	Max	Avg	
49	354	371	12/29/03	12/17/04	1	1,270	12,732	579	921	741	1.71
50	290	425	1/6/05	10/23/05	0.7	1,276	14,525	551	884	728	1.75
51	284	425	11/5/05	8/16/06	0.7	1,276	14,528	543	877	709	1.80
52	281	419	8/31/06	6/8/07	0.7	1,272	14,415	554	904	728	1.75
53	271	416	6/30/07	3/27/08	0.7	1,271	14,453	569	901	693	1.83
54	n/a	235	4/9/08	2008	0.8	1,394	7,390	558	910	709	1.96
55	n/a	221	n/a	2009	n/a	1,394	6,935	585	960	713	1.96
56	n/a	280	n/a	2009	n/a	1,388	8,796	543	915	716	1.94
Average	296	349			0.8	1,317	11,722	560	909	717	1.80

2.3.3.2 Characterization of Emerald Panels

The Emerald mine undermined an additional five panels that crossed I-79. These panels crossed the road at an average angle of 44-degrees. As depicted in the layout of the Emerald panels that interacted with I-79 shown in Figure 20, the fourth panel to be mined, B-6, was cut into two smaller panels to avoid undermining a critical surface structure, with the majority of I-79 in this section passing over the unmined area.

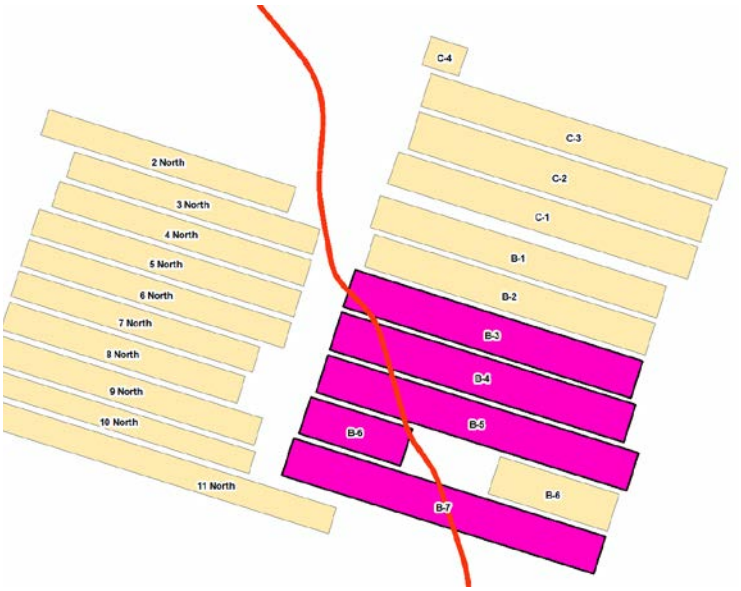

Figure 20 Emerald longwall panels that undermined I-79

The Emerald panels were also very large, with an average size of 331-acres and an average width of 1,435-feet. The average overburden for these panels is 723-feet with minimum and maximum overburdens of 541-feet and 946-feet respectively (Table 6). The average width to overburden ratio for these panels is 2.00, classifying these panels' subsidence basins as supercritical.

Table 6 Characteristics of Emerald Mine panels that undermined I-79

Panel ID	Days to Mine	Acres	Dates Mined		Days to Mine 1 acre	Panel Dimensions		Overburden, ft			Width to height Ratio
			Start	Finish		Width ft	Length ft	Min	Max	Avg	
B-3	252	365	6/30/05	3/9/06	0.7	1438	11094	541	925	739	1.95
B-4	274	374	3/20/06	12/19/06	0.7	1440	11333	574	916	755	1.91
B-5	328	395	12/31/06	11/24/07	0.8	1439	11983	550	946	739	1.95
B-6	n/a	128	n/a	2009	n/a	1429	3910	544	840	659	2.17
B-7	n/a	393	n/a	2010	n/a	1428	12017	547	928	725	1.97
Average	285	331			0.7	1435	10067	551	911	723	2.00

2.3.3.3 Cumberland and Emerald Mines Analyses

A study completed by Gutierrez, Vallejo, and Lin in 2010 analyzed the undermining of I-79 by examining two Emerald panels and six Cumberland panels. Survey data was collected for the highway alignments that crossed all eight panels on multiple dates during the undermining process. This data showed not only the final subsidence basin underneath the highway, but also the dynamic subsidence as the basin formed. The data collected for Cumberland panels LW51 and LW52 can be seen below in Figure 21.

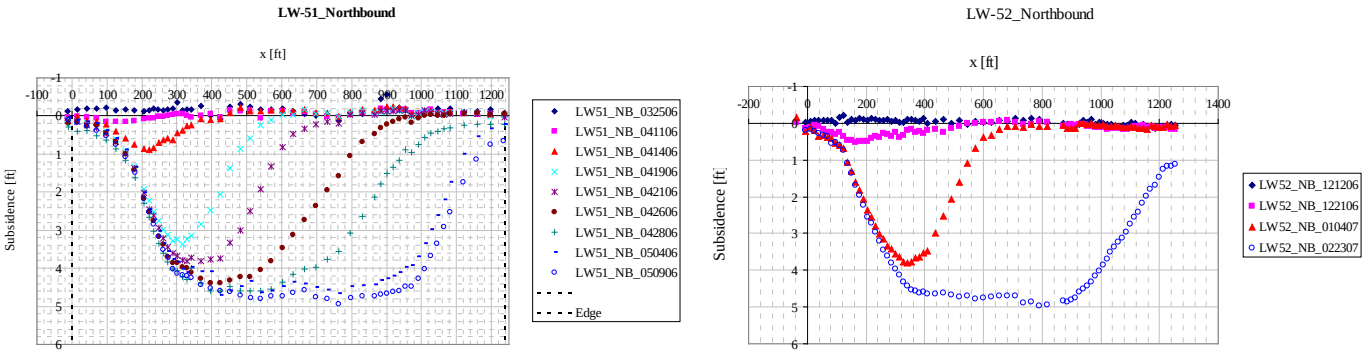

Figure 21 Measured subsidence profiles over time of Cumberland panels LW51 (left) and LW52 (right) (Gutierrez et al., 2010)

Prior to undermining, PennDOT implemented several mitigation techniques to minimize the impact of the longwall subsidence on the drivers. Sections of the concrete base were removed from beneath the asphalt pavement in areas of high predicted stresses and strains to provide the road with additional flexibility to adapt to the subsidence event. During active mining and repair periods, speed-limits were reduced to 45-miles-per-hour and one of the two lanes was closed in each direction. In addition, the interstates were under constant observation and monitoring to ensure the damage was fixed before it could cause accidents or injury.

Throughout the undermining of these panels for both the Cumberland and Emerald mines, PA DEP and PennDOT staff routinely visited I-79. During these visits, they observed a variety of types of damage on the highway surface including compression bumps, transverse cracking, longitudinal cracking, joint faulting, and lane-to-shoulder separations. Some examples of these failures can be seen in Figure 22. Most of the damage was localized and was repaired during or following the undermining process.

Figure 22 Examples of surface damage on I-79 caused by Emerald and Cumberland undermining showing a) compression bump, b) transverse crack, c) joint faulting, and d) lane-to-shoulder separation (Iannacchione et al., 2008)

2.3.4 Monitoring and Mitigation Techniques Implemented During Undermining

Throughout the past undermining of Pennsylvania interstates, a number of monitoring and mitigation techniques were employed. Traditional surveying of interstates and tiltmeters were utilized to characterize the movement of the highway in response to the undermining. The surveying was used primarily to track the vertical subsidence on the highway but was also able to be used to examine slope and surface curvature. With these surveys, little attention was given to the movement in the horizontal plane. The tiltmeters transmitted data regarding the tilt of the ground surface in real-time. This system allowed PennDOT to anticipate major damage to the

roadway as it was occurring and afterwards was used characterize the locations of maximum slope in the subsidence basin.

Many mitigation techniques were also employed during these undermining activities. PennDOT's primary concern during all of the longwall mining activities was to maintain a safe and traversable road throughout the entirety of the undermining processes. The speed limit of these routes was reduced, and the traffic was limited to one lane in each direction to give PennDOT more control over the monitoring and safety of the traveling public. Sections of concrete pavement were removed and replaced with asphalt to provide regions with additional flexibility in the roadway to accommodate the subsidence. In addition, the roadway was under constant observation and monitoring to ensure that any damage was repaired immediately to prevent traffic accidents from occurring.

2.3.5 Financial Analysis

As described previously, both Pennsylvania interstates that were influenced by longwall mining experienced localized damage. Some of these effects were permanent, while others were transitory, and the damage was lessened once the subsidence wave moved through the area. In order to mitigate damage, monitoring, traffic control, and temporary support measures were implemented. Repairs made include milling, temporary patching, and repaving of the pavement, and straightening of guiderails. It is estimated that the Pennsylvania government spent nearly $20 million (Iannacchione et al., 2008) monitoring and rehabilitating sections of I-79 impacted by longwall mining between 2002 and 2008 (Table 7).

Table 7 Estimated cost to monitor, maintain, and repair I-79 during undermining

(Iannacchione et al., 2008)

Year	Detour Preparation ($)	Monitor and Equipment ($)	Construction ($)	Total ($)
2002 - 2003	6,263,597			6,263,597
2004		244,048	467,608	711,656
2005		65,309	1,644,856	1,710,165
2006		239,176	3,192,371	3,431,547
2007		152,871	3,090,231	3,243,102
2008		230,131	4,016,737	4,246,868
Total from 2002 to 2008				19,606,935

During this six-year period from 2002 and 2008, approximately nine panels were extracted, which means that the road cost a little over $2 million to maintain per panel mined. If this cost is extrapolated for all 25 panels extracted in Pennsylvania that influenced interstates, it would be estimated that the Pennsylvania government has spent around $54.5 million on highway repairs due to longwall mining over the last four decades.

2.4 Strains and Deformations on Pavement

Damage to the ground surface above a longwall mine is caused primarily by strains. Though difficult to measure, the earth between the top of the mine and the ground surface has regions of tension and compressive, which result in deformation at the ground surface. The prediction of surface strains due to underground mining can be reported as horizontal strains or ground strain.

Horizontal strain is calculated as the change in horizontal length between two points divided by the original length between the two points. This method of calculating strain assumes

that the points lie on an infinitely horizontal plane. As such, it can only be determined in one orientation but can be defined along a directional path, like a roadway (Agioutantis et al., 2016).

For a more accurate depiction of mining induced impacts on the ground surface, the concept of ground strain can be utilized. Ground strain uses surface points surrounding a point of interest to determine the "overall relative movement" of the surface terrain. This is accomplished by comparing the difference between pre and post mining displacements of the points in question (Agioutantis et al., 2016). Unlike horizontal strain, ground strain considers the topographic elevation of the surface.

Since the ground surface is rarely an infinite horizontal plane, the consideration of the elevation of the surface terrain makes ground strain a better prediction method than horizontal strain. The relationship between measured, axial, and ground strains can be seen in Figure 23 below. As can be seen in this figure, ground strain prediction is a closer estimation of measured strain than axial strain, which overestimates the strain measured on the surface (Agioutantis and Karmis, 2013).

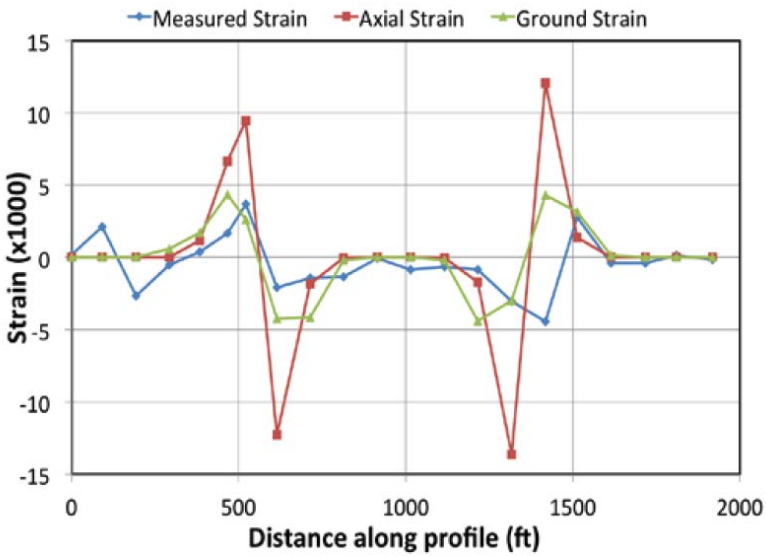

Figure 23 Comparison of measured, axial, and ground strains along monitoring line above longwall panel (Agioutantis and Karmis, 2013)

In 1994, Karmis, Mastoris, and Agioutantis combined a series of ground movement damage classification schemes to characterize the structural damage resulting from horizontal strain caused by underground mining. This characterization system considers the change of length of a structure and class of damage according to the National Coal Board (1975), the severity index according to Bruhn (1982), and suggested damage limits for horizontal strain according to Singh (1992). This characterization system is summarized in Table 8.

Table 8 Characterization of structural damage resulting from horizontal strain

(Karmis et al., 1994)

Change of Length of Structure (N.C.B., 1975)	Class of Damage	Severity Index (Bruhn et al., 1982)	Suggested Damage limit for Horizontal Strain (Singh, 1992)
< 0.1 ft	Architectural	0 – 1	0.5×10^{-3}
0.1 ft – 0.2 ft	Functional	1 – 2	$1.5\text{-}2 \times 10^{-3}$
0.2 ft – 0.4 ft	Functional	1 – 2	$1.5\text{-}2 \times 10^{-3}$
0.4 ft – 0.6 ft	Structural	2 – 4	3×10^{-3}
> 0.6 ft	Structural	4 – 5	$> 3 \times 10^{-3}$

Based on this characterization system, a damage class of "functional" signifies instability of some structural elements, broken windows or doors, and restricted building services (Karmis et al., 1994). As the "structural" amount of damage would be of minimal concern to the structural integrity of a pavement system, the suggested damage limit for horizontal strain of 3 milli-strains (0.3%) should be used as it is associated with structural damage. This small amount of horizontal strain corresponds to the expansion or compression of a 20-foot structural member of about 0.75-inches.

This suggested horizontal strain limit was reinforced by a study completed by Luo, Yiang, and Jiang in 2019 regarding the subsidence effects on interstate highway (2019). In addition to

discussing the impact of subsidence on the highway's geometric layout, the study determines the uplift on concrete slabs, like those beneath the I-70 asphalt surface undermined by Tunnel Ridge's Panel 15, subjected to subsidence induced compressive strain (Figure 24). For a 20-foot concrete slab, uplift begins to occur when subject to compressive strains between 2.5 and 3 milli-strains and a foot of uplift occurs when the compressive strain increases to about 3.75 milli-strains.

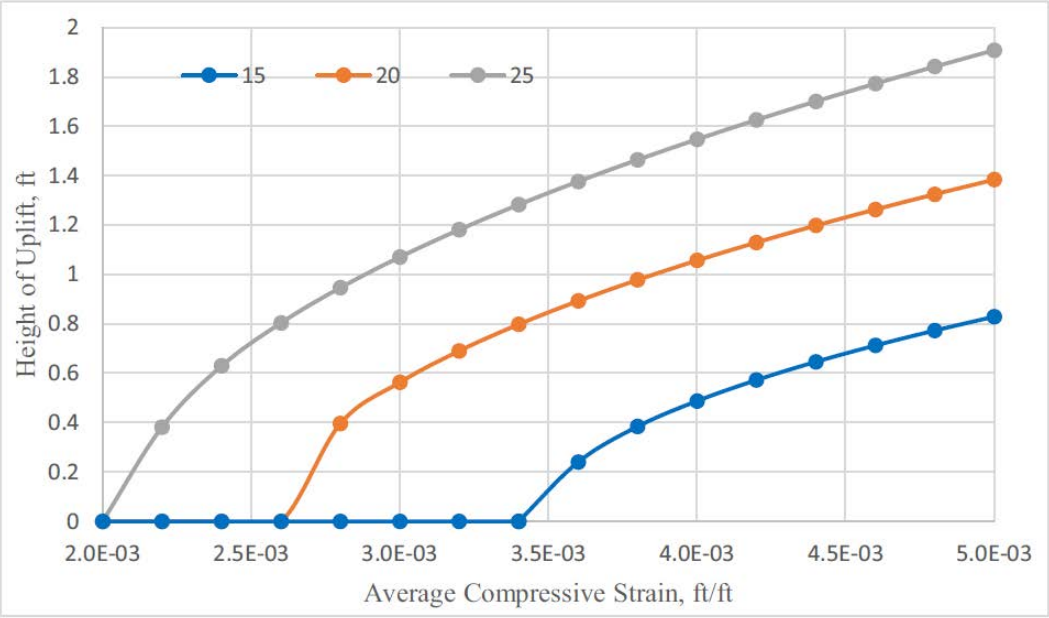

Figure 24 Height of uplift of concrete slabs subjected to subsidence induced compressive strain (Luo et al., 2019)

These uplift calculations were performed using Equation 2-3 and assuming 5/8-inch transverse joints between the concrete slabs (Luo et al., 2019). Using this equation, it can be determined that increasing the width of the transverse crack to 1.5-inches or decreasing the length of the slab to 10-feet would significantly reduce the potential for uplift.

$$\Delta h = \sqrt{D^2 \varepsilon_a (2 - \varepsilon_a) - 2DG(1 - \varepsilon_a) - G^2} \quad \textbf{[2-3]}$$

Where: Δh = height of slab uplift
ε_a = average compressive strain
D = length of slab
G = width of transverse joint

However, this equation is strictly theoretical and does not consider the behavior of partially cut joints in concrete pavement. The width of the joint used in Equation 2-3 is the width at the surface that was cut to promote cracking between slabs; however, these cuts are typically only cut down only a quarter of the thickness of the concrete slab. The crack that forms from this cut is significantly smaller, and as such, there is much less space for compression between the joints than assumed by this equation. This means that uplift in concrete would likely occur when slabs are subjected to smaller amounts of compressive strain than identified in Equation 2-3.

3.0 Data Collection

The data obtained for this study was obtained from multiple sources including publicly available sources, PennDOT, and the Tunnel Ridge Mining company. The analysis included site visits to the study area and data collected by PennDOT's subcontractors to provide instrumentation and survey data.

3.1 Compilation of Pre-existing Information

Before any data could be collected within the study area, a preliminary review of the study area was conducted using documents provided to the University by PennDOT. PennDOT provided as-built drawings from the 1960s for the 5.7-mile stretch of I-70 from the West Virginia border to Claysville interchange in Pennsylvania. These drawings contained plan views of the extent of work, typical sections, areas of cut and fill, logs from borings taken before construction, and select construction details. This information was used to characterize the native soil of the site. No information or details were provided regarding the construction of these embankments. As such, it must be assumed that the embankments were not constructed to modern standards and that the fill placed was not benched into the bedrock.

To further characterize the embankments in the area that was undermined in the winter of 2019, the as-built documents were supplemented with a soils report compiled by PennDOT based on 12 borings taken on the embankment slopes and 2-foot LiDAR contours obtained from the Pennsylvania Spatial Data Access (PASDA) database. There are two large embankments located

within the region undermined by Panel 15. The embankments were constructed at a 2:1 slope and range in length from 550-feet to 650-feet and range in height from about 70-feet to 85-feet. The soils report showed that the embankments were constructed of a granular fill composed of silt, sand, and gravel on a layer of alluvial material and weathered bedrock. The borings collected from these embankments confirm that the fill material was not benched or notched into the bedrock beneath it to prevent sliding.

Additional drawings were provided by PennDOT documenting the reconstruction of the roadway in the late 1980s. In this reconstruction, a 13-inch concrete pavement was placed on an open graded granular base (Figure 25). Skewed transverse joints were cut into the concrete 20-feet apart and were reinforced with 1.5-inch dowels. Tied concrete shoulders were constructed 8-inches thick adjacent to the lanes and tapered down 6-inches at the outer edge. The shoulders were tied to the travel lanes with #5 rebar spaced 30-inches on center. The pavement was constructed on an open graded granular subbase that was 8-inch thick in areas of cut and a 10-inch thick in areas of fill. This section of roadway was overlaid with 4-inches of asphalt prior to the undermining.

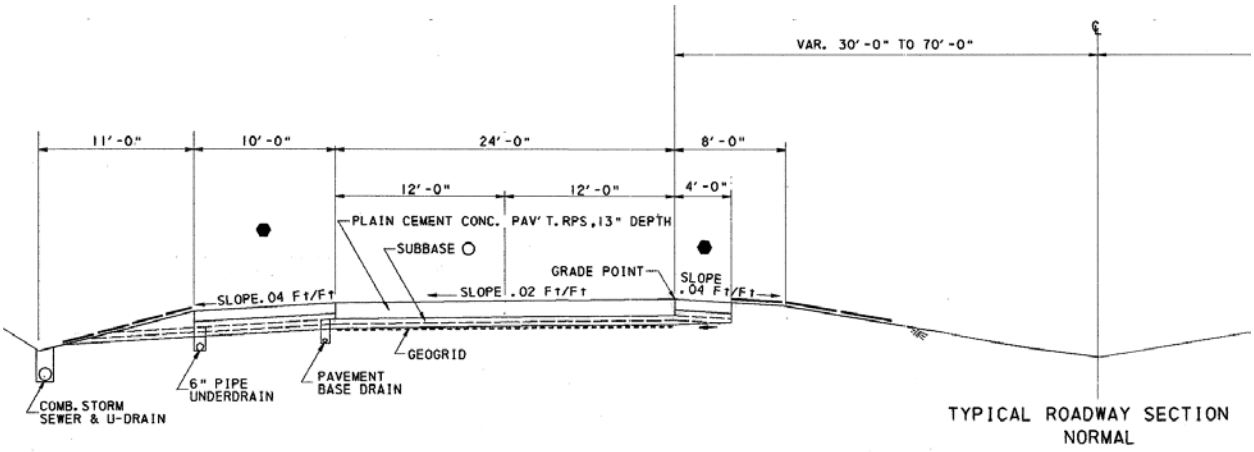

Figure 25 Typical cross section of I-70 from plans of 1980s highway reconstruction

The documents provided by PennDOT were supplemented with information gathered from the PASDA database. The location of Pennsylvania interstates and previously mined longwall panels were obtained from this database. Overburden data for the Pittsburgh Coalbed was also obtained from the PASDA database. It was determined that the rock between the highway and the Pittsburgh Coalbed consisted primarily of limestone and shale, as can be seen in Figure 26, meaning that it is composed of semi-competent hard rock (McCulloch et al., 1975).

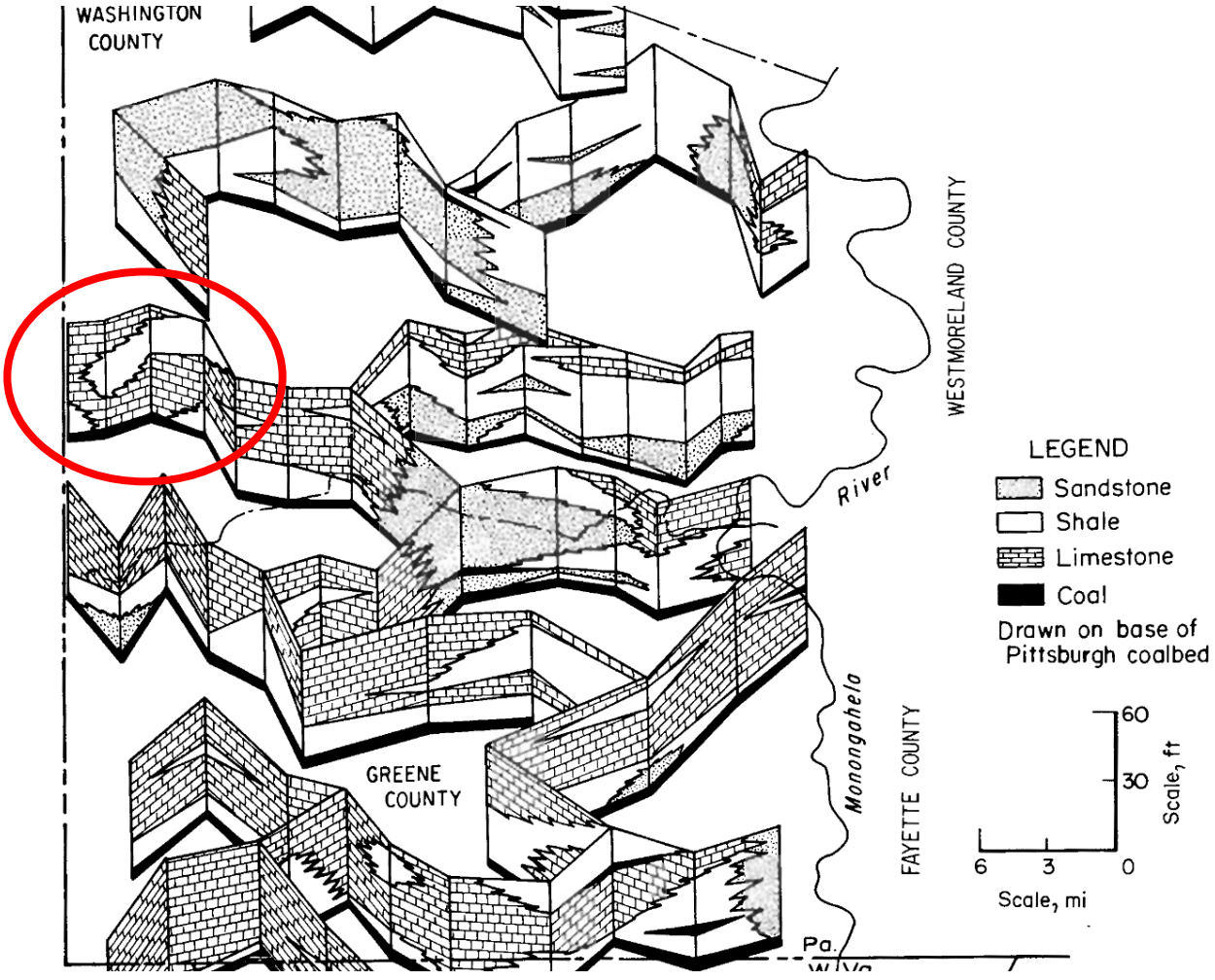

Figure 26 Overburden characterization above the Pittsburgh Coalbed

(McCulloch et al., 1975)

3.2 Field Visits

To accurately observe the impact of longwall mining on the highway, all the observations needed to be properly recorded. Field observations were made by the University once a week during the undermining period. Approximately half a mile of roadway was undermined above Panel 15 and the corresponding gateroads. During the undermining process, the outside lane of the road was closed, which allowed the University to safely use the shoulder to pull off the road. All inspectors made observations from the outside shoulder of the highway to ensure safety.

To ease in locating any signs of failure that may occur on the highway surface, the University of Pittsburgh staff utilized a grid system marked on the roadway. A simplified layout for the gridwork can be seen in Figure 27 below. The full layout shows that in each direction the road was separated into four categories: the inside shoulder, passing lane, travel lane, and outside shoulder. The layout also has cross gridlines that match the PennDOT stations of the baseline median alignment that were marked on the pavement. This allowed the inspectors to identify each feature and the location in which it occurred.

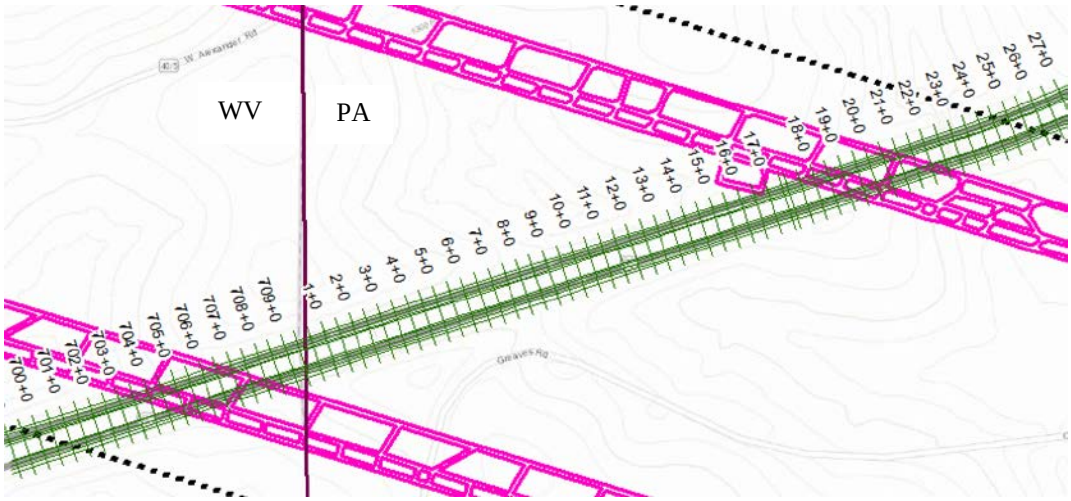

Figure 27 Gridwork on I-70 in study area

The inspectors carried a paper copy of the highway layout with the grid to the site. To the best of the inspector's ability, each sign of failure that was observed was sketched in the corresponding section on the paper grid. Typical forms of failure on the highway surface were described previously. Of these failures, the most common types that are caused by undermining are longitudinal cracking, transverse cracking, widening of contraction joints, compression bumps in the full-depth asphalt sections, blow-ups in the concrete shoulders, and lane-to-shoulder separation and drop-off. Special care was taken in sketching the observations to ensure that they were drawn to scale and in the correct location. Measurements were taken of the features documenting the width, length, height, and orientation as applicable and these measurements were labeled on the sketch. Pictures were also be taken of every feature sketched, ideally in a manner that captured the characteristics and location of the feature.

In addition to observing the road surface, the inspectors also inspected the slopes of the embankments. An inspector went down the slopes to monitor for any sign of increased wetness or slope instabilities. Signs of slope instability include bulges, tension cracks, and small scarps near the toe. Pictures were taken of any features that developed. Cut slopes were also observed for signs of instability during site visits, though only from the road surface as they could not be traversed.

After returning from the field, the inspectors downloaded the pictures taken of the highway and slope failures and scanned the paper grids with sketched features. The photographs were given descriptive names and archived so that they could be easily retrieved for future use. Photograph naming included the location and type of feature in addition to any measurements made to characterize the feature. Using the ArcGIS software, the features observed and recorded on the paper grid in the field were digitized.

3.3 Subcontractor Data Collection

3.3.1 Instrumentation

In preparation for undermining of I-70, a series of instruments were installed to monitor the behavior of the highway as the longwall face approached the study area. The behavior of the embankments was of particular interest and, as such, the instruments were placed primarily on the embankment slopes and the berm of the road. A total of 18 instruments were installed: nine (9) tiltmeters, six (6) inclinometers, and three (3) piezometers; however, only the tiltmeters and inclinometers will be discussed.

3.3.1.1 Tiltmeters

PennDOT subcontracted Earth Inc. to supply nine (9) tiltmeters in shallow boreholes to monitor the subsidence caused by Panel 15; eight (8) of the tiltmeters were located along the berm of the eastbound lane of I-70 and one (1) was located on the southern side of embankment #1, towards the bottom of the slope (Figure 28). As only eight (8) instruments were originally contracted for this project, on January 24th, 2019, the instrument from TM-1 was removed and installed in TM-9's location at the bottom of the southern slope. These instruments allowed for the examination of change in tilt that occurred at different points along the highway as the undermining took place.

Each tiltmeter was installed in a casing and suspended 3-feet below the surface. These tiltmeters are described as "in place inclinometers". Readings, including the time, temperature, degree of tilt, and millivoltage, were taken for each instrument every ten (10) minutes. Temperature readings were measured in Celsius and the degree of tilt and millivoltage readings

were measured in both the X and Y planes. The degree of tilt could vary +/- 12 degrees and reportedly had an accuracy of 0.005 degrees. The locations and axes orientation of the tiltmeters are shown below in Figure 28.

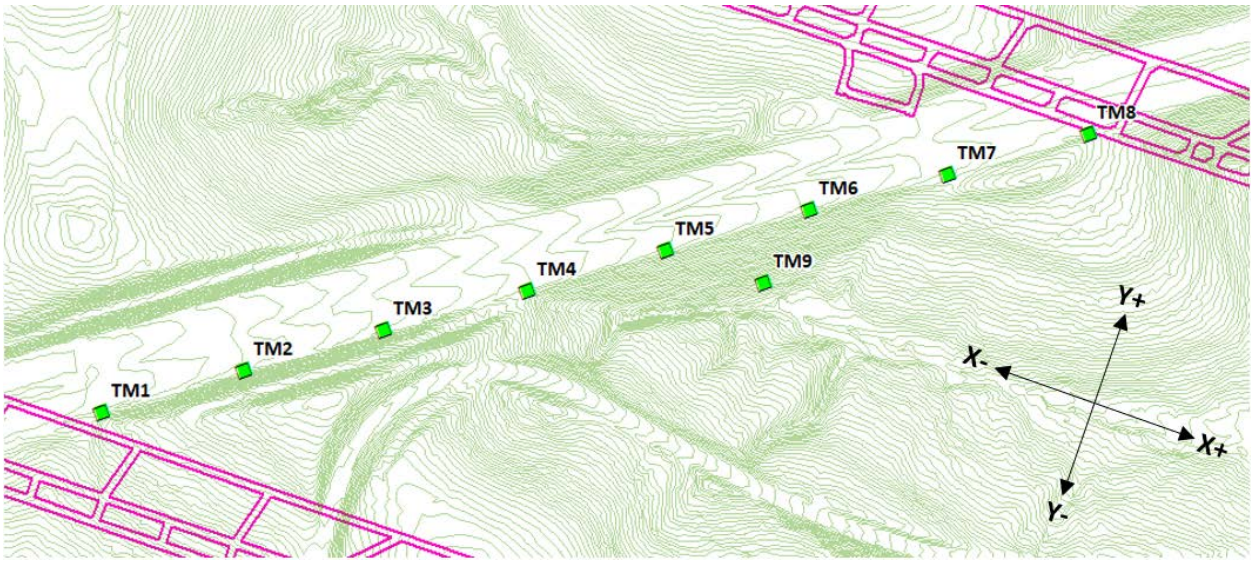

Figure 28 Locations and orientation of the tiltmeters within I-70 study area

TM-1 (TM-9) through TM-8 used the "Model 906 Little Dipper" model tiltmeters. TM-1 (TM-9) through TM-5 were an older version of the model, while TM-6 through TM-8 were a newer version of this same model. The tiltmeters were connected to one another and continuous readings were transmitted to a central data reader, which could be accessed remotely.

The software package Cambel Scientific (LoggerNet) was used by the tiltmeters and accessed the cell modem every 30 minutes to collect data. It contains a built-in alarm system to alert users via SMS text or email if there was more than 0.5 degrees of movement between readings. This could be altered to any point but, for the purposes of this project, the alert was set so that once the 0.5-degree alarm was triggered, the alarm trigger was increased to 1.0 degrees. Conversely, it could also alert users when the direction of tilt reversed.

Although the tiltmeters have not had data examined for the temperature impact, the specifications state that they can operate between -13 and 158 degrees Fahrenheit, meaning that variation in air temperature should not affect the accuracy of readings for this project.

All data gathered from the tiltmeters was put into a database, where the files were stored on a server with a local and offsite backup for storage and analysis. The data files were to be kept and analyzed to obtain the most critical results.

Due to a technology malfunction beyond the control of the University or PennDOT, data was lost for the older model of tiltmeters. The motherboard for the instrumentation to that was to be used to transmit the data in real time was stolen from the side of the highway. Though news of the theft was shared immediately, appropriate measures were not taken to collect the data from the instruments regularly. The older tiltmeters did not have the data storage capacity to keep all of the data between collections, so five of the tiltmeters lost two-weeks' worth of data recorded during the heart of the undermining; this data was overwritten and lost forever.

3.3.1.2 Inclinometers

PennDOT installed inclinometers in six boreholes within the study area and the PennDOT survey crews collected regular readings from these inclinometers throughout the undermining process. The RST Digital Inclinometer Probe, Model No. IC 35202 was used to take readings at these locations. These probes have an accuracy of +/- 0.1-in per 100-feet and can operate within +/- 30 degrees, and in temperatures ranging from -40 to 158 degrees Fahrenheit.

Figure 29 shows the locations and orientations of the borehole casings. Notice that the orientations differ based on their locations; TB-4 and TB-2 share an orientation, while TB-6, TB-8, TB-9 and TB-13 all share a different orientation. The orientation as installed shows the A+

direction pointing down the slope of the embankments and the B+ axis clockwise from the A+ orientation.

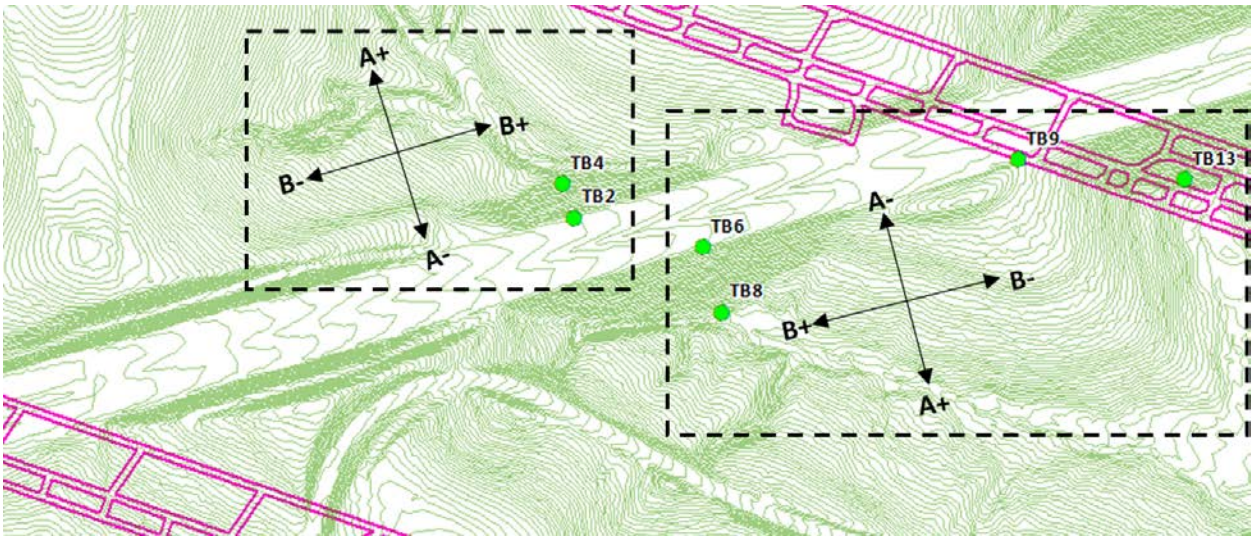

Figure 29 Locations and orientation of the inclinometers within I-70 study area

The installation of an inclinometer is a multi-step process. Inclinometers are installed in boreholes, that were drilled to collect soil samples. An inclinometer casing is placed into the borehole and the area surrounding the casing is backfilled with granular material. This set up allows the casing to deform due to movement in the soil layers, as seen in Figure 30.

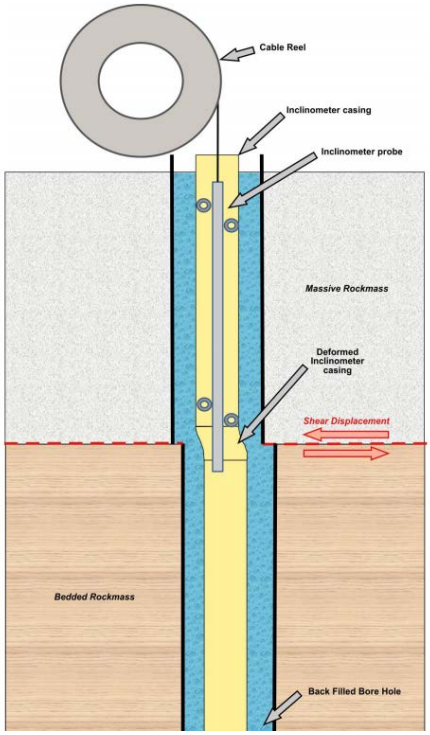

Figure 30 Schematic view of inclinometer casing and inclinometer probe

(Diagle and Mills, 2017)

Proper installation of the inclinometer casing attempts to align one set of grooves in line with the axis of expected movement. This set of grooves is referred to as the A axis. The perpendicular set of grooves is the B axis. For this site, movement was expected to run outward from the slope, so the A+ direction pointed down each instrument's respective slopes. The B+ axis ran along the slopes, clockwise from the A+ direction. To take a reading, the inclinometer was placed in the A axis groove and was lowered to the bottom of the hole with the wheels facing the A+ direction, as shown in Figure 31. The probe was then raised in 2-feet increments, with readings taken at each increment; at each position, the probe was stabilized before accepting the inclination reading. Results were accepted once the probe reaches the top. Once lifted to the top of the hole, the probe was reversed and the process was repeated in the A-, B+, and B- directions.

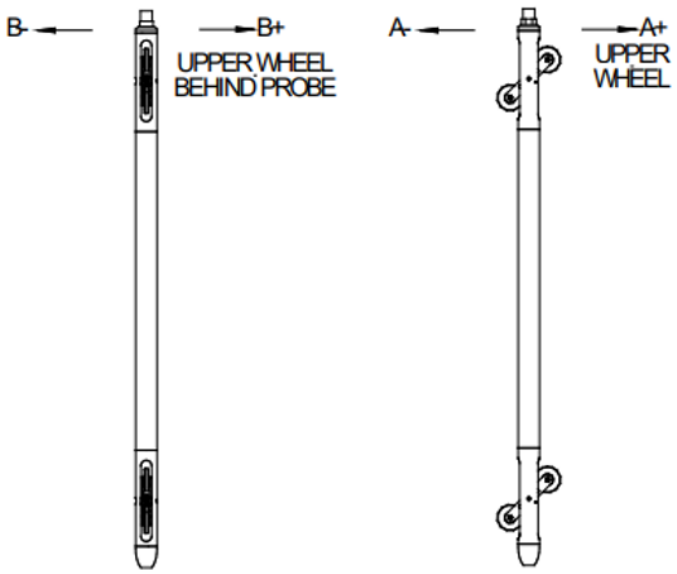

Figure 31 Upper and lower wheel diagram

(*RST*, 2019)

Readings collected from the inclinometer probe are deviations from the vertical over the distance between the upper and lower wheels, as can be seen in Figure 32. The deviation measurements for each reading were taken in feet and calculated Equation 3-1 (RST, 2019).

$$D = L * \sin(\alpha) \quad \textbf{[3-1]}$$

where: L = inclinometer probe length
α = inclination angle of probe from vertical axis

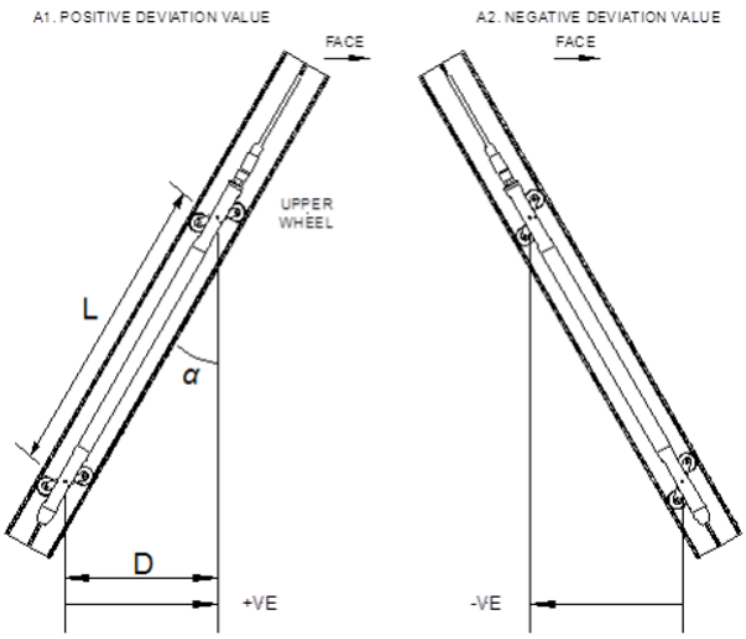

Figure 32 Sign convention in the A-axis and deviation D measured by the inclinometer probe (*RST*, 2019)

These results were recorded on the portable instrument and were transferred to PennDOT's equipment calibration log in the office. They were then supplied to the University for analysis.

3.3.2 Monitoring Movement of Ground Surface Through Surveys

When Panel 15 undermined I-70, ground movement occurred in all three dimensions due to the subsidence. To monitor this movement, a series of surveys including highway alignment surveys, slope surveys, and LiDAR surveys were employed.

3.3.2.1 Highway Alignment Surveys

The PennDOT survey crews tracked the movement of the highway alignment throughout the undermining process. This monitoring was necessary to redefine the highway's position once

subsidence had concluded. The centerline alignment was staked for approximately 3,500-feet with 2,600-feet in Pennsylvania and 900-feet extending into West Virginia. The alignment was offset 62-feet right and left to create the two baselines with over 140 points along the alignment to be monitored. The location of the points surveyed can be seen in Figure 33.

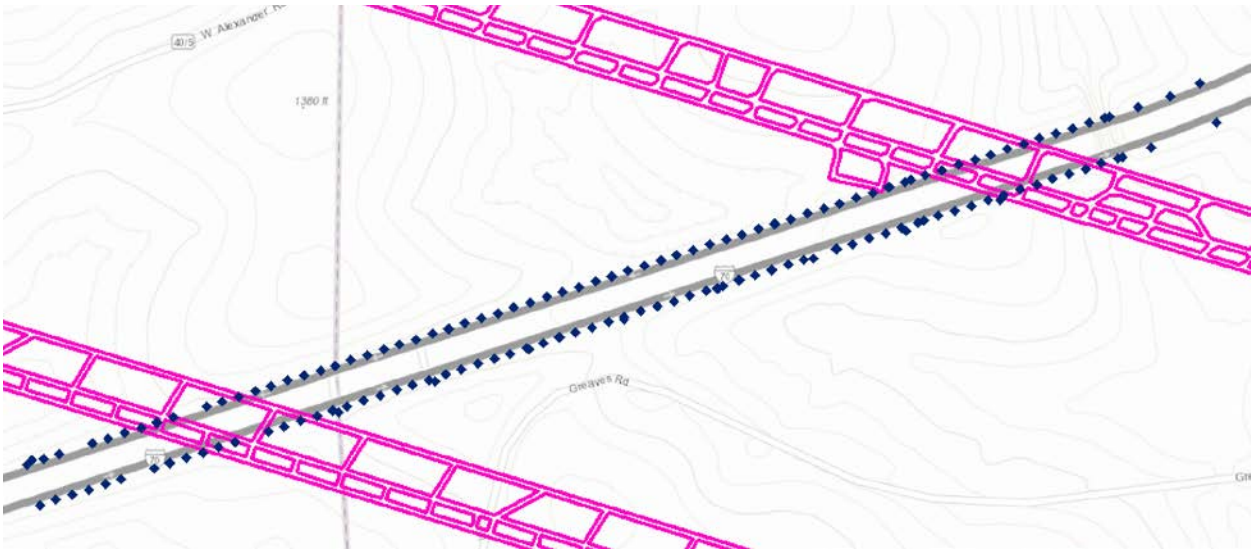

Figure 33 Points monitored by highway alignment surveys

This set of points was surveyed regularly during the undermining, for a total of 11 contracted monitoring surveys. PennDOT's survey crew performed 3D surveys using a Trimble R10 GPS unit with Virtual Reference Station (VRS) methodology. For this methodology, observational data was created from the data of surrounding, imaginary reference stations as though it had been observed by a GPS receiver. Vertical control was added using existing benchmarks and a differential leveling technique. This combination of survey techniques resulted in a horizontal accuracy of 0.02-feet and a vertical accuracy of 0.05-feet to 0.10-feet. The data collected through these surveys was provided to the University of Pittsburgh and utilized to characterize the behavior of the road surface's behavior resulting from undermining.

3.3.2.2 Surveys of Cut Slopes and Embankments

PennDOT subcontracted SPK Engineering to monitor the movement of the cut slopes and embankments within the study area being undermined by Panel 15. The locations of over 590 points were collected twice a week to monitor the behavior of the slopes as the longwall panel undermined the road. These points were categorized into 11 survey stake groups, as can be seen in Figure 34.

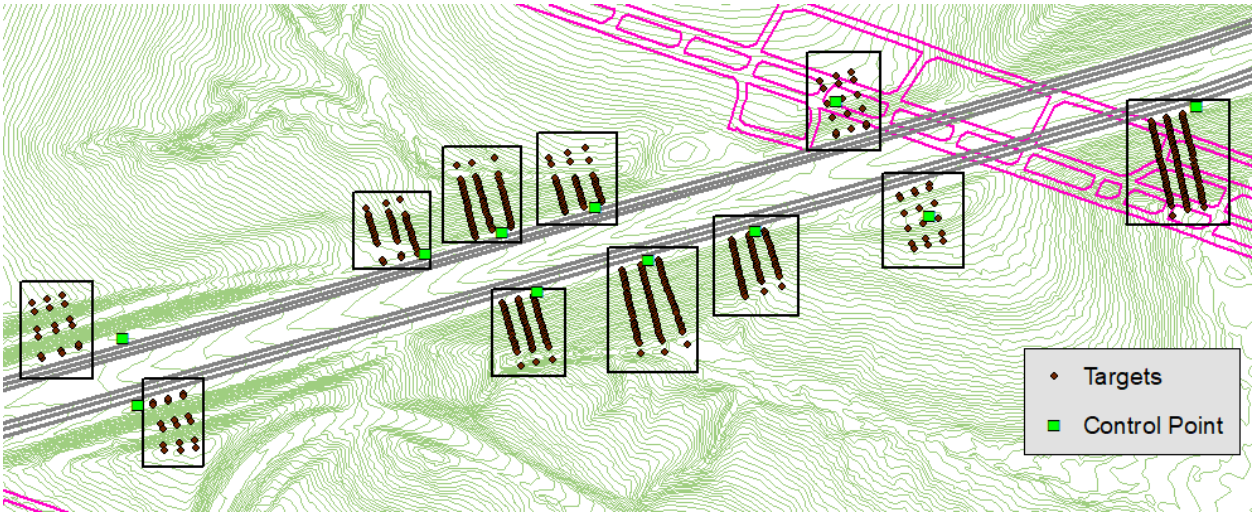

Figure 34 Points monitored by surveys of cut slopes and embankments

SPK Engineering utilized a Total Station to obtain angles and degrees from control points to the target points on the slopes. A Total Station utilizes trigonometry and triangulation to determine the location of surveyed points relative to a known point. There were 11 control points, or traverse points, located both inside and outside of Panel 15 that were used as known points to locate the other 590 target points. The horizontal location of these control points was identified using GPS and the elevation was determined using an engineer's level before each survey was performed. Though the GPS precision was approximately 0.026-feet, the elevation precision was

approximately ±0.01-feet, and the Total Stations were accurate to ±0.02-feet, the surveys generated combining both methods were only accurate to ±0.05-feet. The data gathered from these surveys by SPK Engineering was provided to the University of Pittsburgh as it was collected and was used to characterize the behavior of the slopes and embankments resulting from subsidence.

3.3.2.3 LiDAR Surveys

PennDOT contracted T3 Global Services to monitor the movement of the road surface as I-70 was undermined. T3 Global Services subcontracted ESP Associates to collect data and images to generate an engineering grade topographic survey. ESP deployed a Riegl VMX-1HA mobile LiDAR device based in Indianapolis to monitor this movement. This system was equipped with two (2) Riegl VUX-1HA laser scanners, a POS LV 610 INS, and four (4) 5 mp Riegl cameras.

Using this mobile LiDAR unit, the positions of millions of points were collected each time the road was driven. There were ten (10) LiDAR scans contracted to be performed for this study. The data from these scans was processed using Riegl RiProcess. RiProcess uses plane to plane matching in conjunction with POS data to calculate errors in the POS solution to establish the most probable location for the LiDAR data. This was then used to analyze the provided control to search for potential blunders in the provided control points. Once the LiDAR and control data were found to be consistent, the control points were held as fixed and RiPrecision was run to finalize the alignment of the LiDAR data to the controls.

For the scans of the highway alignment, the control points were located using the traverse method of land surveying. The traverse method uses a series of lines with predetermined and measured lengths to connect various points at determined locations. These traverse lines can be open or closed and can move easily around uneven terrain or obstacles. By using this method of control point surveying, T3 Global Services determined the LiDAR scans have an accuracy of

0.016-feet to 0.033-feet (5-mm to 10-mm) in the horizontal plane and 0.016-feet (5-mm) in the vertical plane.

T3 Global Services provided the University of Pittsburgh the LiDAR surveys at the conclusion of the contract. This data was used in conjunction with the highway alignment surveys to characterize the behavior of the road surface. Additional accuracy was maintained in the horizontal plane so that the University of Pittsburgh could analyze the change in movement and strains between concrete contraction joints.

3.4 Other Sources of Data

In addition to information collected in the field and by the PennDOT subcontractors, the University gathered information through direct communications with involved parties. Throughout the undermining process, the University communicated regularly with the Tunnel Ridge Mining company. These communications provided a range of information including the exact parameters of Panel 15 and the progression of the longwall face. Based on the information provided, the University was able to determine that the longwall face progressed at an average rate of 115-feet-per-day.

The University also communicated regularly with PennDOT and were provided information in addition to the construction drawings of I-70. They were able to answer clarifying questions about the construction drawings and the data collected by the subcontractors. Additionally, PennDOT took cores of the pavement after the undermining completed, which were provided to the University for observation.

3.5 Limitations of Data Collected

Despite the best intentions, there are some concerns with the collected data. As all of the observations made on the highway were made from the shoulder, much of the observed damage was seen across the travel lanes and through passing vehicles. This made it nearly impossible to precisely locate and measure much of the damage. The observations were then digitized, which inherently added another layer of potential error to the observed features.

The data collected through the instruments also have potential error. Due to the limited number of instruments installed for the undermining process, it was difficult to tell when data collected was accurate and identify trends. Only two inclinometers were installed on each slope, making it difficult to characterize what happened in the middle of the slope or along a different cross section. Additionally, only three of the eight tiltmeters successfully collected data during the undermining, meaning that an opportunity for pattern and trend recognition was lost.

The survey data inherently has a significant amount of error. The surveys were completed by three different subcontractors that did not coordinate with each other. As a result of this lack of coordination, the surveys did not share any control points that could be used to compare the data. In addition, the surveys are each only accurate to between about 0.5 and 1.0-inches. Though individually this accuracy would be sufficient, when comparing the datasets, the accuracy compounds; this means that when the data between surveys are compared the small movements are within the margin of error of the data. As each dataset has error, the compounded error between datasets makes it difficult to compare the various types of data collected.

4.0 Data Collected during Undermining of I-70

4.1 Survey Data throughout Study Area

Regular surveys were conducted throughout the undermining process. A total of 147 points along the highway surface were surveyed by PennDOT's surveyors 11 times during the undermining event. These points were based on the center highway alignment and were offset 62-feet to be located in the shoulder of the highway. These surveys had a horizontal accuracy of 0.02-feet and a vertical accuracy of 0.05-feet to 0.10-feet. An additional 590 points located on the embankment and cut slopes were surveyed by SPK Engineering to characterize the movement of the slopes. The SPK surveys are accurate to between 0.03-feet and 0.04-feet in both the horizontal and vertical planes.

4.1.1 Final Subsidence Basin Movement

Traditionally, a supercritical longwall subsidence basin is bathtub shaped. The panel subsides symmetrically along the long and short axis. The ground surface at the center of the panel drops by the maximum vertical subsidence and then slopes up to the original ground elevation beyond the longwall panel. As a result of this extension and bending of the ground surface, the points on the surface move on the horizontal plane towards the center of the longwall panel.

4.1.1.1 Vertical Subsidence

Survey data was compiled from the highway alignment points and the slope points. These points can be analyzed to determine the final subsidence of the highway surface and the adjacent slopes. Figure 35 shows the final subsidence throughout the study area. As can be seen in this figure, the majority of subsidence occurred over the central embankment on the highway surface.

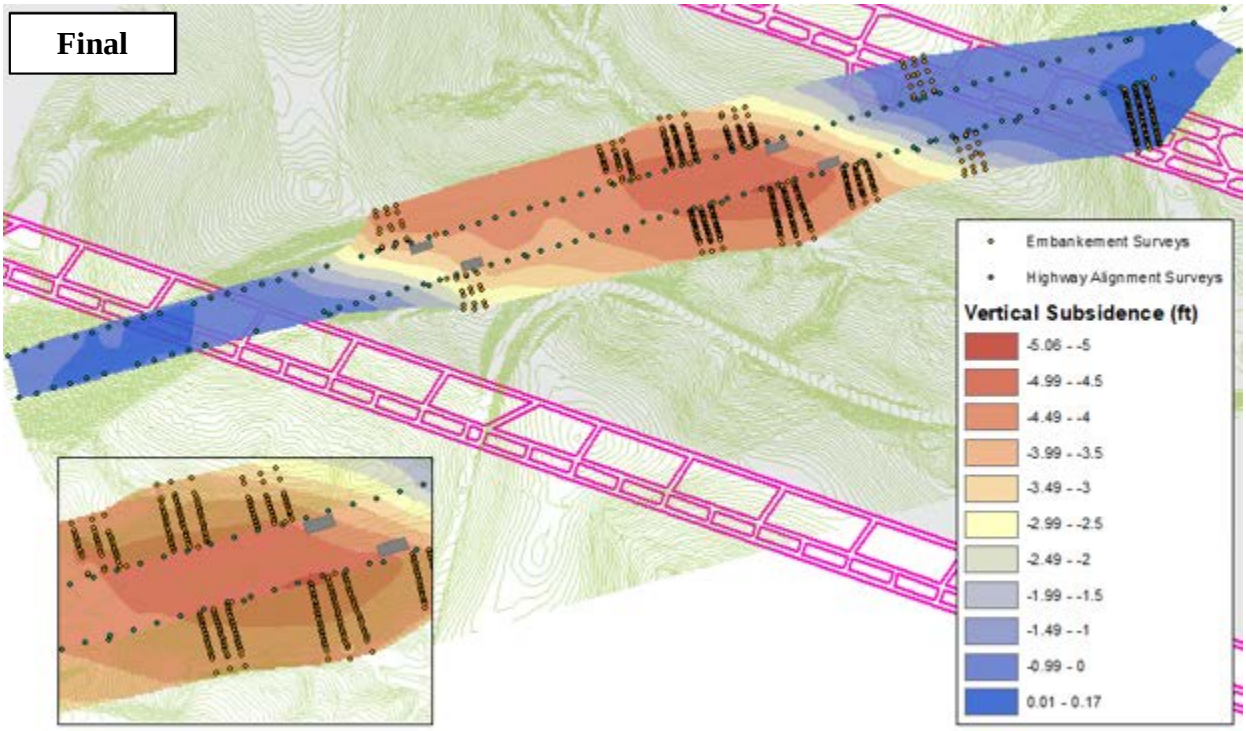

Figure 35 Final vertical subsidence of I-70 caused by mining of Panel 15

4.1.1.2 Horizontal Movement

The highway alignment and slope points can also be combined to analyze the movement of the study area in the horizontal plane. Figure 36 shows the final horizontal movement throughout the study area. This figure shows the magnitude and direction of horizontal movement of the points surveyed during the undermining. The maximum horizontal movement was observed

at the bottom of the northern slope of embankment #1. The point at this location moved over 2-feet north in the horizontal plane, which indicates movement out from the slope.

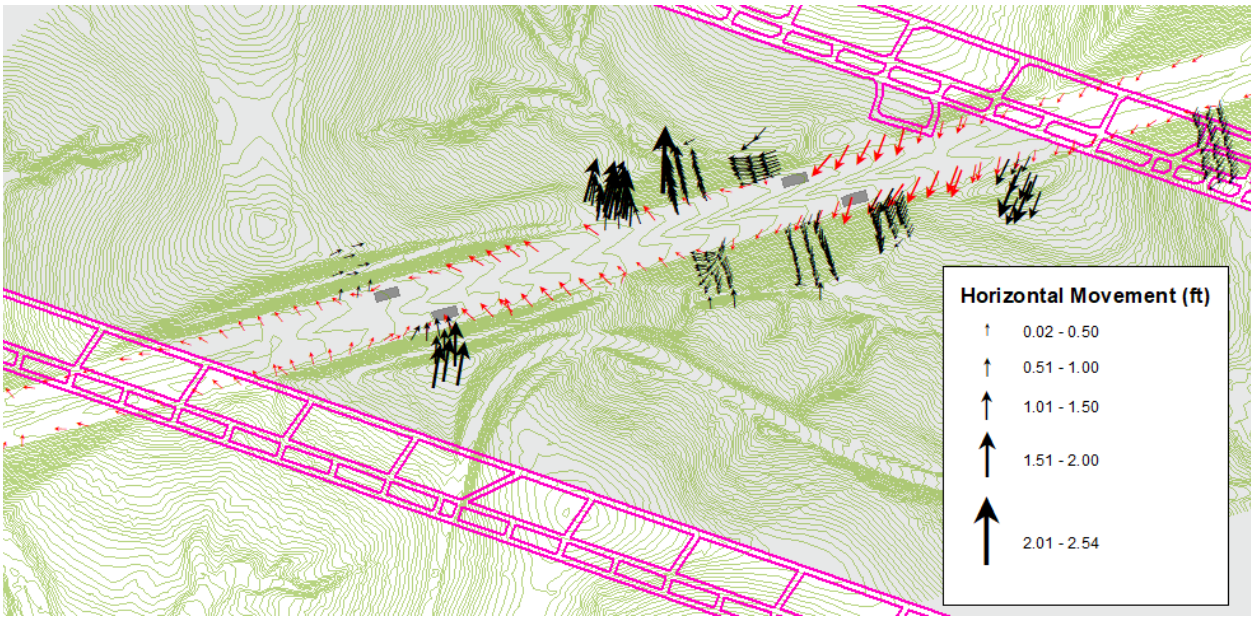

Figure 36 Final horizontal movement of I-70 caused by the mining of Panel 15

Overall, more horizontal movement was observed on the slopes than on the highway surface. The western side of northern slope of embankment #1 moved primarily in the north-northeast direction at large magnitudes, showing that the embankment slope was moving outwards from the core of the embankment. Though this movement was not towards the center of the basin, it can be explained by a spreading phenomenon of the embankment when subjected to subsidence. The opposite side of the embankment also showed movement primarily moving outward from the core of the embankment, but at significantly lower magnitudes. This indicates that more spreading occurred on the northern slope than the southern slope of the embankment.

Unlike the central embankment, the movement of the cut slopes and embankment #2 are more typical of a traditional subsidence basin. These points moved horizontally towards the center

of longwall panel. The points on the southern cut slopes move at larger magnitudes, between 1.5-feet and 2-feet, due to the ground surface sloping from the original elevation to the final subsidence elevation at these locations. This indicates that without the presence of the embankment, the ground likely would have performed as a typical, well-behaved subsidence basin.

The highway surface experienced less horizontal movement than the slopes, with a maximum movement of around 1.5-feet observed. The eastern side of highway experienced the most horizontal movement, which was oriented primarily towards the center of the subsidence basin. This direction of movement is typical of a traditional subsidence basin. This movement dissipated at the eastern asphalt relief sections at the edge of embankment #1, which absorbed the excess movement. The movement over the embankment was minimal and in no specific orientation. The highway surface adjacent to cut slope #1 to the east of the western asphalt relief sections also experienced significant movement. These points moved primarily in a north-west orientation at a magnitude between 0.5-feet and 1-foot. The western asphalt relief sections also dissipated the horizontal movement, causing minimal movement at the western most edge of the study area.

The direction of movement of the highway surface adjacent to cut slope #1 is not typical for subsidence basins. When looking only at the magnitudes and directions of all of the movement of the highway surface (Figure 37), it appears that the pavement structure is twisting throughout the study area. Rather than both extents of the highway moving towards the center of the panel, the eastern side of the highway moved towards the center of the panel and the western side of the highway moved parallel to the gate roads towards the longwall face. The pivot point appears to be over the central embankment, indicating that the granular fill material may have absorbed movement and facilitated the twisting.

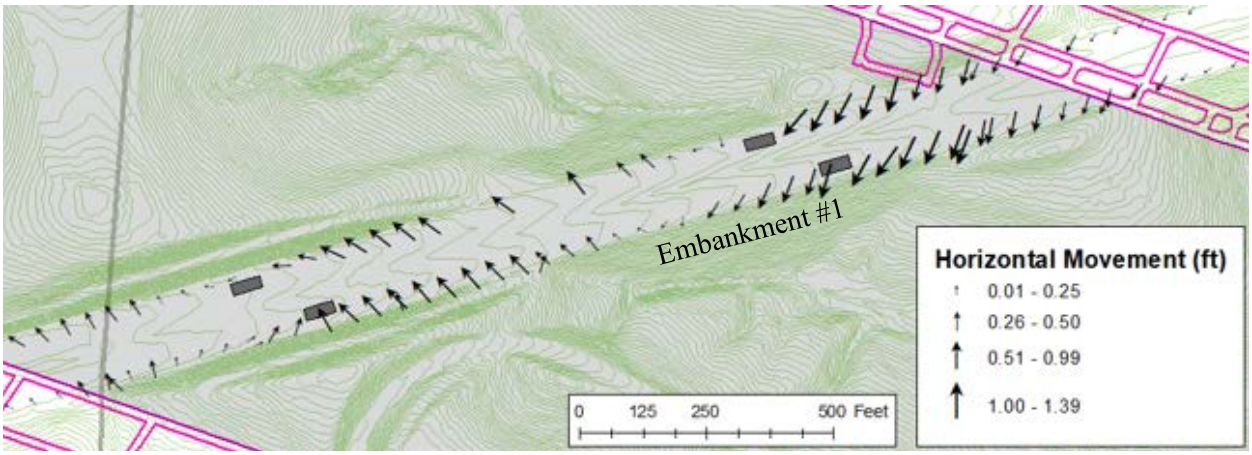

Figure 37 Final horizontal movement of I-70 on the highway surface caused by the mining of Panel 15

4.1.2 Ground Movement caused by Dynamic Subsidence

As longwall mining occurs over time, the subsidence basin forms gradually in a dynamic wave. The dynamic subsidence wave subjects the ground first to tension beyond the face and between the longwall face and the inflection line and then to compression behind the inflection line (Figure 9). This gradual change causes the surface to experience horizontal stresses and strains at different magnitudes and locations than represented by the final subsidence event.

Panel 15 was mined at an average rate of 115-feet/day and was beneath the highway for about a month. The longwall operated on a standard schedule, meaning it did not extract coal on the weekends. There was one unscheduled shutdown day when the panel was underneath I-70.

4.1.2.1 Vertical Subsidence over Time

As the longwall face progressed, the ground surface subsided vertically and the ground surface moved gradually as the longwall basin formed. The surveys collected weekly show the

progression of the vertical subsidence basin as the longwall face progresses, which can be seen in Figure 38 through Figure 41.

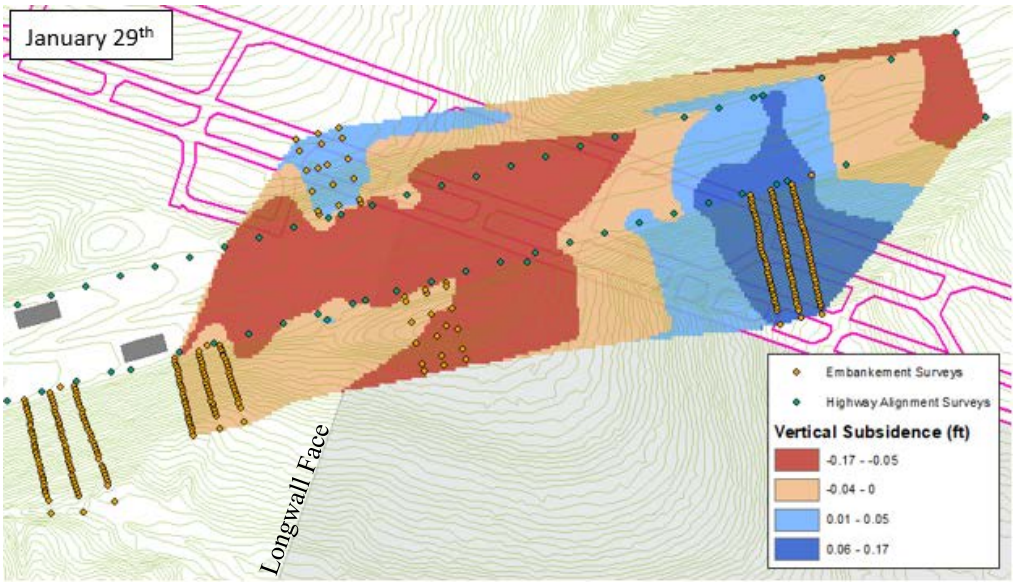

Figure 38 Vertical subsidence on January 29th

Figure 38 shows very small movements as the longwall face begins to influence the interstate. Up to 0.17-feet of heave was observed over embankment #2 and up to 0.17-feet of vertical subsidence was observed on the eastern-most portion of the highway alignment. The majority of the movement observed is likely due to noise in the surveys.

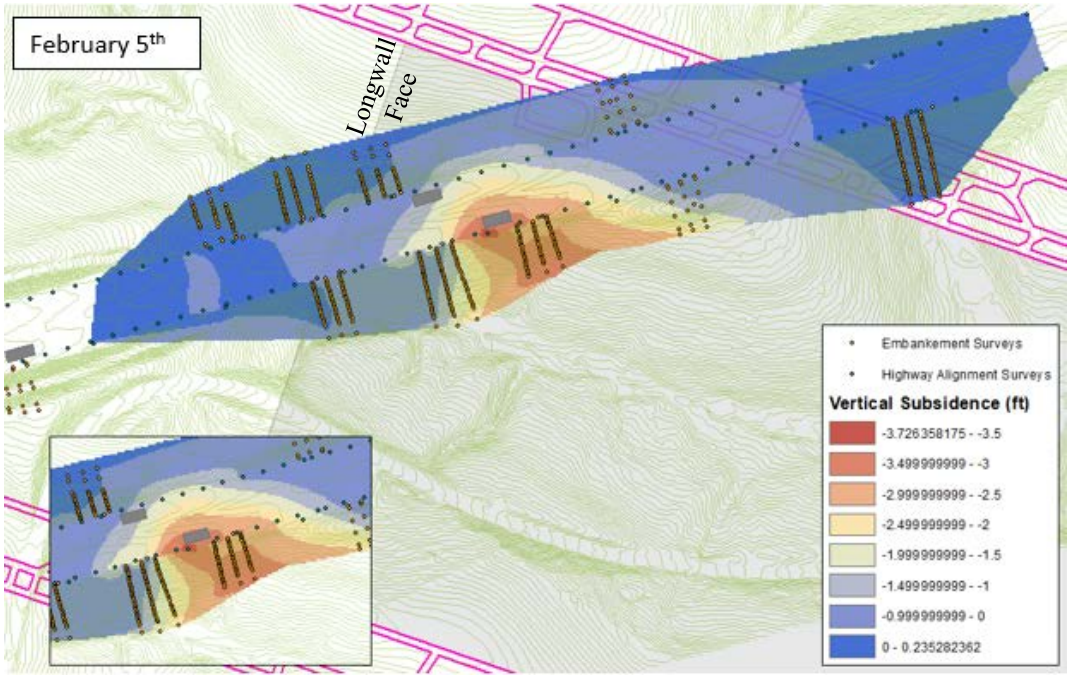

Figure 39 Vertical subsidence on February 5th

Figure 39 shows the vertical subsidence when the longwall face was below embankment #1. This shows the maximum subsidence of about 3.75-feet at the top of the south slope of embankment #1, occurring about 300-feet behind the longwall face. No point in the study area had reached the maximum predicted subsidence at this point in time. This is due to the fact that the points far enough behind the longwall face to drop to the maximum allowable subsidence are too close to the gateroads to experience this maximum drop in surface elevation.

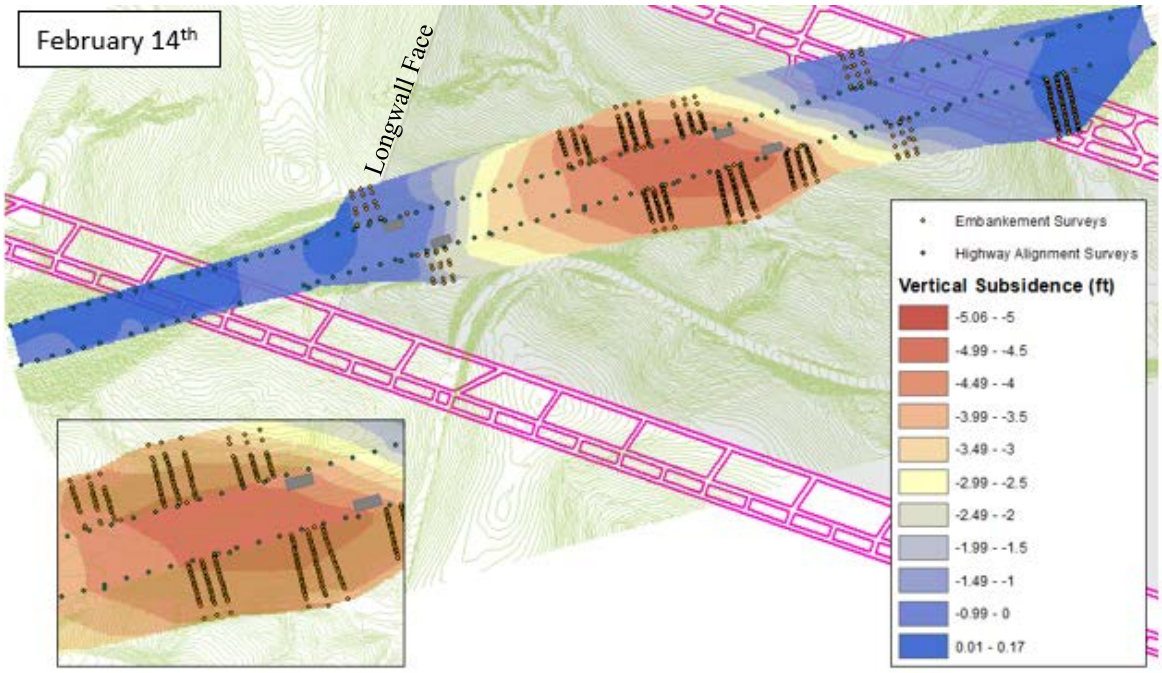

Figure 40 Vertical subsidence on February 14th

Figure 40 shows the vertical subsidence when the longwall face was just beyond the western asphalt relief sections. At this point in time, a maximum subsidence of about 5-feet was observed over the center of the embankment. The embankment was approximately 650-feet behind the longwall face on February 14th. The entire embankment subsided over 4.5-feet. It can also be seen that the change in surface drop between the gate road and the maximum subsidence occurs in a shorter distance on the eastern side of the study area than the western, meaning the slope is steeper on the eastern half of the study area.

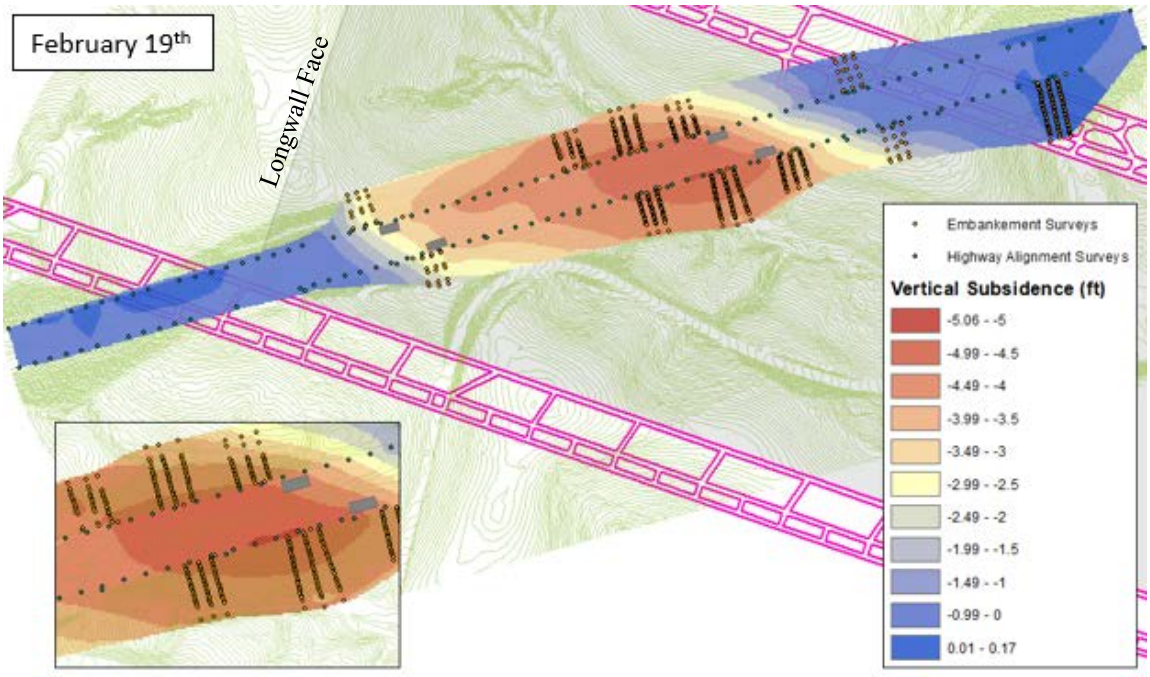

Figure 41 Vertical subsidence on February 19th

Figure 41 shows the vertical subsidence when the longwall face was at the end of the highway section. This shows a small area of maximum subsidence of just over 5-feet at the top of the south slope of embankment #1, occurring about 1,200-feet behind the longwall face. By this point in time, the slope on the western side of the study area is closer to that on the eastern side, making the subsidence basin more symmetrical throughout the panel. It is also worth noting that small amounts of heave were observed over the gateroads of the panel.

4.1.2.2 Horizontal Movement over Time

As the longwall face progressed, the ground surface also moved horizontally. The surveys collected weekly show the progression of the horizontal movement of the subsidence basin as the longwall face progressed, which can be seen in Figure 42 through Figure 45.

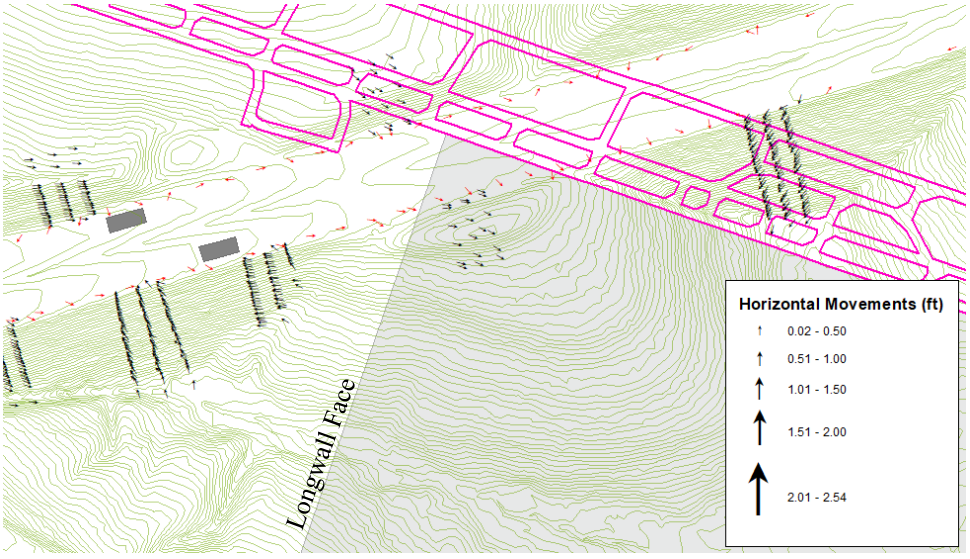

Figure 42 Cumulative horizontal movement on January 29th

Figure 42 shows the horizontal movement on the eastern portion of the study area on January 29th. As the longwall face just started to influence the interstate at this point, the horizontal movements are very small, less than 0.5-feet in any direction. The movement is generally oriented into the subsidence basin.

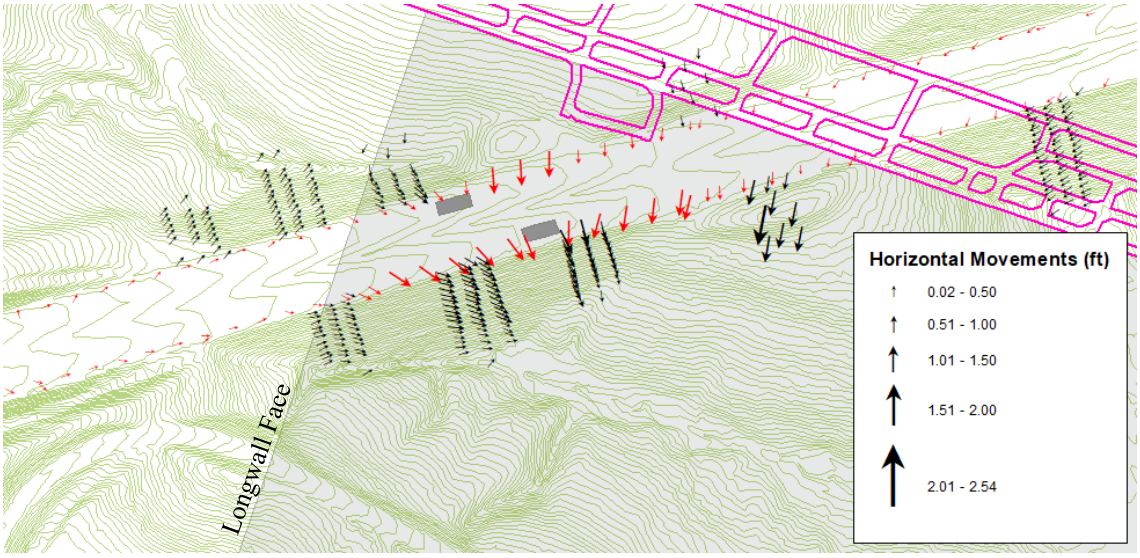

Figure 43 Cumulative horizontal movement on February 5th

Figure 43 shows the cumulative horizontal movement of the ground surface on February 5th, when the longwall face was beneath the central embankment. At this point in time, most of the points along the embankments experienced minimal movement, with magnitudes of less than 1-foot. The cut slope nearest to the gateroads experienced larger movements, with magnitudes of almost 2-feet, oriented towards the center of the longwall panel. This section of highway also experienced significant horizontal movement, with magnitudes around 1.5-feet, oriented towards the center of the longwall panel. These movements on the highway surface are dissipated at the asphalt relief section, causing there to be minimal movement beyond the longwall face.

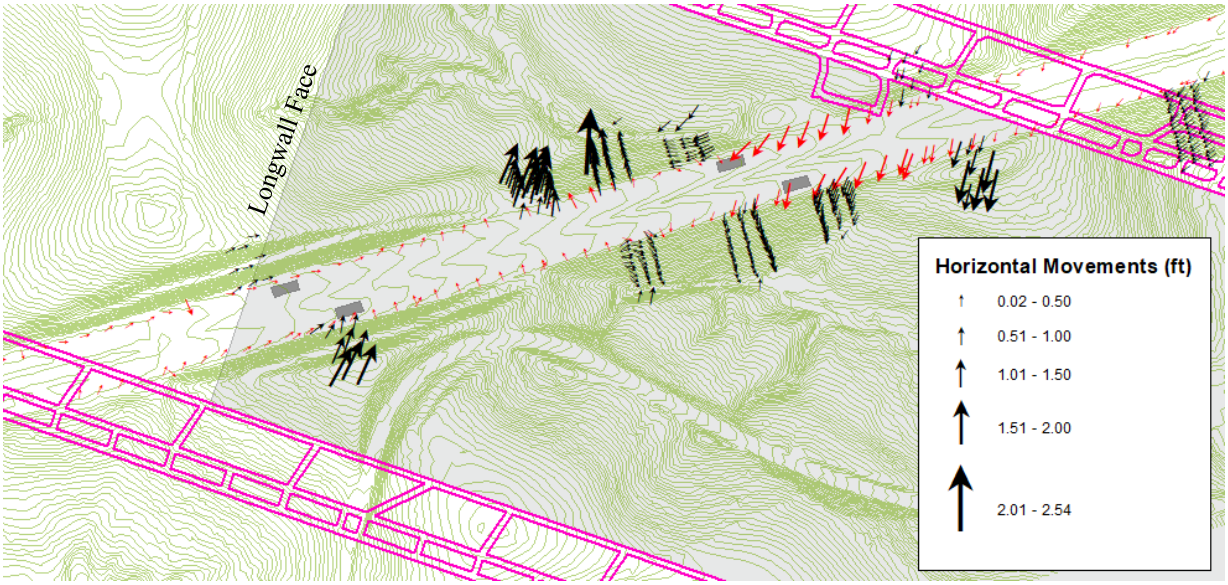

Figure 44 Cumulative horizontal movement on February 14th

Figure 44 shows the cumulative horizontal movement of the ground surface on February 14th, when the longwall face was just past the western asphalt relief sections. At this point in time, some of the slopes within the study area had begun to experience significant movement. The northern slope of embankment #1 moved away from the center of the embankment, with

magnitudes as high as 2.5-feet. These movements are larger than and in a different orientation than that which would typically be expected on a longwall panel, but this is likely due to spreading of the embankment. Like on February 5th, the eastern side of the highway surface experienced horizontal movements with magnitudes around 1.5-feet that are oriented towards the center of the longwall panel. These movements are dissipated at the asphalt relief sections, causing there to be very minimal movement west of these relief sections.

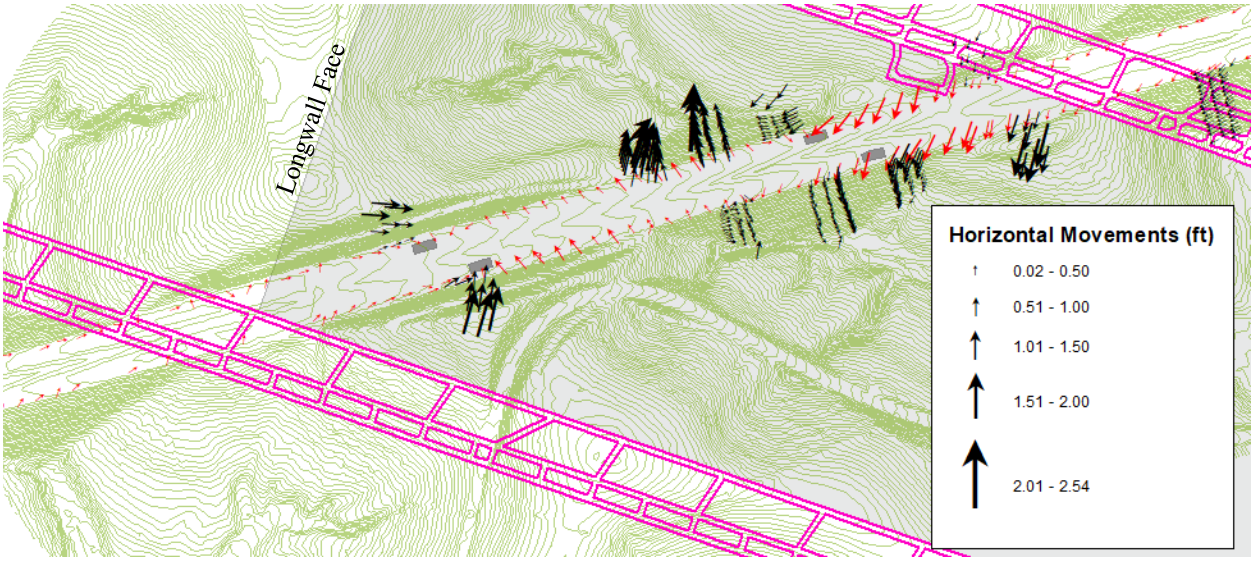

Figure 45 Cumulative horizontal movement on February 19th

Figure 45 shows the cumulative horizontal movement within the study area on February 19th when the longwall face was at the end of the area of highway influence. At this point in time, most of the slopes within the study experienced significant movement. The northern western cut slope moved away from the longwall face with magnitudes of movement up to 1.5-feet. The movement of the remainder of the slopes remained mostly unchanged from that observed on February 14th. The movement observed on the highway surface had magnitudes of up to 1.5-feet on the eastern side of the study area oriented towards the center of the basin and up to 1-feet on

the western side of the study area oriented towards the longwall face. These movements were dissipated at the asphalt relief sections, causing the areas just west of the asphalt relief sections to experience minimal horizontal movement.

The horizontal movements can also be examined incrementally between surveys. The incremental movements can be seen in Figure 46. As this figure shows, the eastern side of the highway surface experienced the majority of movement between January 29th and February 5th, when it was about 150-feet behind the longwall face. The western side of the highway surface experienced the majority of movement weeks later between February 19th and March 7th, when the longwall face was far beyond the movement area. It is also worth noting that between February 5th and February 14th, there was significant change in the direction of the horizontal movement adjacent to the southern slope of embankment #1. Embankment #1 experienced the majority of movement between February 5th and February 14th, when the longwall face was approximately 550-feet beyond the embankment. The western cut slopes each experienced the majority of movement when the longwall face was approximately 250-feet past the points. By looking at the movements of the surface incrementally, it is evident that the progression of the longwall face has a significant impact on the horizontal surface movements.

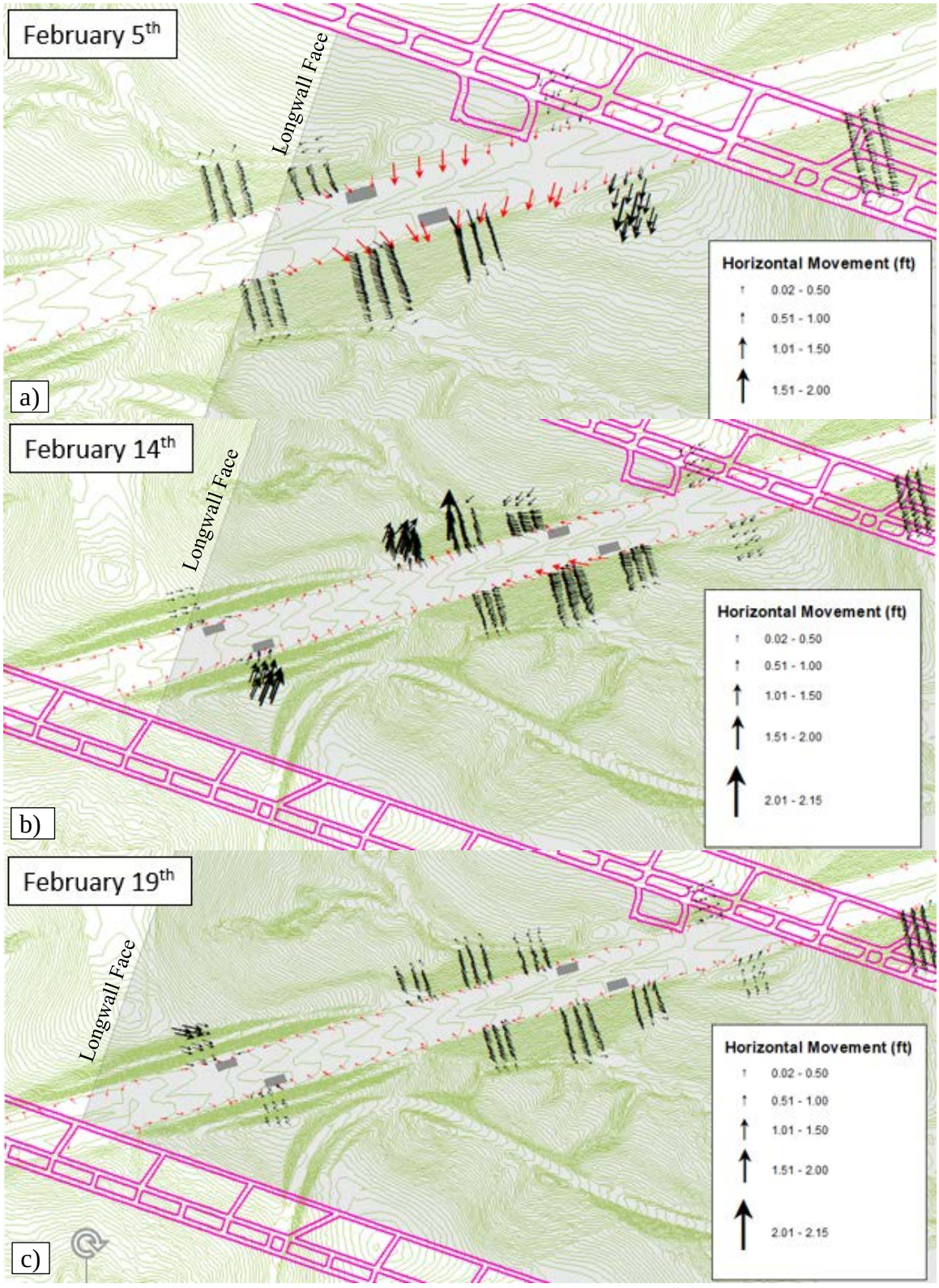

Figure 46 Incremental horizontal movement throughout study area influenced by undermining

4.2 Reaction of Roadway to Mining

4.2.1 Observational Data

Throughout the undermining of I-70 by Panel 15, the University visited the site weekly to observe the condition of the pavement surface. The failures of the pavement observed during these visits were recorded in the field and then digitized in ArcGIS. There were eight types of failures observed during these site visits. It is worth noting that the pavement surface in Pennsylvania was overlaid with asphalt shortly before the mining occurred, so it was devoid of any failures prior to the effects of subsidence.

The following types of failures occurred on the pavement surface:

- Transverse cracks – cracks that are predominately perpendicular to the pavement centerline
- Longitudinal cracks – cracks that are predominately parallel to the pavement centerline that tended to occur above the lane-shoulder joint
- Blow-ups – localized upward movement (buckling) of the pavement surface caused by large in-plane pressure buildup in the concrete slab.
- Compression bumps – Large transverse bumps in the asphalt created by high in-plane pressure build-up in regions with full-depth asphalt
- Shear failures – cracks that formed along the lane-shoulder longitudinal joint that are caused by shear forces generated when the mainline expanded/contracted at different rate than the shoulder.
- Widened contraction joints – the opening of transverse contraction joints
- Separations – the widening between the edge of the slab and the soil adjacent to the structure

- Guiderail deformations – shear or compression failure of guiderail due to movement of pavement surface

The longwall face was mined five days a week and progressed at an average rate of 115-feet/day, meaning that in a week it progressed about 575-feet. The longwall mine first interacted with the highway when the face was adjacent to the gateroads below the interstate on January 25th. A summary of the damage observed can be seen in Table 9, and detailed accounts can be seen in the sections that follow.

Table 9 Summary of damage observed on highway through undermining

Date	Distance of highway impacted (ft)	Types of damage observed
January 29	N/A	Open joints
February 5	1,450	Widened contraction joints, transverse cracking, shear failures, longitudinal cracking, compression bumps, and separations between the pavement and adjacent soil
February 14	1,900	Transverse cracking, longitudinal cracking, shear failures, compression bumps, blow-ups, widened contraction joints, displaced guiderails, and separations between the pavement edge and the adjacent soil
February 19	2,000	Transverse cracking, longitudinal cracking, shear failures, compression bumps, blow-ups, widened contraction joints, displaced guiderails, and separations between the pavement edge and the adjacent soil
February 26	2,400	Small transverse cracks and widened contraction joints
March 5	All	N/A

4.2.1.1 January 29th

The observed distresses on the highway surface were first seen on January 29th when the panel first crossed beneath the highway. During this visit, four contraction joints at the edge of the study area began to open from the subsidence forces. These contraction joints were located

over the edge of the gate roads approximately 250-feet behind the longwall face. The location of the observed features can be seen in Figure 47.

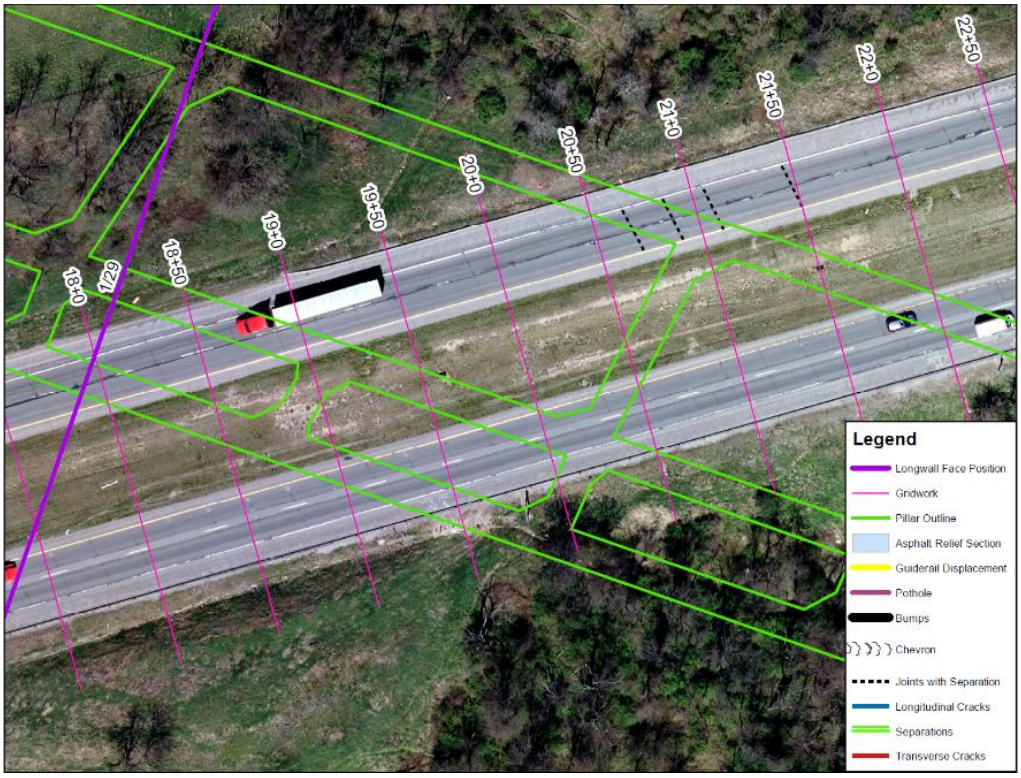

Figure 47 Pavement features observed on January 29th

4.2.1.2 February 5th

The University returned to the site on February 5th to observe the condition of the pavement surface. The longwall panel had progressed about 835-feet since it first influenced the highway, which caused impacts on approximately 1,450-feet of the interstate. Damage was observed as far as 725-feet behind the longwall face and 450-feet in front of the longwall face. The distress observed included joint separations transverse cracking, chevron cracking, longitudinal cracking, compression bumps, and separations between the pavement and adjacent soil. The location of the distresses closest to the longwall face can be seen in Figure 48, while the remainder of the damage can be seen in Appendix A.

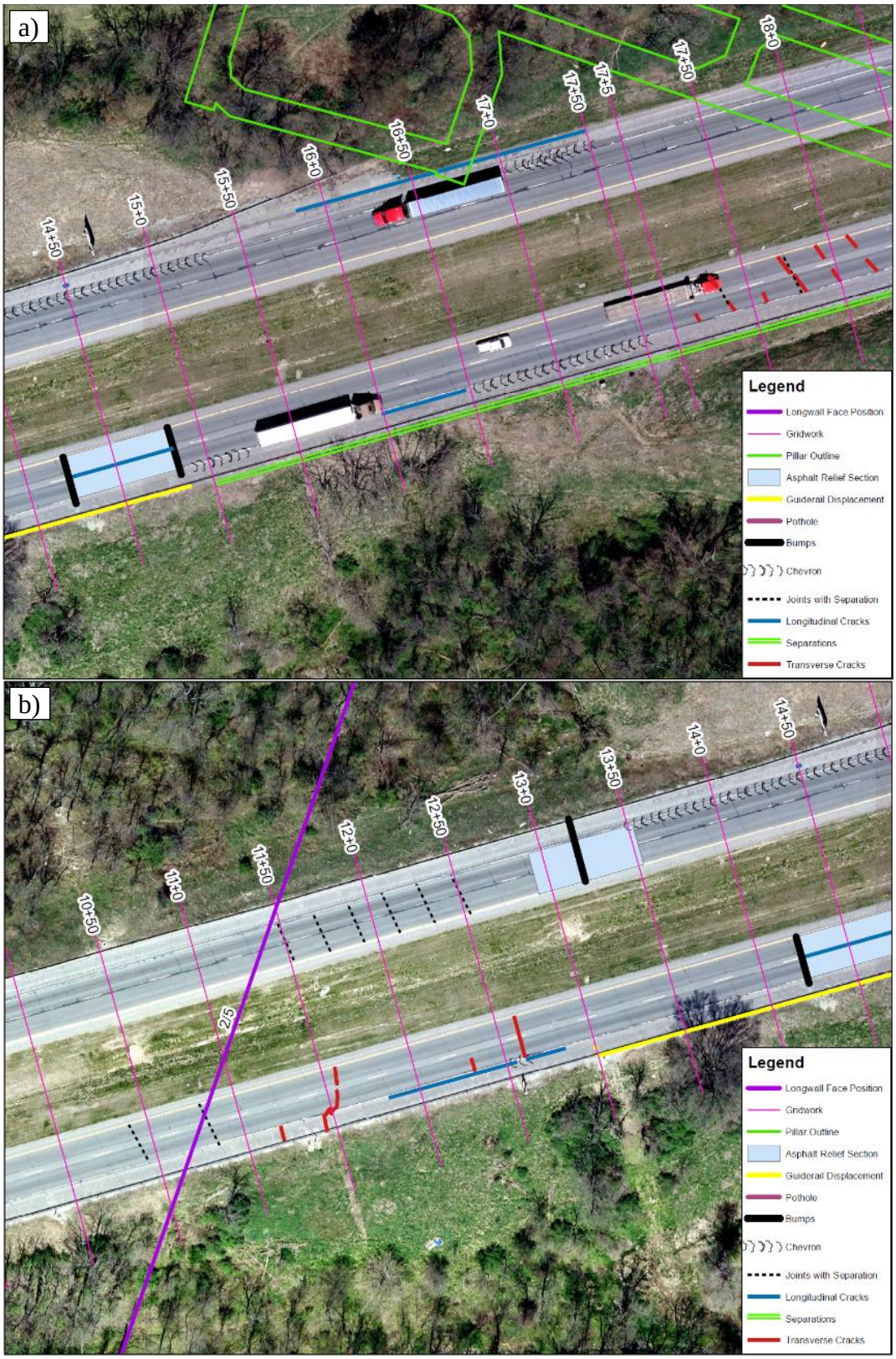

Figure 48 Pavement features observed on February 5th

Some of the most notable distresses observed during this site visit were the three compression bumps and a large transverse crack. The compression bump on the westbound lane formed on February 5th, approximately 150-feet behind the longwall face. The two compression bumps on the eastbound lane formed on February 4th, between 175-feet and 225-feet behind the longwall face. All three of these compression bumps formed in the asphalt relief sections. The large transverse crack formed about 60-feet behind the longwall face and opened to a width of more than 2.5-inches wide. Images of these distresses can be seen in Figure 49 below.

Figure 49 Field images of observed features on February 5th from left to right; eastbound compression bump/blow-up 1-foot tall, westbound blow-up, and eastbound transverse crack 2.5-inches wide

4.2.1.3 February 14th

Due to inclement weather, the University was unable to return to the site until February 14th, which was seven active mining days after the prior visit. In this time period, the longwall face progressed about 800-feet. During this site visit, damage was observed on approximately 1,900-feet of the interstate. The types of distress observed throughout the highway included transverse cracking, longitudinal cracking, shear failures, compression bumps, widened contraction joints, displaced guiderails, and separations between the pavement edge and the adjacent soil. The locations of the failures closest to the longwall face that were observed on February 14th can be seen in Figure 50, while the remainder of the features can be seen in Appendix A.

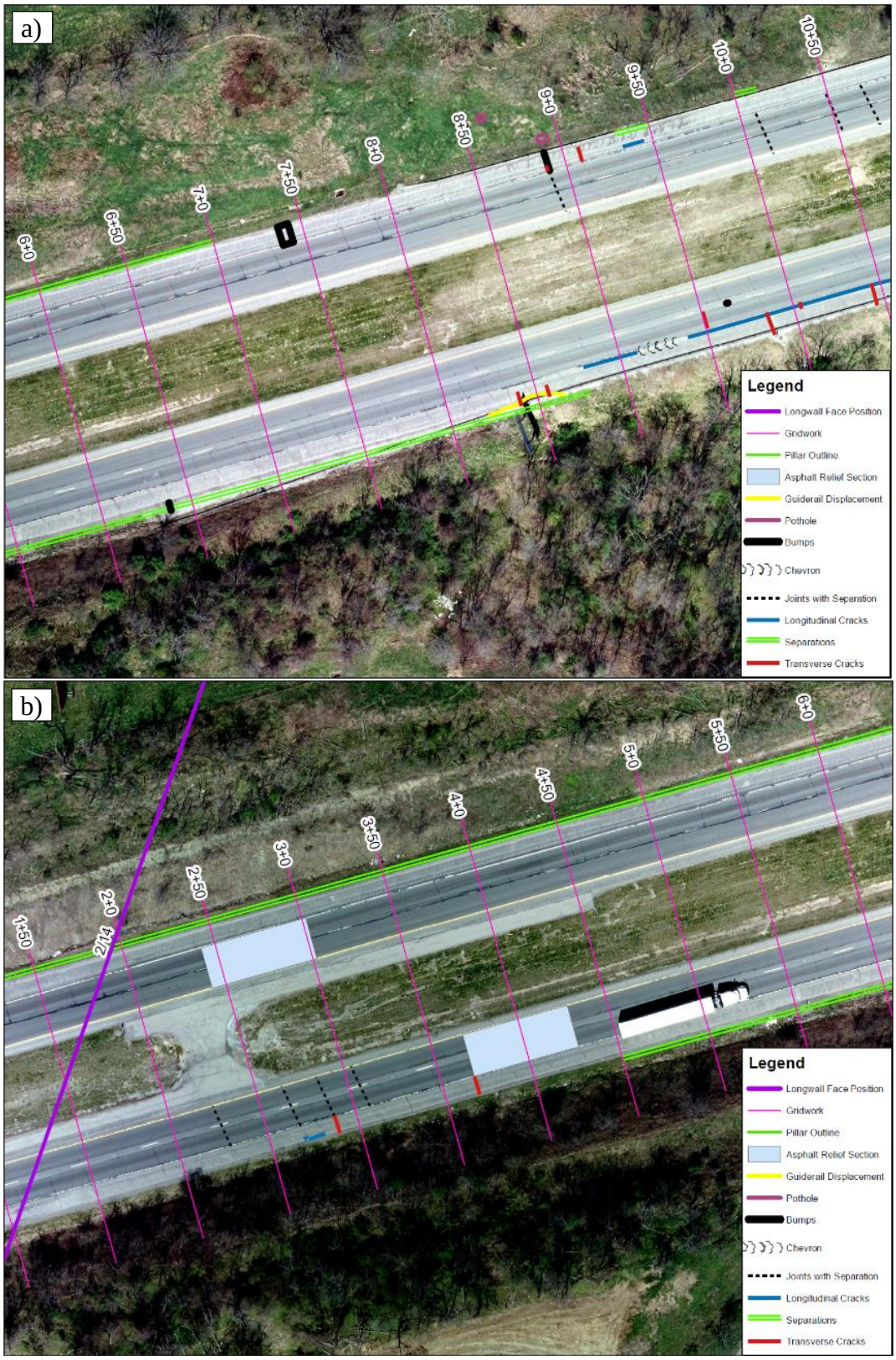

Figure 50 Pavement features observed on February 14th

Two new compression features formed between the observations made on February 5th and February 14th. On the outside shoulder of the eastbound lanes, a blow-up approximately 7-inch tall formed on top of the existing transverse crack. This blow-up occurred on February 6th when the longwall face was about 200-feet past the location of the original crack. On the other side of the road, a compression bump formed on February 14th approximately 450-feet behind the longwall face. Images of these compression features can be seen in Figure 51.

In addition to these two new compression features, significant separations between the edge of the pavement and the adjacent soil on both sides of the road, guiderail displacements, and open expansion cracks were observed. On the eastbound side of the road, separations as much as 6-inch wide were observed. Joints 0.75-inch wide, which was three times their original width, were observed on both sides of the road. These features can also be seen in Figure 51.

Figure 51 Field images of observed features on February 14th from left to right; westbound blow-up, eastbound blow-up 7-inches tall, eastbound separation of pavement from soil, joint width of 0.75-inches, sheared guiderail in westbound lanes, sheared guiderail in eastbound lanes

4.2.1.4 February 19th

The University next visited the site on February 19th. Between February 14th and February 19th, the longwall face progressed approximately 275-feet. By this point in the undermining process, almost the entirety of the portion of Panel 15 that was beneath the interstate had been undermined. During this site visit, approximately 2,000-feet of the interstate had experienced damage. Like in the previous observational visit, the types of distress observed throughout the highway included transverse cracking, longitudinal cracking, shear failures, compression bumps, widened contraction joints, displaced guiderails, and separations between the pavement edge and the adjacent soil. The locations of these failures observed on February 19th closest to the longwall face can be seen in Figure 52, while the remainder of the features can be seen in Appendix A.

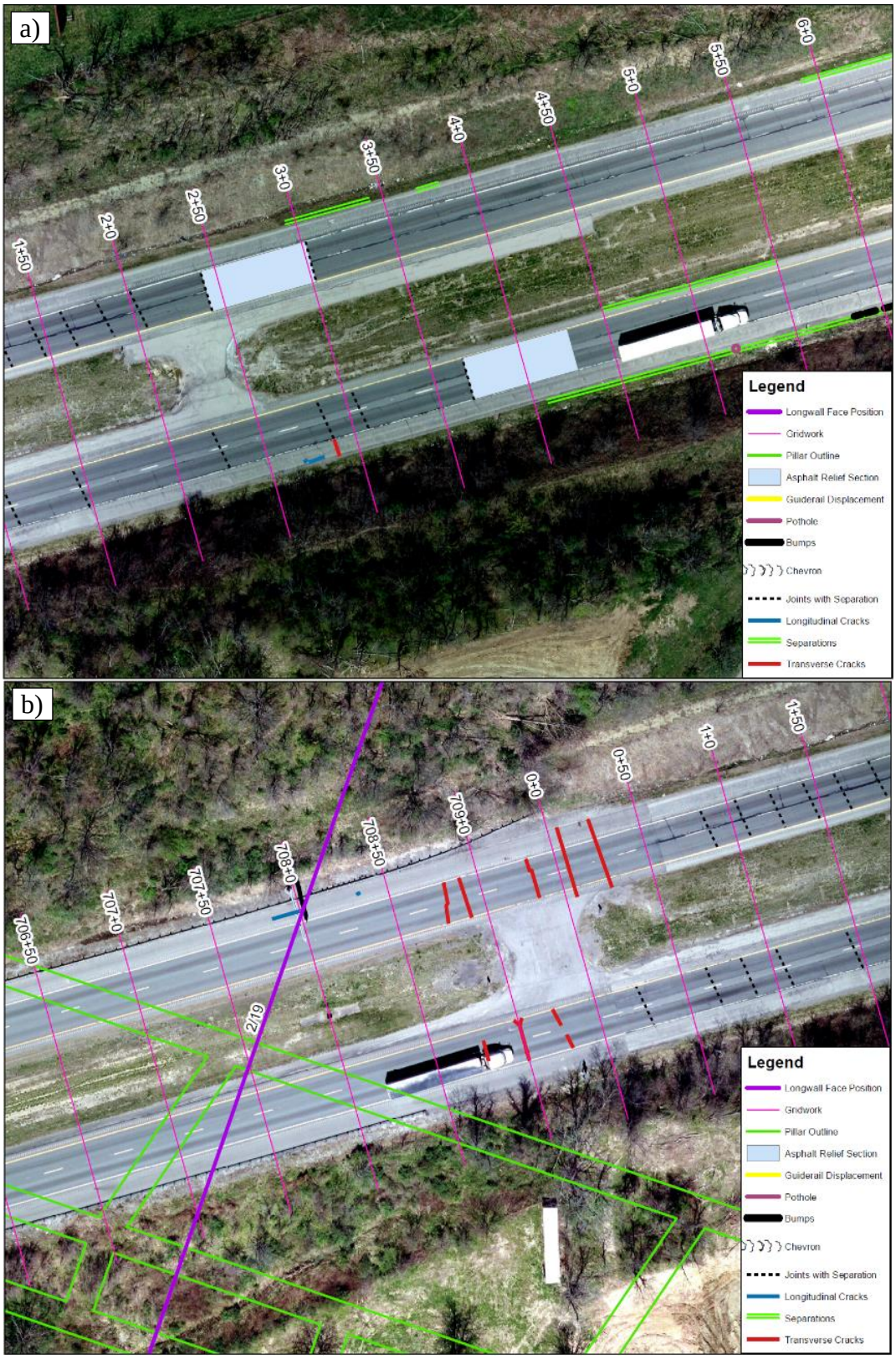

Figure 52 Pavement features observed on February 19th

Very few new features were observed during the site visit on February 19th. Additional contraction joints had widened, and small transverse cracks formed as much as 300-ft behind the longwall face. Additionally, additional portions of the longitudinal lane-shoulder joint reflected up into the overlay had widened just beyond the longwall face. The new damage observed on this site visit was not as significant as the damage observed in similar features near the center of the panel. Slight separations also occurred on the inside of the eastbound lanes between the pavement and the adjacent soil.

4.2.1.5 February 26th

By February 26th, the longwall face was approximately 465-feet beyond the extent of I-70. Various types of distresses were present throughout the entire 2,400-foot section of interstate as a result of the subsidence basin. The location of damage observed near the western edge of the panel during this site visit can be seen in Figure 53, while the remainder of the observed damage can be seen in Appendix A.

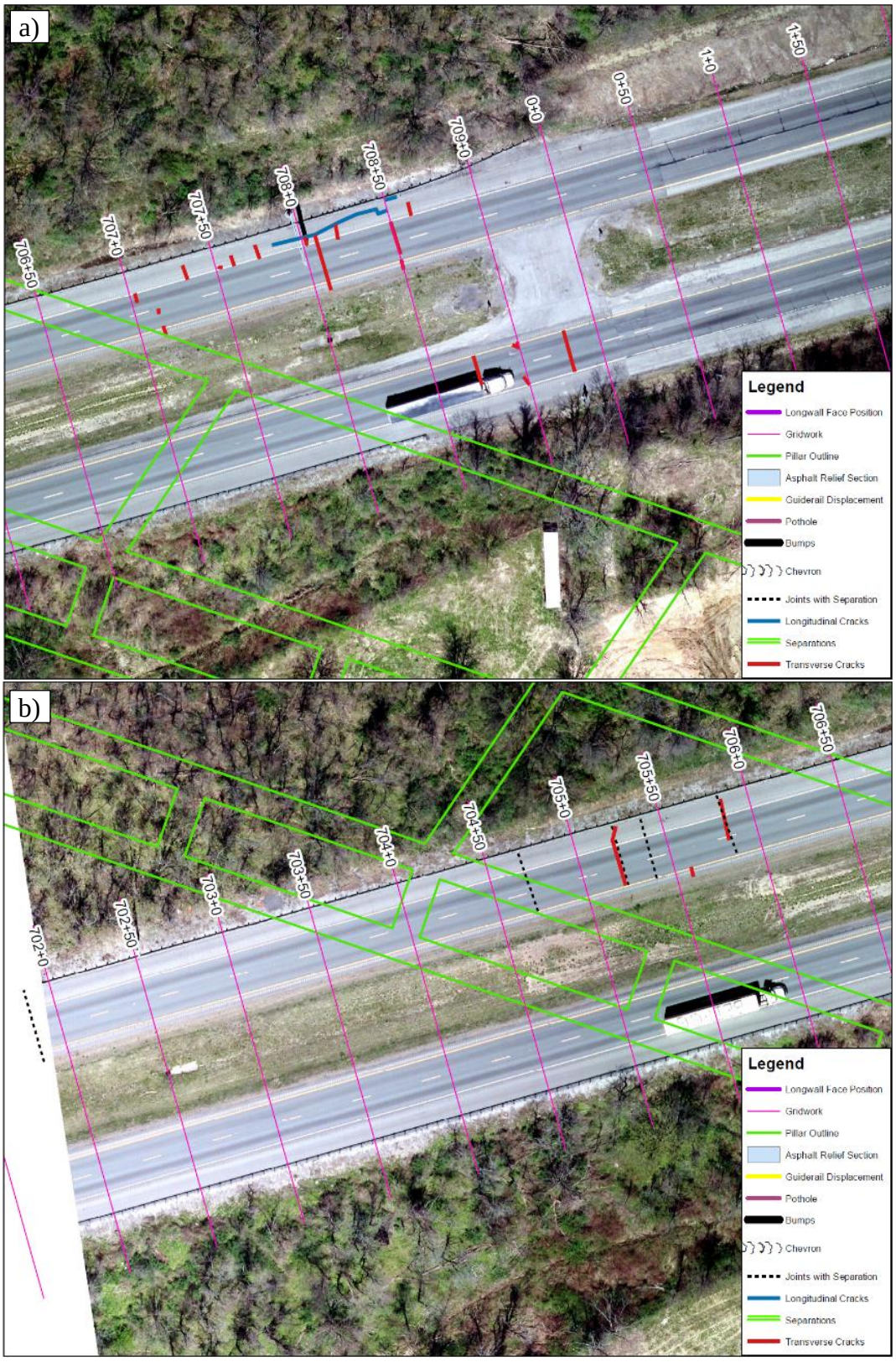

Figure 53 Pavement features observed on February 26th – Longwall face is beyond the extend of study area

With the longwall face beyond the extent of the interstate, only a small amount of new distress was observed, and it was in the section of highway in West Virginia section of the highway. In this section, small transverse cracks and widened contraction joints were observed on the westbound lanes. This distress was observed over the western gateroads and just inside the panel.

4.2.1.6 March 5th

By the site visit on March 5th, the longwall face was over 1,000-feet beyond the extent of the highway. Due to repairs made by the PennDOT maintenance team and the natural subsidence progression, the University found that the distress on the highway had been repaired by this observation.

4.2.2 Tiltmeter Data

As described previously, eight tiltmeters were installed along the eastbound lanes of I-70. The locations of the tiltmeters can be seen in Figure 28. The instrument located furthest west at the TM-1 location was relocated to the bottom of the southern slope of embankment #1 and renamed TM-9 at the end of January.

Unfortunately, due to a malfunction of the tiltmeter data acquisition system, much of the data collected by the tiltmeters was lost. Tiltmeters 1 through 5 (TM-1/9, TM-2, TM-3, TM-4, and TM-5) all experienced an override in data that led to data loss as the longwall approached and passed underneath these instruments. A review of the pre and post mining tilt data from these instruments indicates that they likely became uncalibrated during the undermining, meaning that the data is not usable for analysis.

However, TM-6, TM-7, and TM-8 were a newer model of instrument and did not experience this data loss. As such, a complete characterization of tilt of the roadway can be made for these three tiltmeters. No change in tilt was expected until the longwall face approached the tiltmeter, so it was only necessary to consider the movement of the instruments when the longwall face was approximately 600-feet of the instrument in each direction. Figure 54 depicts the location of the tiltmeters with usable data and the orientation of the axes in relation to the orientation of Panel 15 and expected subsidence curve.

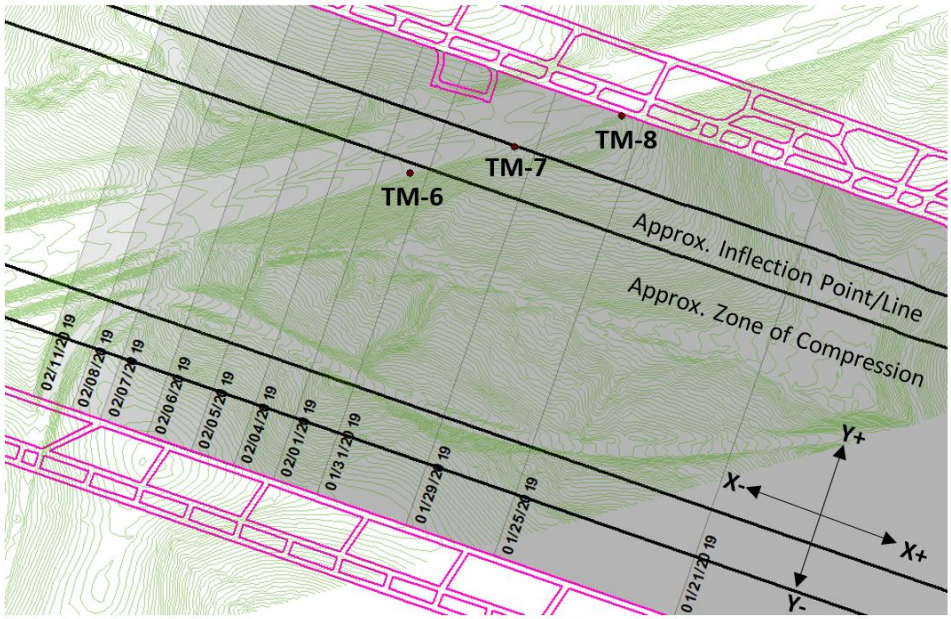

Figure 54 Location and orientation of tiltmeters that did not expereince data loss

In an analysis of the tiltmeters, the data was viewed as cumulative tilt, so each data point represents the total amount the instrument tilted from the original position, zero-tilt orientation. This type of analysis provides a representation of the positioning of the instrument as the undermining progressed. Figure 55 through Figure 57 show the plots of movement of TM-6, TM-

7, and TM-8 on a scatterplot over time. The dates used were based on when movement began to occur and when they began to settle.

Figure 55 depicts TM-6 as it began to tilt in the X+ and Y- directions as the longwall face approached the instrument. As can be seen, as the longwall face approached the TM-6, it began to tilt towards the position of the longwall face and into the center of the basin. It continued to tilt in this direction until February 3rd, when the longwall face was approximately 180-feet past the tiltmeter. At this point, the tilt reversed its direction and began to tilt in the direction of mining, which continued until the longwall face was approximately 550-feet past the instrument on February 7th. It settled with very little change in tilt on the x-axis and a more dramatic change on the y-axis, indicating permanent tilt towards the center of the basin.

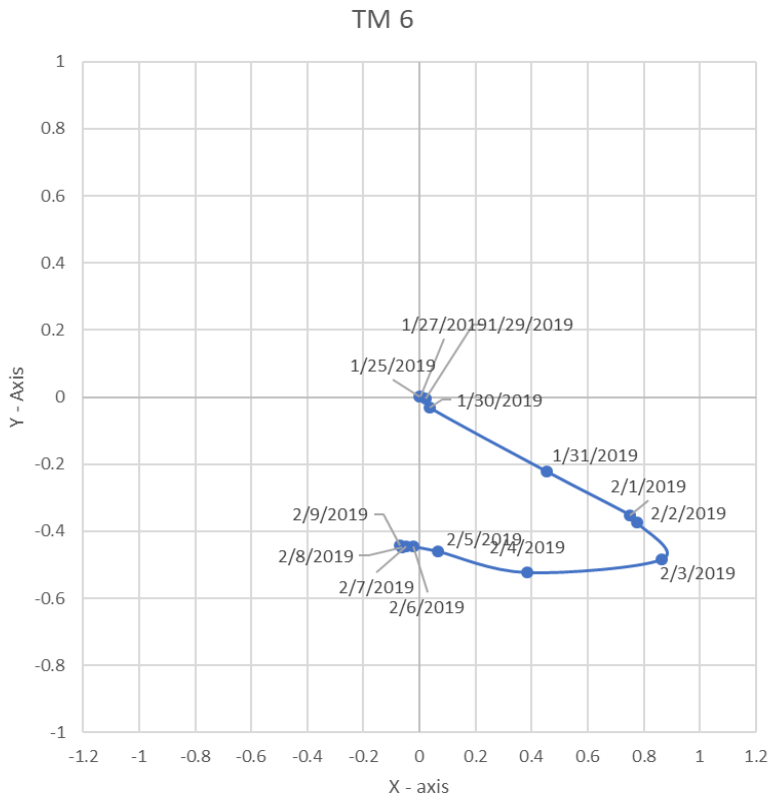

Figure 55 Tilt measurments of TM-6 as undermining occurred

The movement of TM-7 was very similar in orientation to that experienced by TM-6 in that it first tilted in the X+ and Y- directions and then reversed direction, tilting towards the active longwall face. However, the permanent tilt change was approximately 50% more for TM-7 than TM-6, as TM-7 was located within the portion of the subsidence basin where large permanent surface slope changes were expected. The movement of TM-7 can be seen in Figure 56.

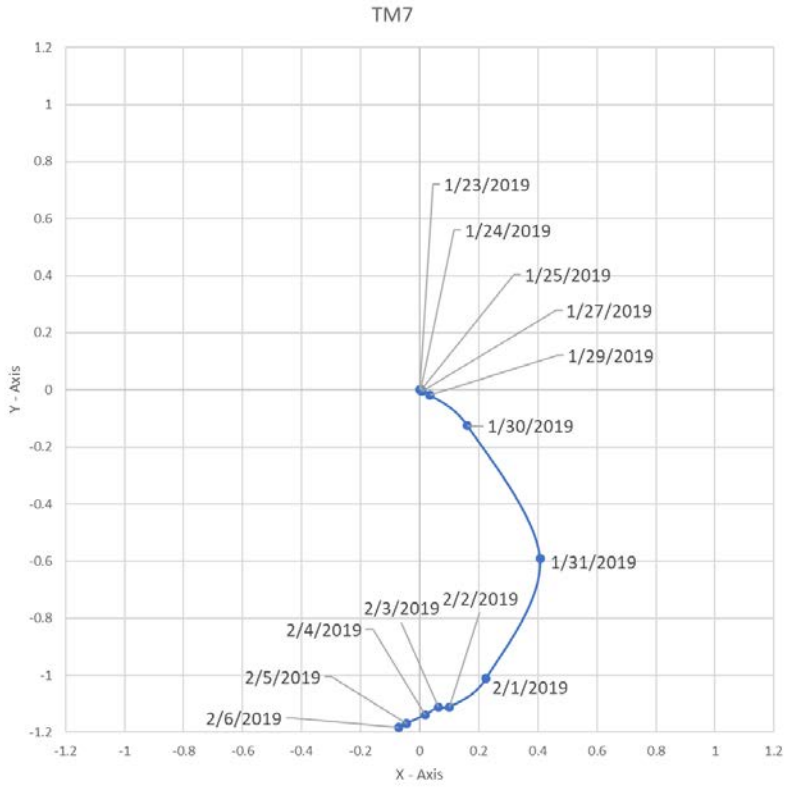

Figure 56 Tilt measurements of TM-7 as undermining occurred

Figure 57 represents the movement of TM-8. As can be seen in Figure 54, TM-8 was located very close to the edge of the panel, causing it to experience significantly less change in tilt than the other two instruments. The tiltmeter did not begin to move until January 29th, when the longwall face was approximately 300-feet past the instrument. TM-8 began to tilt in the Y+

direction, and slightly in the X+ direction, meaning that the tiltmeter began to point away from the center of the basin and in the opposite direction of mining. When the longwall face was approximately 430-feet past the instrument, TM-8 reached its maximum in both the X+ and Y+ directions and then reversed its direction. Like the other tiltmeters, TM-8 settled to approximately the same tilt on the x-axis and moved slightly on the y-axis when the longwall face was approximately 660-feet away.

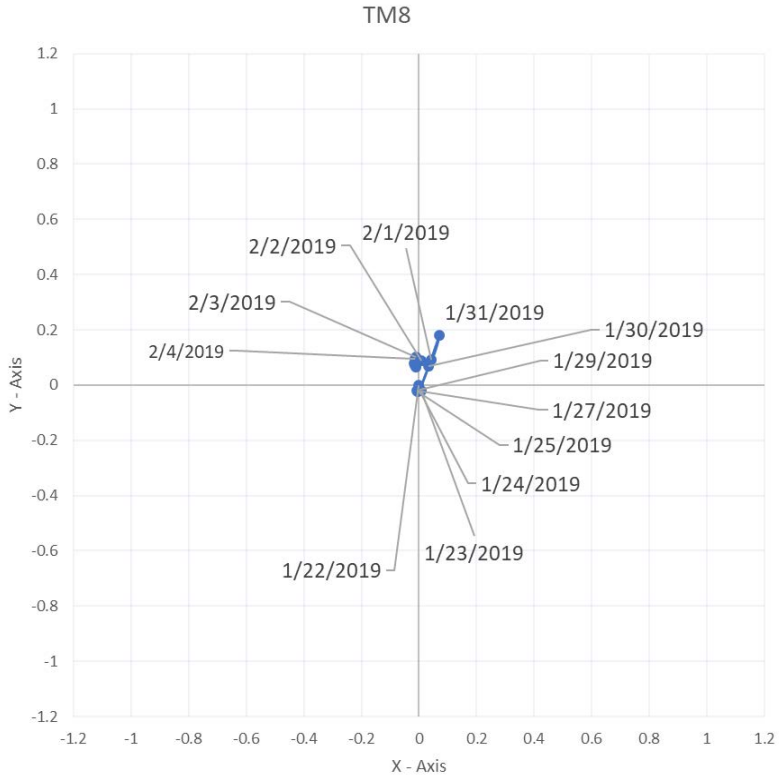

Figure 57 Tilt measurements of TM-8 as undermining occurred

The movements of all three tiltmeters were summarized on a map shown in Figure 58. The map contains vectors displaying the movements of the tiltmeters and the face positions of the longwall on the days when this section was undermined. The vectors and face positions are color

coded so it can be determined where the longwall face position started on the day each movement occurred. As can be seen in this figure, aside from TM-8, which experienced a very small degree of tilt away from the basin, the general trend seen was tilt towards the center of the longwall basin. The severity of movement varied based on where in the basin the instrument was located. TM-7 experienced the highest degree of permanent tilt in the Y- direction as it was close to the inflection line, where a higher degree of slope was expected, while TM-6 experienced a larger degree of tilt on the x-axis during the dynamic subsidence event.

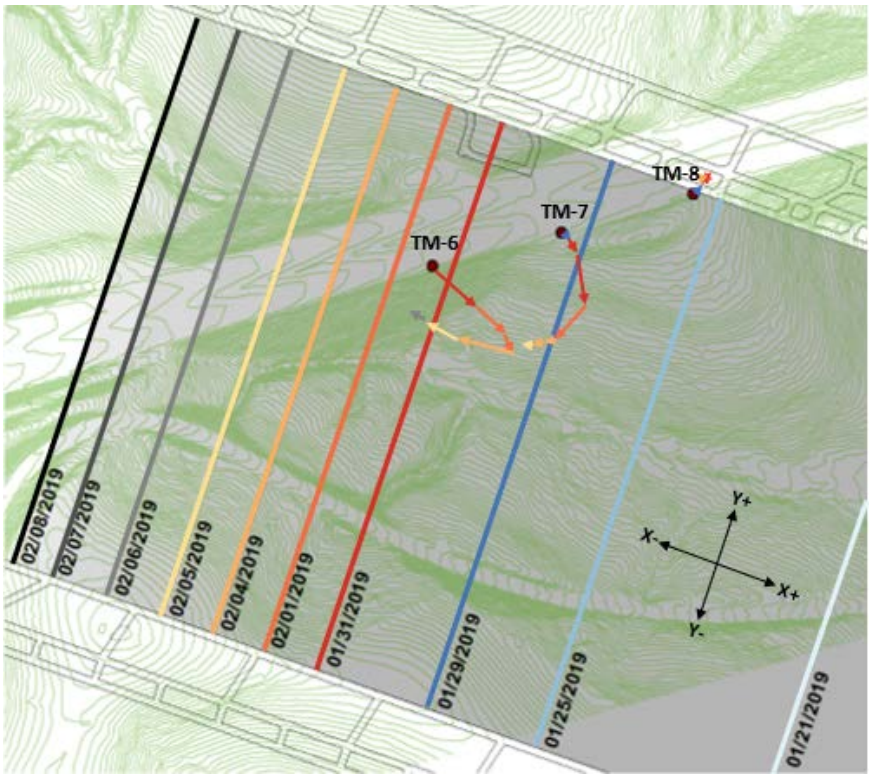

Figure 58 Vector representations of the tilt of TM-6, TM-7, and TM-8 with respect to the longwall face position

4.3 Reaction of Slopes to Mining

4.3.1 Inclinometer Data

As explained previously, six inclinometers were installed on the slopes of the embankments. The location and orientations of these inclinometers can be seen in Figure 29. As can be seen in this figure, the orientations of the instruments differ based on their locations; TB-4 and TB-2 share an orientation, while TB-6, TB-8, TB-9 and TB-13 all share a different orientation. The orientation as installed shows the A+ direction pointing down the slope of the embankments and the B+ axis clockwise from the A+ orientation. The inclinometers were placed either on the top or the bottom of the embankments, so their measurements could be compared and characterize the movement of the overall slope.

Measurements of the movement of the slope were recorded at 2-foot intervals in the inclinometer casing. A cumulative displacement analysis was utilized, which adds readings together as the data moves upwards at each interval. This is the best method of analysis as it represents the true ground movement at each interval, as the upper layers of the ground move when the lower layers move.

4.3.1.1 Movement of Embankment #1 South Slope

TB-6 and TB-8 were located on the southern slope of embankment #1, with TB-6 at the top of the embankment and TB-8 at the bottom. TB-8 was undermined on January 31st and TB-6 was undermined the following day. As such, inclinometer TB-8 began to experience movement the day before TB-6. Both instruments recorded movement one active mining day after the longwall face past beneath the casing.

The behavior of TB-8 and TB-6 were very similar and the movement of TB-6 at the top of the embankment slope can be seen in Figure 59. Both instruments experienced movement that were most pronounced in the A+ direction, indicating movement down the slope and towards the center of the basin. This trend in movement continued as the longwall face moved away from the instruments. As this occurred, movements varied back and forth on the B-axis. Finalized movements were similar for both instruments, showing approximately 6-inches of movement in the A+ direction and 1.5-inches to 2.5-inches of movement in the B+ direction, indicating the casings shift towards the center of the basin. The inclinometers began to settle into their final positions when the face was between 600-feet and 850-feet, or between six and eight active mining days, past the instrument. The movement of both inclinometers also show that movement was greatest at the bottom of the casing and experience the highest change in movement at sediment interfaces.

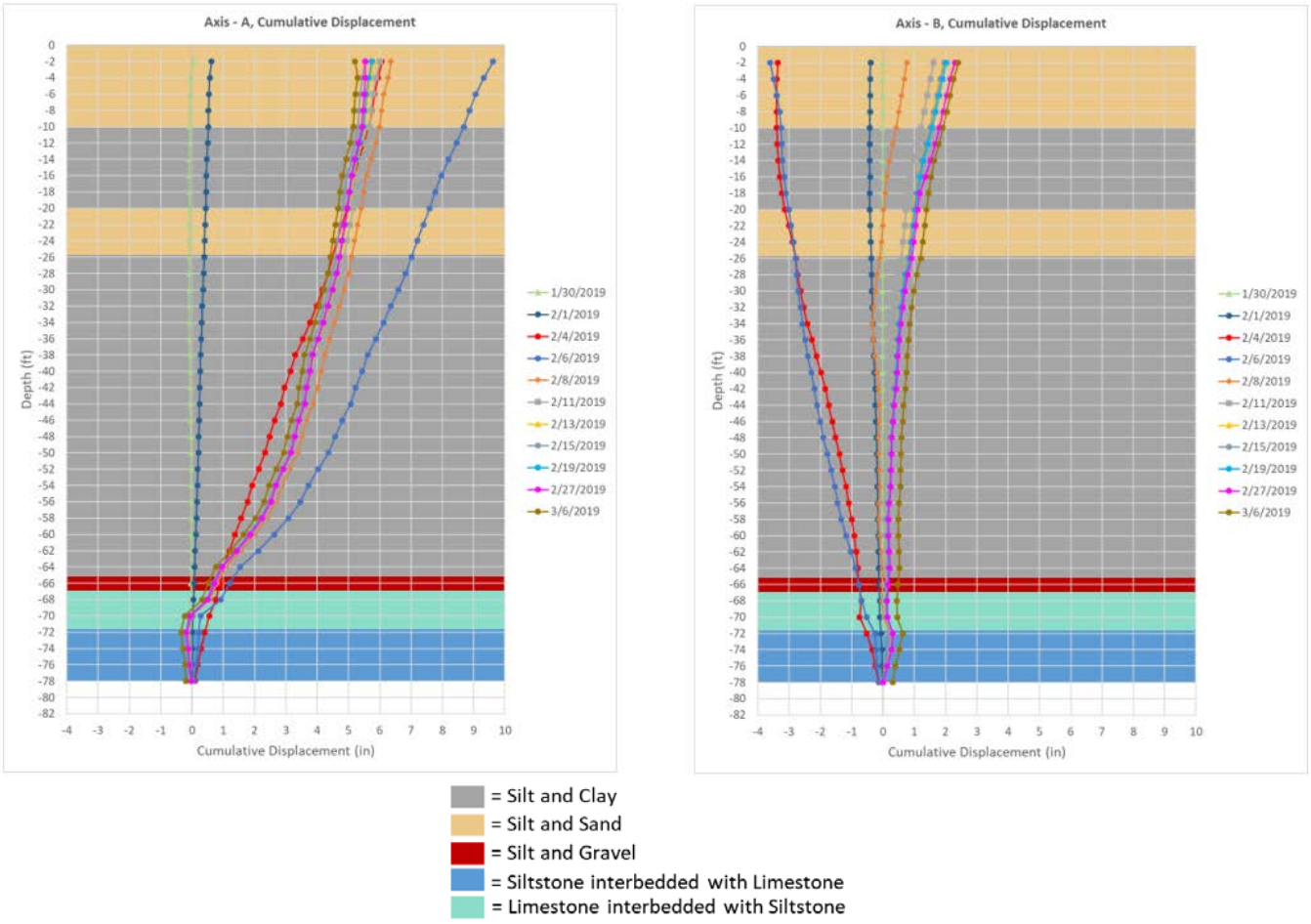

Figure 59 Cumulative displacement of inclinometer TB-6 on southern slope of embankment #1

4.3.1.2 Movement of Embankment #1 North Slope

TB-2 and TB-4 were located on the northern slope of embankment #1, with TB-2 at the top of the embankment and TB-4 at the bottom. TB-2 was undermined on February 5th and TB-4 was undermined the following day. Both instruments began moving on February 6th, which was the day after undermining for TB-2 and the day of undermining for TB-4.

The movement of TB-4 can be seen in Figure 60. Both instruments began to settle on February 15th, when the longwall was approximately 750-feet to 800-feet, or seven to eight active mining days, past the instruments. Unlike the inclinometers on the southern slope, TB-2 and TB-

4 experienced different amounts of movement at the top and bottom of the slope. The inclinometer at the bottom of the slope (TB-4) moved outward an additional 4-inches in the A+ direction than the inclinometer at the top of the slope (TB-2). The movement on the B-axis were very similar between the two instruments, showing initial movement in the B+ direction before settling close to its original point on the B-axis. As with the inclinometers on the southern slope, much of the differential movement in TB-2 and TB-4 was concentrated at deep intervals near the bottom of the casing and at various sediment interfaces.

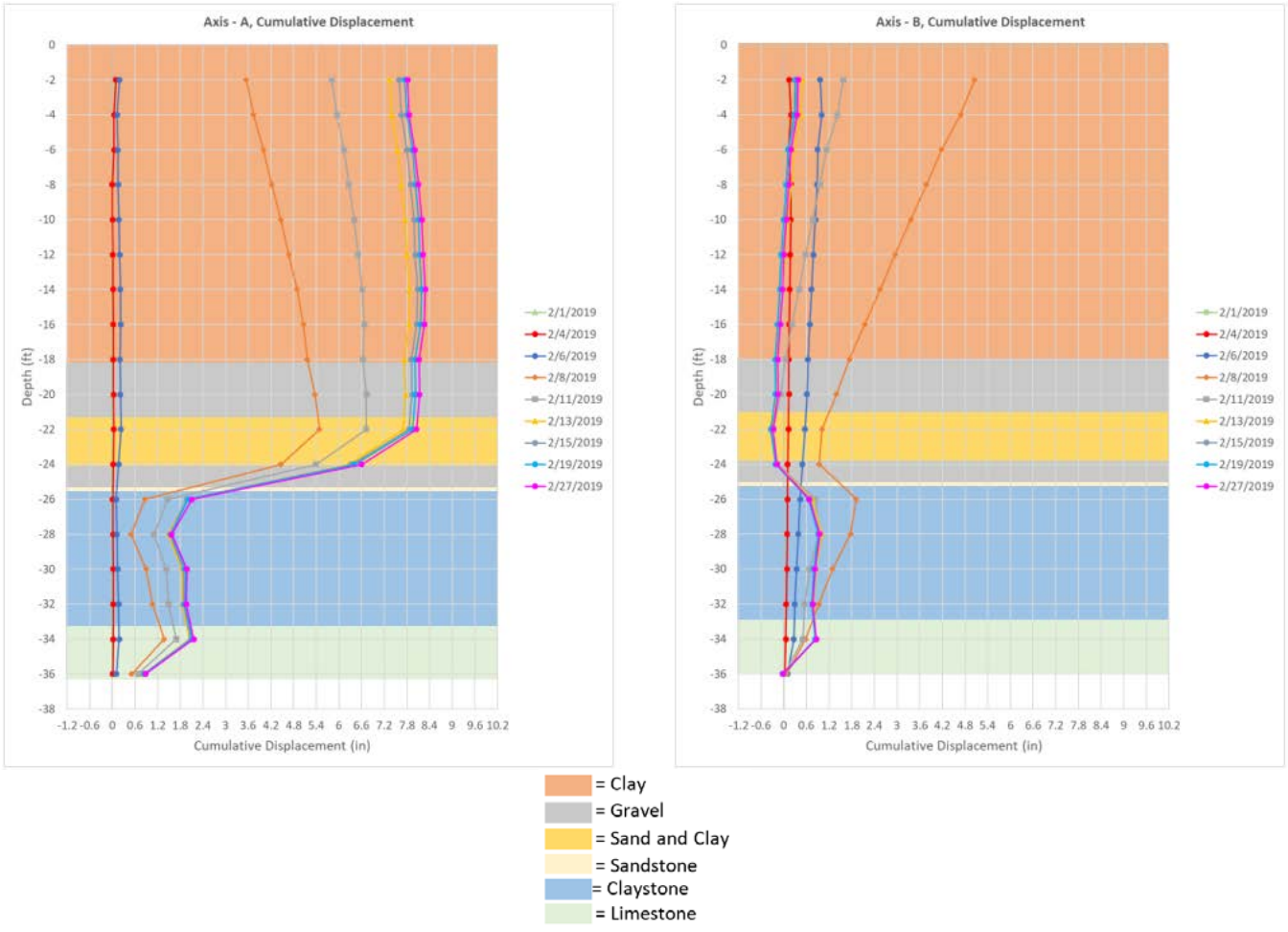

Figure 60 Cumulative displacement of inclinometer TB-4 on northern slope of embankment #1

4.3.1.3 Movement of Embankment #2 South Slope

TB-13 was installed at the bottom of the southern slope of embankment #2, over Panel 15's gateroads. As it was outside the area of active longwall mining, not much movement was expected in this inclinometer. TB-13 began to experience movement on January 21st, when the longwall face was 200-feet from the instrument. The initial readings indicated movement outward from the slope and towards the longwall face. Movement continued in this direction as mining progressed, before eventually settling on February 4th when the longwall face was approximately 1000-feet past the instrument. Very little movement was observed in this inclinometer during the mining of Panel 15.

4.3.1.4 Movement of Cut Slope

TB-9 was located on the edge of the longwall panel and at the base of the cut slope on the eastern side of the study area. Movement was first recorded on January 30th, when the longwall face was approximately 300-feet past the borehole. The movement was primarily in the A+ direction, indicating movement into the basin and opposite of the direction of mining. Additional movement occurred in the B+ direction, however, these movements were not as severe. The casing eventually stopped moving on February 4th, when the longwall face was approximately 650-feet past the instrument. The final movements on the surface totaled approximately 0.8-inches on the A-axis and 0.4-inches on the B-axis.

4.3.2 Summary of Embankment #1 Movement

The vertical displacement throughout the study area was measured using the highway alignment points surveyed by PennDOT and the slope stakes surveyed by SPK Engineering, as

described previously. Using these surveys, the subsidence of each point was measured over time. The final vertical subsidence is displayed in Figure 35. This figure shows that over 5-feet of subsidence was observed at the top of the embankment and on the highway adjacent to the embankment slopes, while only around 4-feet of subsidence was observed at the bottom of the embankment slopes. As there is more fill material at the top of the slope than at the bottom, the larger vertical displacement in the region with more fill indicates that the fill material likely experienced consolidation causing the larger vertical subsidence.

The slope surveys can also be used in combination with the inclinometer data to further characterize the movement of the embankment. The final horizontal movements of the embankments can be seen in Figure 36. This figure shows that the points on the embankment moved away from the roadway and towards the bottom of the slope. This movement was reinforced by the inclinometer data from TBB-2, TB-4, TB-6, and TB-8, which show that the primary direction of movement within the slope is oriented in the A+ direction, indicating movement towards the bottom of the slope. These data sets indicate that the embankment also experienced lateral spreading when subjected to the subsidence forces. Luckily, the fill material demonstrated strain-hardening behavior so the embankment did not experience catastrophic failure as a result of this spreading.

5.0 Analysis of Subsidence through Modeling

As described previously, longwall mining subsidence can be predicted using either empirical relationships, the profile functions, or the influence function. Before Panel 15 undermined I-70, these methods were implemented to predict the subsidence effects that may have occurred during longwall mining. After the mining of Panel 15, the subsidence basin was modeled again using a combination of the empirical relationships and profile function and with the influence function in SDPS to calibrate the basin's shape to the observed movement. These models were compared with the data and observations that were collected to better understand the movement of the study area.

5.1 Empirical and Profile Function Model

5.1.1 Preliminary Predictions using Empirical and Profile Function Model

Empirical relationships were employed to characterize the subsidence basin of Panel 15 in the Pittsburgh Coalbed. As described previously, Peng and the department of mining engineering at West Virginia University collected approximately 40 case studies of longwall mines in the Pittsburgh Coalbed to develop these relationships. For supercritical panels, the maximum vertical subsidence, inflection point location, and influence radius can be determined using these relationships and are provided with Equation 5-1 through Equation 5-4 (Peng and Cheng, 1981).

$$a = 0.6760821 * 0.9997678^{h} = 0.6760821 * 0.9997678^{675}$$

$$a = 0.578 \quad \textbf{[5-1]}$$

Where: a = subsidence factor
h = overburden

$$S_{max} = a * m = 0.578 * 7.25$$

$$\boldsymbol{S_{max} = 4.19\ ft} \quad \textbf{[5-2]}$$

Where: S_{max} = maximum subsidence predicted
a = subsidence factor
m = extraction thickness

$$d = 0.45439 * h * e^{-0.000914*h} = 0.45439 * 675 * e^{-0.000914*675}$$

$$\boldsymbol{d = 165.5\ ft} \quad \textbf{[5-3]}$$

Where: d = distance from edge of mining to inflection line
h = overburden thickness

$$r = \frac{h}{\tan(\beta)} = \frac{675}{\tan(67)} \rightarrow \boldsymbol{r = 286.5\ ft} \quad \textbf{[5-4]}$$

Where: r = radius of influence measured from the point of zero surface subsidence to the inflection line and from the inflection line to the point of maximum subsidence
β = angle of influence, 67 degrees for Pittsburgh Coalbed
h = overburden thickness

With the aid of these empirical relationships and the hyperbolic tangent profile function defined previously in Equation 2-2, the subsidence basin can be predicted. Figure 61 shows a sketch of the predicted final subsidence basin based on these relationships. As can be seen from

these relationships, the maximum subsidence predicted for Panel 15 is about 4.2-feet and the inflection line is approximately 165-feet from the edge of the longwall mining.

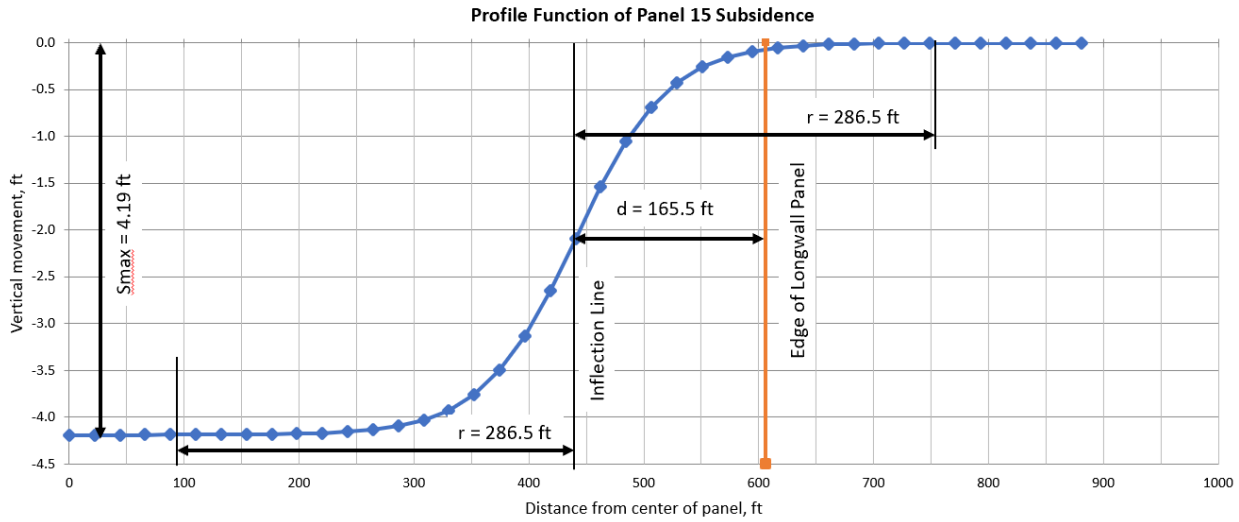

Figure 61 Final subsidence basin sketched using the profile function and empirical relationships derived for the Pittsburgh Coalbed

5.1.2 Comparison of Predictions from Empirical/Profile Function Model with Observed Deformations

The empirical/profile function model can be compared with the final vertical subsidence survey data collected on the highway alignment (Figure 62). As can be seen in this figure, the maximum amount of subsidence predicted by this model matches the maximum subsidence observed in areas of cut along the highway. The large amount of subsidence observed on the eastern portion of the highway occurred over embankment #1; the movement in this area was influenced by the embankment and therefore cannot be accurately predicted by a predictive model. The curvature of the model also matches very well with the data observed on the eastern side of

the highway; however, the curvature does not match as well with the data observed on the western side of the highway. Like most models, the empirical/profile function cannot predict heave like that which was observed over the gateroads when mining Panel 15. Based on this overview, the empirical/profile function model would be effective to be used to predict the vertical subsidence on the highway surface.

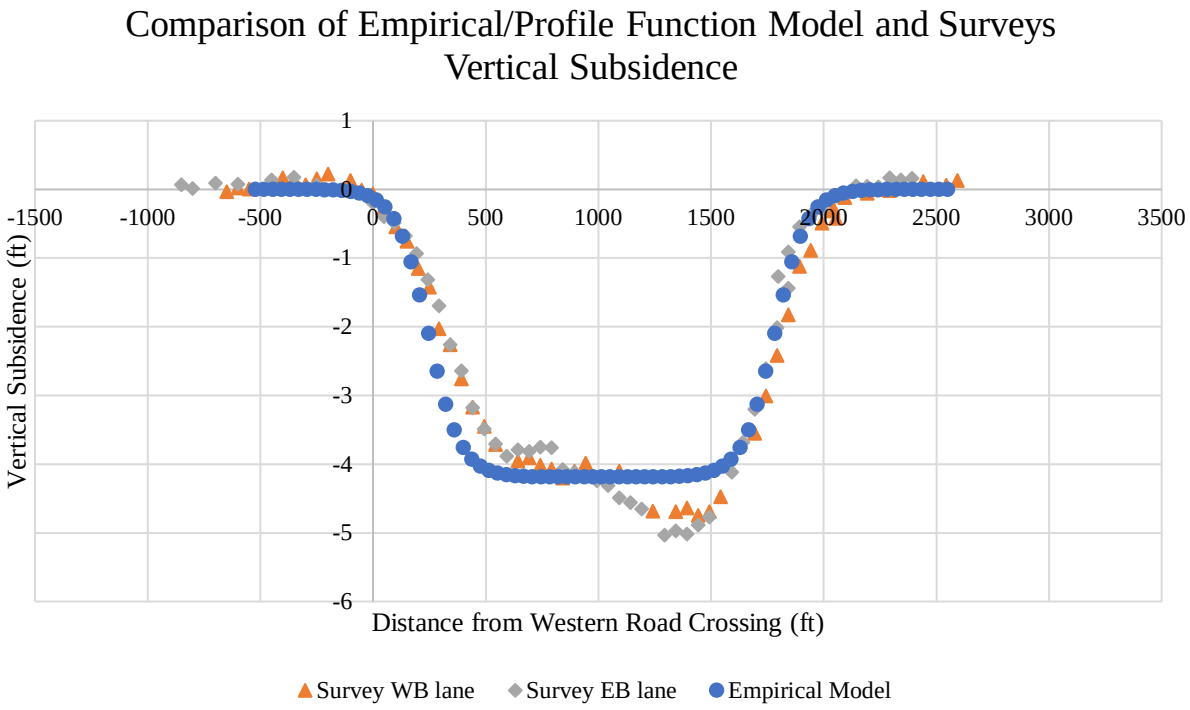

Figure 62 Vertical Subsidence relationship between empirical/profile function model and survey data

Based on the empirical relationships set forth previously, the distance from the edge of the longwall panel to the inflection line should be about 165-feet. Assuming that the inflection line remains the same distance away from the active mining as it does from the edges of the longwall panel, the location of the inflection line can be monitored throughout mining. The inflection line is the location that stress that mining induces on the ground surface transfers from tension to

compression. Based on this principal, tension features were expected to occur between the longwall face and the inflection line and compression features were expected behind the inflection line. The relationship between the longwall face, the inflection line, and the observed distresses is shown in Figure 63 and Figure 64.

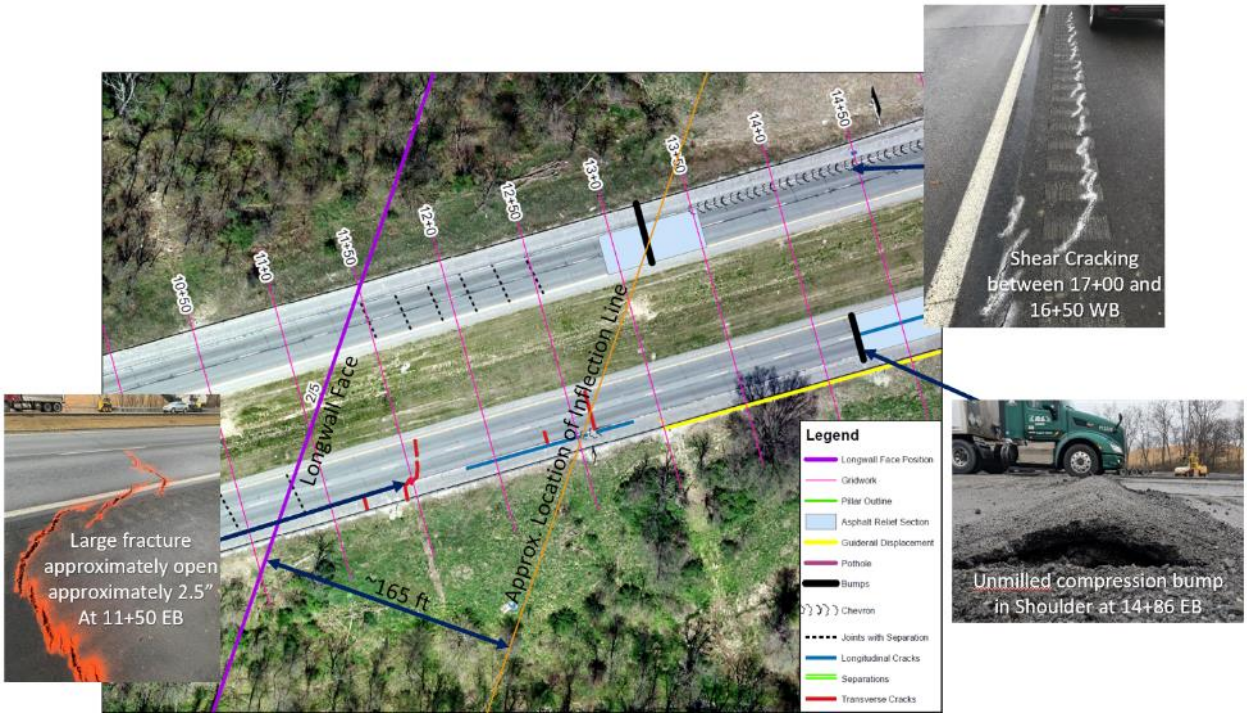

Figure 63 Failures of the highway surface as the subsidence basin formed on February 5th, demonstrating areas of tension and compression

Figure 64 Failures of the highway surface as the subsidence basin formed on February 14th, demonstrating areas of tension and compression

As can be seen in Figure 63 and Figure 64, the trends in the observed distress show that the tensile regions exhibited behavior, such as separation and widened contraction joints, and tended to occur within 150-feet beyond the longwall face and 165-feet behind the longwall face. Once the longwall face was approximately 165-feet past a point, the surface stresses and strains switched from tension to compression, causing the formation of compression features, such as blow-ups. These figures help to confirm that the empirical relationships were accurate in predicting the zones of compression and tension for the mining of Panel 15. The survey and observation data collected through the mining of Panel 15 beneath I-70 verifies the validity of the empirical/profile function model for the Pittsburgh Coalbed, therefore these relationships can also be utilized to predict future mining operations.

5.2 SDPS Model

An analysis of Panel 15 in the Tunnel Ridge Mine was developed using the Surface Deformation Predication System (SDPS) modeling software to consider the effects of undermining on I-70. This analysis considered primarily how the final subsidence basin impacts the highway and the embankments. Based on the mine maps received from the Tunnel Ridge Mine, the panel has a width of approximately 1,200 feet and a length of approximately 14,500 feet. The layout of Panel 15 and the highway intersection can be seen below in Figure 65. A detailed overview of how the model was generated can be found in Appendix B.

Figure 65 Orientation of I-70 alignment crossing Panel 15

5.2.1 Preliminary Predictions using SDPS Model

An initial analysis of Panel 15 was completed using SDPS before the undermining took place. The analysis was performed to make predictions regarding the deformations that would

occur during the undermining process. The following assumptions were made for this initial analysis:

- Extraction thickness is approximately 7.25-ft (provided by Tunnel Ridge Mine)
- Supercritical Subsidence Factor = 64.2%
- Average overburden thickness is 675-feet
- Average percentage of hard rock is approximately 25% (lower extreme of typical range for greater Pittsburgh area)
- All pillars will remain rigid, minimizing vertical subsidence over the gate roads and creating an edge effect of 135-feet
- Surface is at a constant elevation
- The longwall face progresses at an average rate of 115 feet/day

This analysis was completed in the SDPS program and predicted deformation and strain over the extent of the longwall mining operation. The results were displayed using graphs. The models can be generated for the entire panel and displayed as a three-dimensional graph or can be generated for points and displayed as a two-dimensional cross-sectional graph. Using the SDPS final predictive model, the vertical subsidence, horizontal displacement, and horizontal strain, that could affect the ground surface as a result of mining Panel 15 were predicted. As the surface for this model was flat, ground strain could not be calculated. The visual representations of some of these factors for a cross section through the highway alignment can be seen below in Figure 66 through Figure 68.

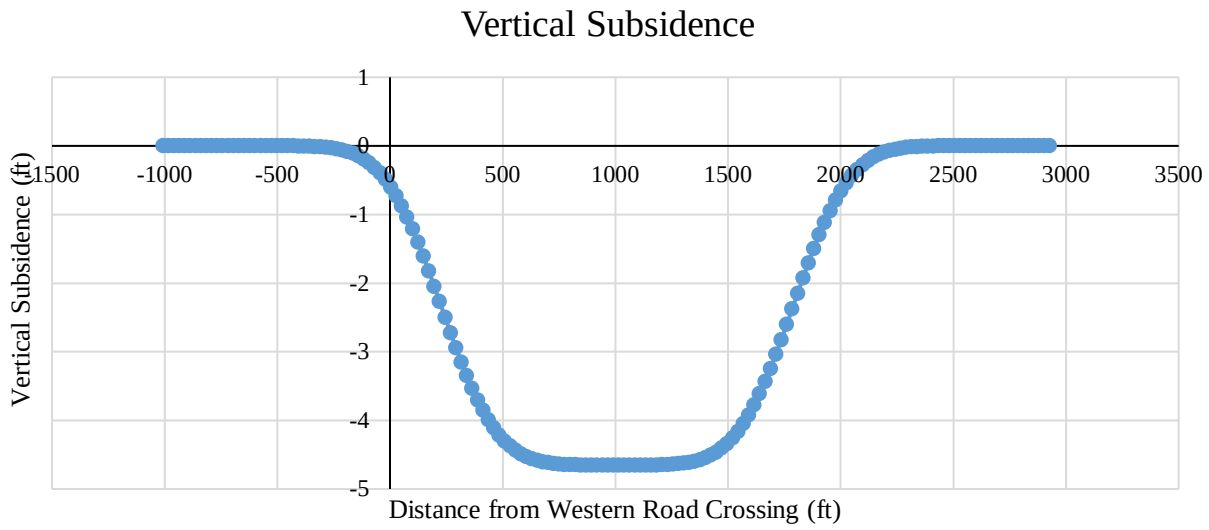

Figure 66 Preliminary model of vertical subsidence on I-70 alignment from undermining of Panel 15

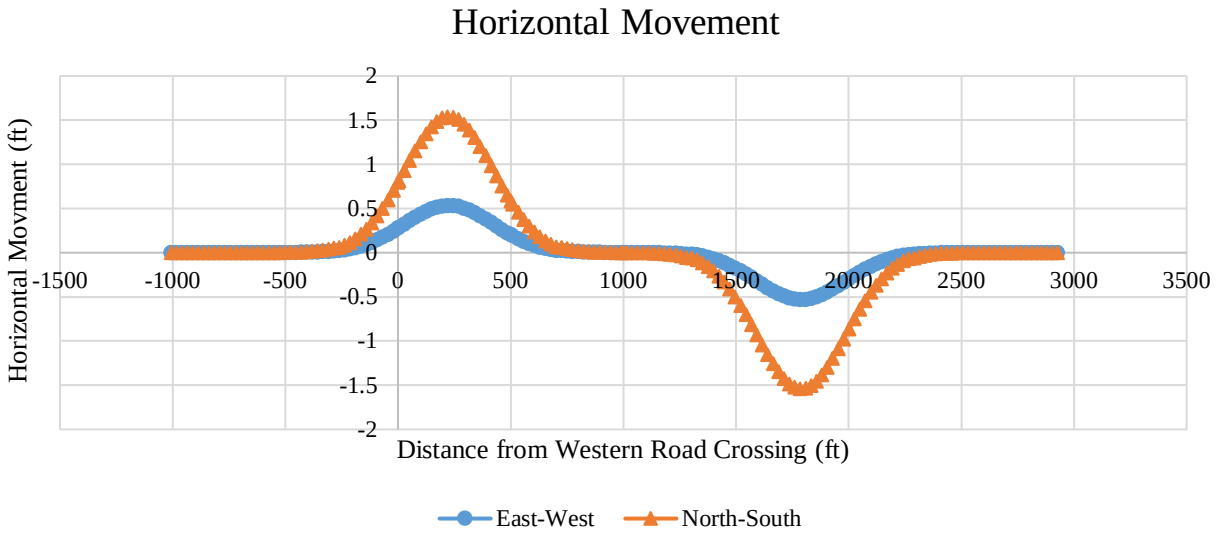

Figure 67 Preliminary model of horizontal displacement on I-70 alignment from undermining of Panel 15

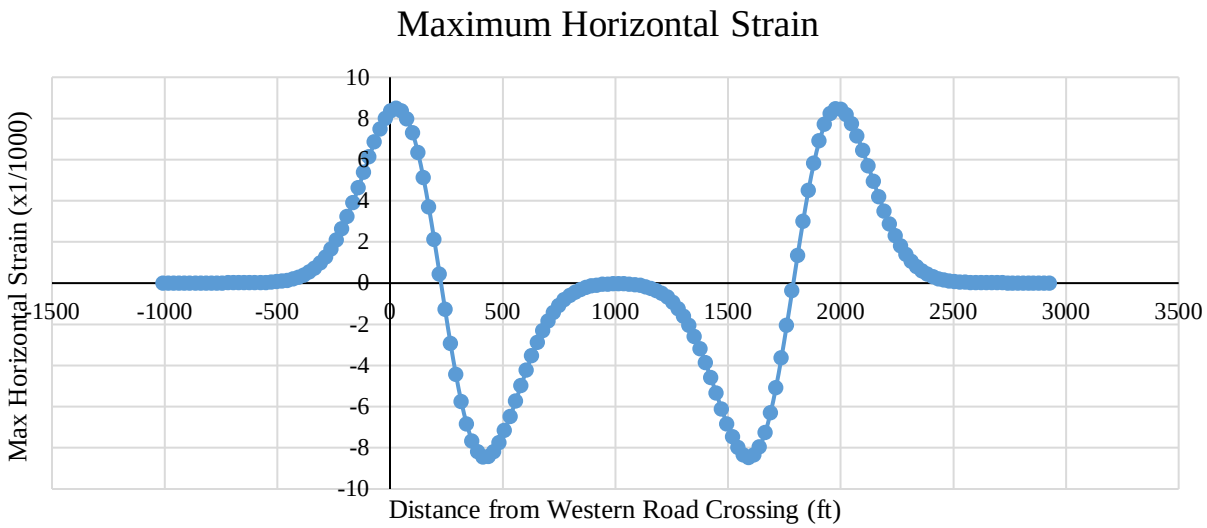

Figure 68 Preliminary model of maximum horizontal strain on I-70 alignment from undermining of Panel 15

An analysis of this model shows that, under the aforementioned parameters, the maximum amount of vertical subsidence expected is -4.66-feet. The horizontal deformations are expected to be a maximum of 1.53-feet in the north-south plane and 0.52-feet in the east-west plane, for a total maximum horizontal displacement of about 1.6-feet.

5.2.2 SDPS Model Refinement

Following the undermining of I-70 by Panel 15, the initial SDPS model was refined to emulate the movement of the highway surface. An analysis of the survey data collected from the highway alignment showed a significant difference in the predicted values from the preliminary SDPS model and the survey data. As a result of these differences, the SDPS model had to be modified from the preliminary model. The following factors for used for the refined model:

- Extraction thickness is approximately 7.25-ft (provided by Tunnel Ridge Mine)
- Supercritical Subsidence Factor = 59.5%

- Average overburden thickness is 675-feet
- Average percentage of hard rock is approximately 30% (upper extreme of typical range for greater Pittsburgh area)
- All pillars will remain rigid, minimizing vertical subsidence over the gate roads and creating an edge effect of 175-feet
- Surface points are at the initial topographic elevation
- The longwall face progresses at an average rate of 115 feet/day

Using SDPS, graphs were generated to represent the subsidence basin that formed over the extent of the longwall mining operation. The vertical subsidence, horizontal displacement, horizontal strain, and ground strain that could affect the ground surface as a result of mining Panel 15 were predicted. The visual representations of these factors for a cross section through the highway alignment can be seen below in Figure 69 through Figure 71.

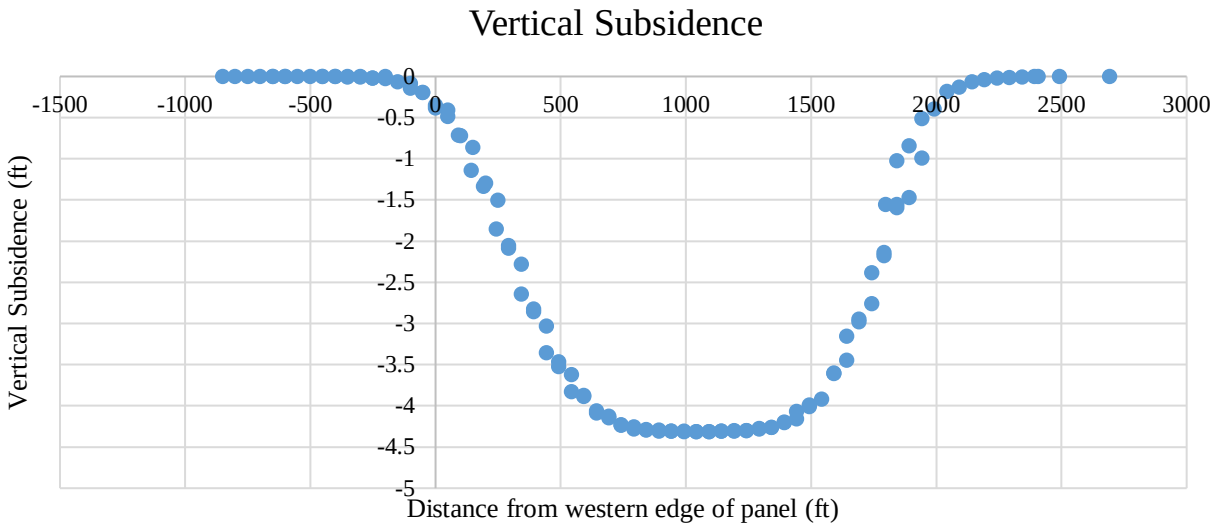

Figure 69 Refined model of vertical subsidence on I-70 alignment from undermining of Panel 15

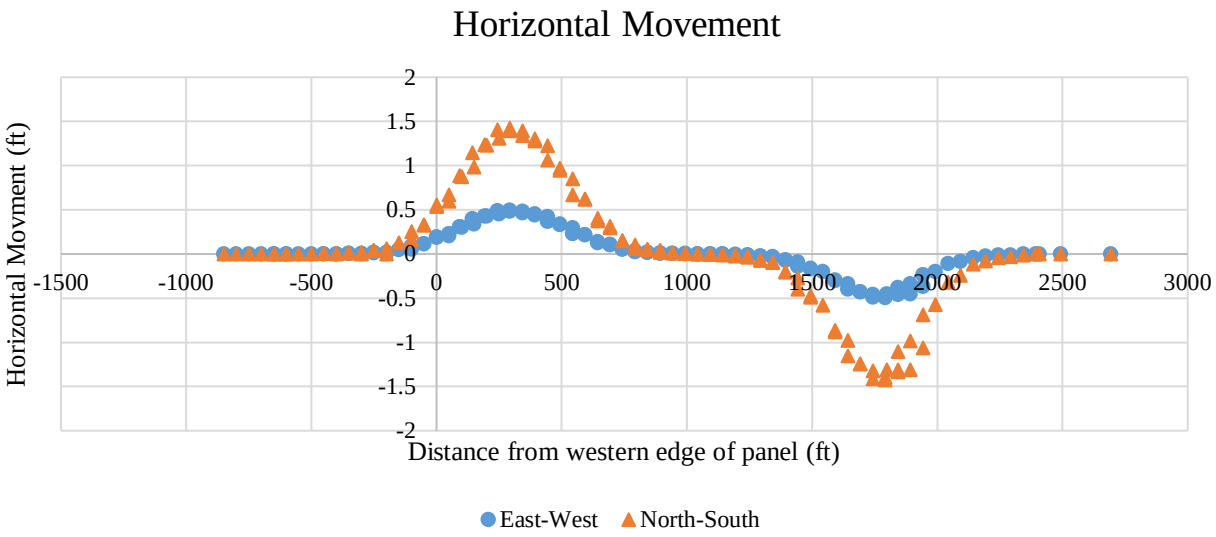

Figure 70 Refined model of horizontal displacement on I-70 alignment from undermining of Panel 15

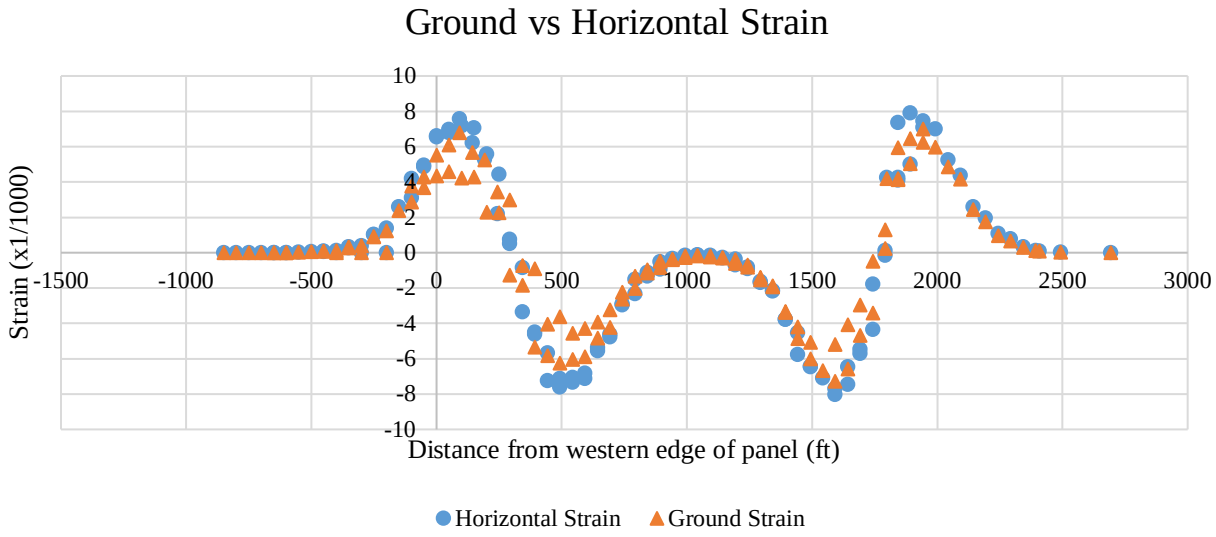

Figure 71 Refined model of maximum horizontal and ground strain and on I-70 alignment from undermining of Panel 15

An analysis of this model shows that, under the calibrated parameters, the maximum amount of vertical subsidence expected is -4.31-feet. The horizontal deformations are expected to be a maximum of 1.43-feet in the north-south plane and 0.49-feet in the east-west plane, for a total maximum horizontal displacement of about 1.5-feet.

5.2.3 Comparison of Predictions from SDPS Model with Observed Deformations

Based on the refined SDPS model, the vertical subsidence and horizontal deformations predicted can be compared to the final survey data. Due to the nature of real survey data and the presence of surface irregularities, no model will be able to match the data perfectly. Figure 72 through Figure 74 show the correlation between the SDPS model data and the survey data.

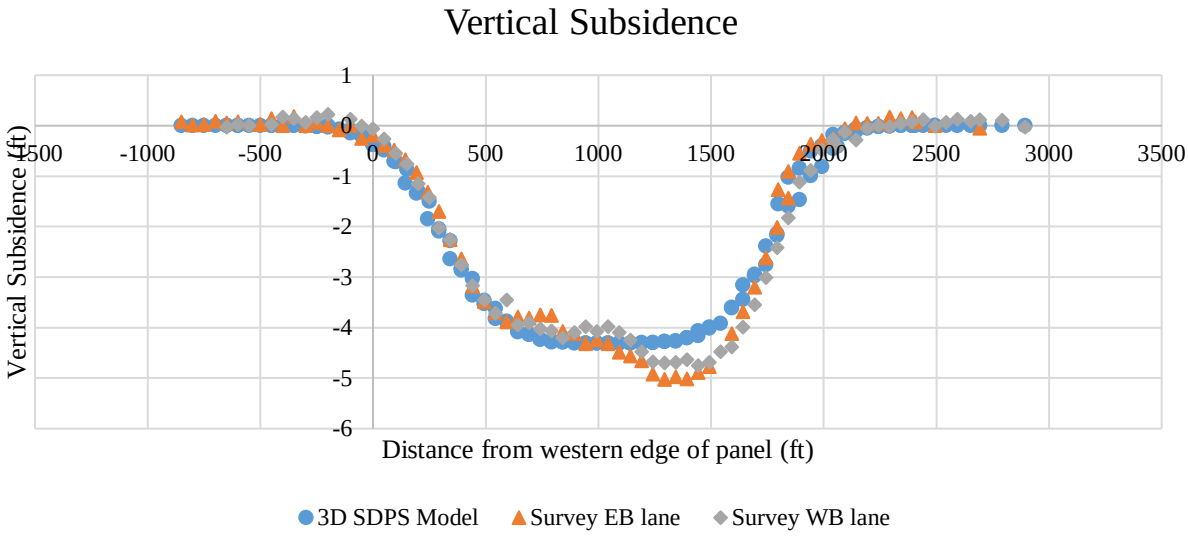

Figure 72 Vertical subsidence relationship between refined SDPS model and PennDOT survey data

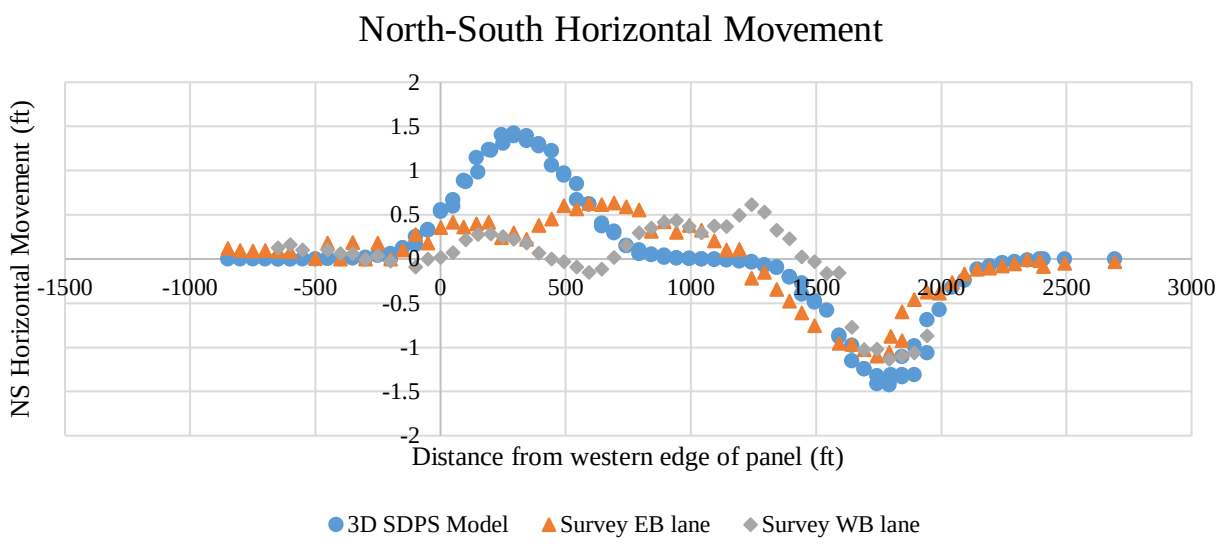

Figure 73 North-south horizontal movement relationship between refined SDPS model and PennDOT survey data

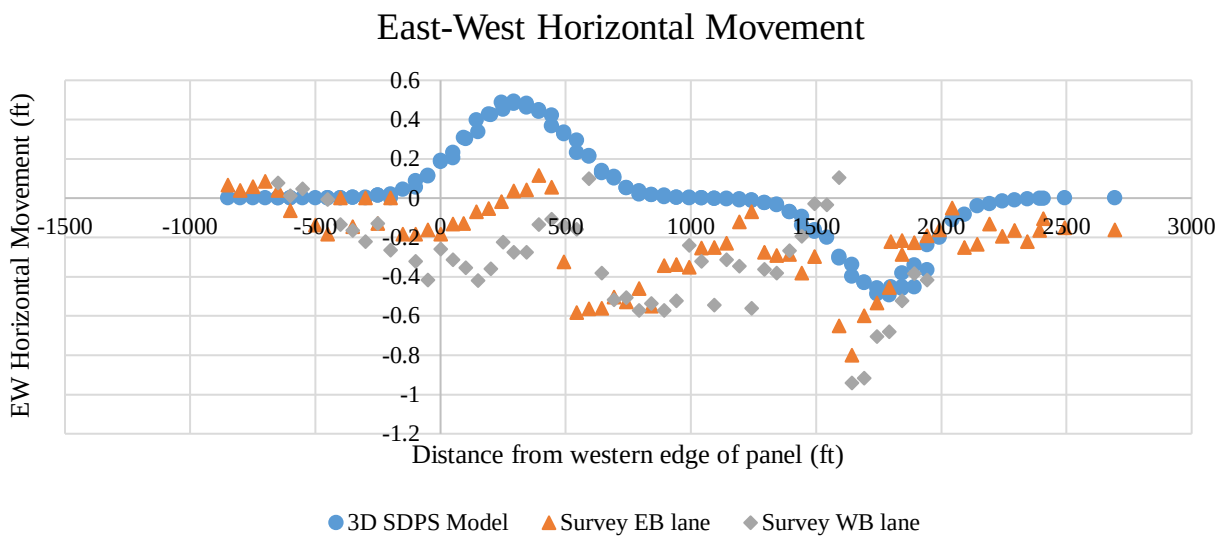

Figure 74 East-west horizontal movement relationship between refined SDPS model and PennDOT survey data

These figures show the relationship between the model predictions and the survey data. Looking at Figure 72, it is evident that the model is well calibrated to the observed highway movement; the area in the figure that shows subsidence greater than the model is the location of embankment #1, which experienced additional vertical movement due to consolidation and spreading of the fill. Unfortunately, the horizontal deformations observed did not match those predicted by the model. The inconsistencies displayed in Figure 73 and Figure 74 are likely due to the variation in the fill and cut materials, the mitigation techniques employed, and the damage that occurred on the surface.

The impact of the central embankment, asphalt relief sections, and surface damage can be seen in Figure 75 and Figure 76. Each lane and direction of movement was compared separately to better understand the pavement movement. As can be seen in Figure 75, both the north-south and east-west horizontal movements on the eastbound lane experienced substantial deviations from what was predicted west of the location of the large blow-up and tensile crack at EB11+05. It also shows that both asphalt relief sections impacted the east-west and north-south horizontal movement, with more significant deviation caused by the western asphalt relief section. Based on this data, it appears that the sheared guiderail and the edges of the central embankment had little correspondence with the horizontal movement of the roadway.

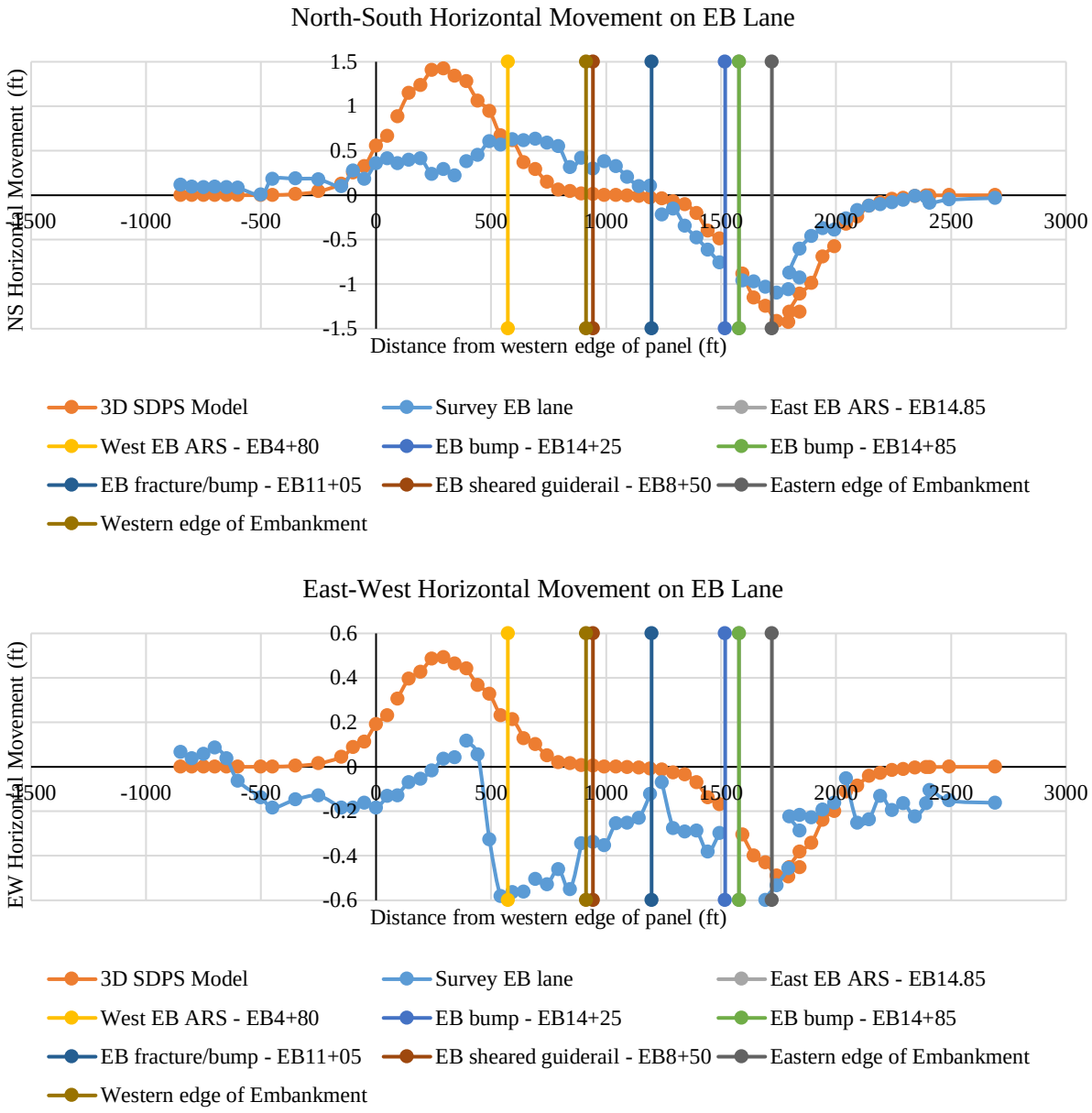

Figure 75 Horizontal on Eastbound lane of I-70 compared with location of surface features

As can be seen in Figure 76, both the north-south and east-west horizontal movement experienced substantial deviations from what was predicted west of the location of the eastern asphalt relief section, which coincided with the formation of a substantial compression bump. It also shows that both asphalt relief sections also impacted the east-west and north-south horizontal

movement, with more significant deviation caused by the western asphalt relief section. Based on this data, both the sheared guiderail and the western edge of the embankment correspond with small deviations in the horizontal movement on the westbound lane.

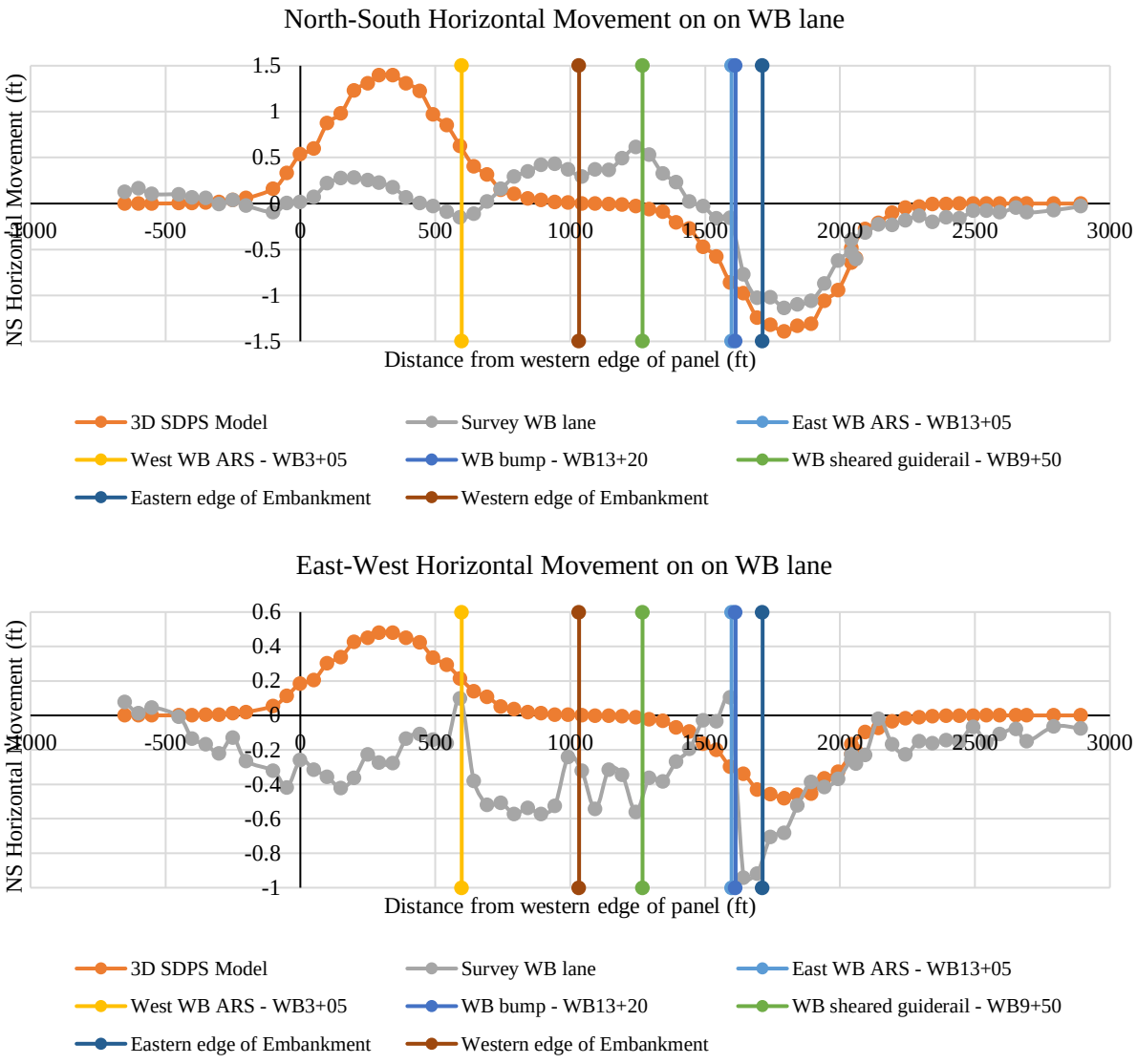

Figure 76 Horizontal on Westbound lane of I-70 compared with location of surface features

Through a review of this data, the influence of the asphalt relief sections on the behavior of the pavement structure is evident. These features allowed for the absorption of the compression stresses and strains different than that allowable in the concrete, causing different horizontal movements to occur on the highway than are predicted by the SDPS model created for soil surface materials. The data also suggests that the formation of significant compression bumps and blow-ups and the central embankment influenced the horizontal movements that were observed.

Table 10 shows the relationships between the preliminary SDPS model, the refined SDPS model, and the observed data at a variety of points throughout the subsidence basin. Comparing the preliminary model and the refined model, it can be seen that the refined model predicts 0.34-feet less vertical subsidence, 0.04-feet less east-west horizontal deformation, and 0.11-feet less north-south horizontal deformation than the preliminary model. This shows that the increased percentage of hard rock in the overburden lessens the effects of subsidence on the surface, which better represented what was observed on the highway.

Comparing the results of the calibrated model and the observed results, it is evident that the model fits the data well. The percent error between the vertical profile and the observed data is less than 20%, which indicates a good correlation. Contrarily, the horizontal deformations do not fit the model profiles as well, except on the eastern side of the study area. When compared with features that occurred on the surface, the horizontal movement indicates the influence of the pavement, asphalt relief sections, slopes and colluvium in the surface behavior.

Table 10 Comparison of subsidence values between SDPS models and PennDOT survey data

		Distance from Western Panel Edge (ft)	Vertical Subsidence (ft)	EW Horizontal Deformation (ft)	NS Horizontal Deformation (ft)	Maximum Horizontal Strain (1/1000)	Ground Strain (1/1000)
Preliminary Model	POI 1	0	-0.585	0.275	0.795	8.290	--
	POI 2	500	-4.270	0.202	0.587	-7.396	--
	POI 3	1000	-4.656	0.000	0.000	-0.043	--
	Max	--	0.000	0.532	1.540	8.479	--
	Min	--	-4.656	-0.532	-1.540	-8.479	--
Calibrated Model	POI 1	0	-0.353	0.186	0.538	6.535	5.527
	POI 2	500	-3.524	0.335	0.948	-7.613	-3.623
	POI 3	1000	-4.311	0.003	0.002	-0.154	-0.281
	Max	--	0.000	0.493	1.426	7.887	6.997
	Min	--	-4.313	-0.493	-1.427	-8.029	-7.274
Highway Alignment Survey Data	POI 1	0	-0.263	-0.315	0.072	--	--
	POI 2	500	-3.732	0.392	-0.037	--	--
	POI 3	1000	-4.067	-0.538	0.389	--	--
	Max	--	0.224	0.632	0.392	--	--
	Min	--	-5.031	-1.136	-0.917	--	--

5.3 Subsidence Modeling Limitations

Like with any prediction model, there is a limit to the efficacy of the empirical, profile, and SDPS models. As applied in this analysis, the empirical relationships are used to predict the values of parameters that can be used to characterize the subsidence basin, the profile function is used to predict a two-dimensional subsidence profile through a cross section of the longwall panel, and the SDPS model is used to predict a two-dimensional profile through a cross section of the longwall panel or a three-dimensional profile of the longwall panel.

As mentioned previously, the empirical relationships used for the first method of prediction are based on data gathered over years of mining in the Pittsburgh Coalbed. The data was compiled and summarized by a series of equations that can be used to predict the size and shape of the

subsidence basin. However, the validity of the implementation of these equations for current and future longwall mining operations is dependent on the accuracy of the initial data, the conditions under which the initial data was collected, and the conditions under which the new longwall panel is being mined. As such, variability in factors such as overburden height, overburden geology, and panel dimensions can impact the ability to accurately apply these empirical relationships to be used to predict longwall subsidence (Saeidi et al., 2013).

Like the empirical relationships, the profile functions were developed to match data gathered and observed conditions from previously mined longwall panels. As such, the limitations of the empirical relationships also apply to the profile functions. In addition to these limitations, the profile function also has the added limitation of being based on a mathematical equation. This means that the subsidence profile is simplified to follow a constant curve.

As the SDPS program is more sophisticated than the other models, it has additional limitations. The program utilizes the influence function which considers the displacements caused by subsidence on the surface as a function of the sum of surface subsidence due to the extraction of an infinite number of elements in the coal seam. As such, the method requires a lot of assumptions to model the displacements. In addition to the assumptions made by the program, there are additional limitations associated with the SDPS program. It does not account for material properties or geologic features in the overburden, meaning that the occurrence of features such as sandstone channels will not affect the shape of the subsidence basin predicted. The program also does a poor job of estimating the compaction of the gob, especially adjacent to the gateroads, requiring the manual modification of the edge effect factor. It also is limited in its ability to determine the impact of irregular topography or surface features, such as escarpments and embankments. These limitations could impact the profile of the predicted subsidence basin.

6.0 Discussion

6.1 Horizontal Movement and Damage

Many interesting trends were observed regarding the behavior of the pavement surface when subjected to longwall subsidence by reviewing the observations made during the undermining process. As can be seen in Figure 63 and Figure 64, the trends in the observed features show that the tensile features, such as separations and widened contraction joints, tended to occur within 300-feet beyond the longwall face and 150-feet behind the longwall face. Once the longwall face was approximately 150-feet past a point, the surface forces switched from tension to compression, causing compression related distresses, such as blow-ups. These distresses tended to concentrate in the asphalt relief sections, as these sections did not have a concrete base and, therefore were able to absorb additional movement.

A particularly interesting distress observed was the occurrence of the large transverse crack that formed on the eastbound lanes that then transitioned into a blow-up. Side by side images of these failures can be seen in Figure 77. The transverse crack that occurred in this location was 2.5-inches wide, making it the largest that formed on the pavement surface. The section of this fracture in the shoulder transitioned into a 7-inch tall blow-up, while the other sections of the initial fracture remained open as a crack. This distress developed halfway between two contraction joints in the asphalt that were cut 40-feet apart. Generally, the contraction joints were placed 20-feet apart in the existing concrete below the asphalt. Therefore, this contraction joint must have been missed when the joints were sawed in the overlay above the existing contraction joints in the underlying jointed plain concrete pavement. The large opening of the joint in the underlying

concrete pavement beneath the overlay likely resulted in the reflection of this movement up into the overlay.

This failure was located about halfway between the two asphalt relief sections on the eastbound lanes. The blow-up associated with this failure formed only in the shoulder, which did not have predefined areas of the concrete slab removed and filled with asphalt to absorb the compressive forces. As such, the asphalt relief section allowed the mainline lanes to contract to a larger extent as compared to the concrete shoulder. This nonuniform contraction between the mainline and the shoulders most likely contributed to the blow-up that developed in the shoulder. The formation of this failure at this location emphasizes the importance of the joints and the asphalt relief sections in the behavior of the pavement when undermined.

Figure 77 Image of tensile crack that formed at EB 11+05 on February 5 (left) and compression bump that formed in shoulder at EB 11+05 on February 6 (right)

Another interesting distress is the shear failures that formed throughout the study area, primarily along the rumble strip between the lane and the shoulder. In this case, shear failures are caused by differential movement between the outside lane and the shoulder. An analysis was

performed comparing the movement of the highway alignment points in the outside shoulders with the movement of the contraction joints in the travel lanes. The results of this analysis around the eastern asphalt relief section on the eastbound travel lane can be seen in Figure 78. It shows that the travel lanes primarily moved towards the asphalt relief sections while the shoulders moved towards the slope, confirming that the shear failures indicate differential movement. However, the occurrence of these shear failures in the rumble strips rather than on the asphalt seam indicates that the tie bars connecting the concrete slabs in the shoulder and travel lanes likely needed to deform or shear before these failures could develop.

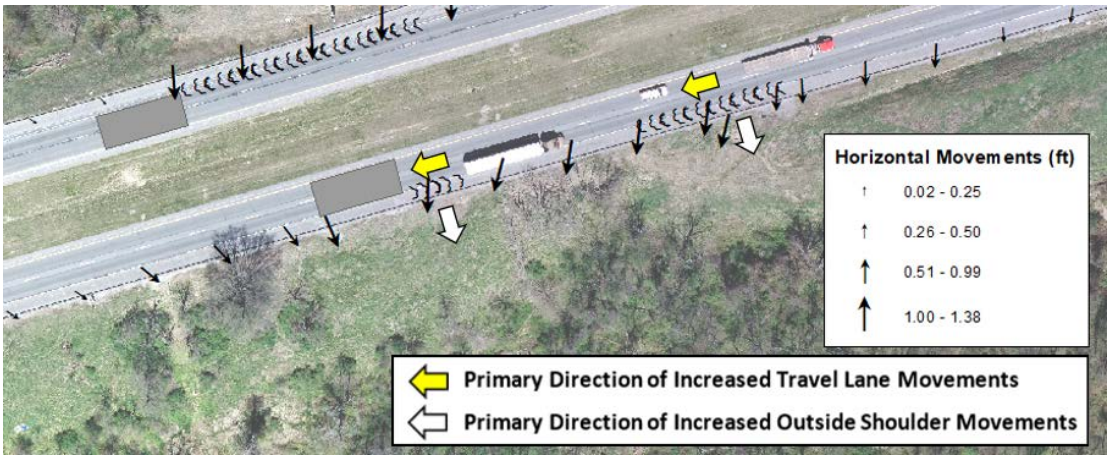

Figure 78 Map showing primary direction of joints on highway surface (yellow) and highway alignment points on the outside shoulders (white)

To better understand the cause of the distresses exhibited on the highway surface, the concentration of horizontal movement on the surface should be considered to reveal important relationships. As can be seen in Figure 79 and Figure 80, the damage observed on the highway tended to form in the areas experiencing large horizontal movements.

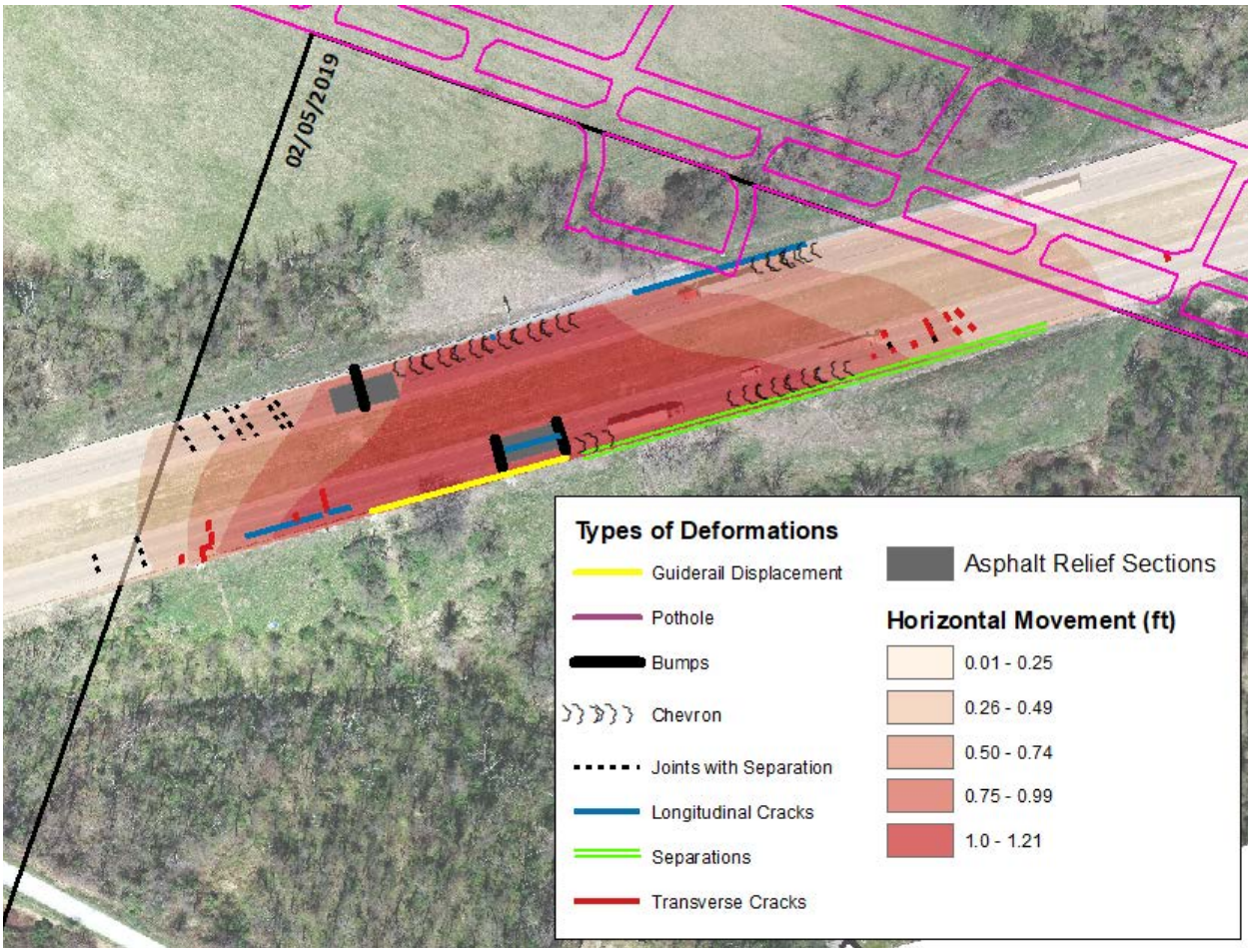

Figure 79 Highway observations in areas of large horizontal movements on February 5th

Figure 79 shows the distresses observed on the highway in the areas of high horizontal movement on February 5th. Damage observed in this region on this day included three compression bumps in the asphalt relief sections and extended shear failures on both sides of the highway. Significant lane-to-shoulder separations and guiderail displacements were also observed on the eastbound lanes.

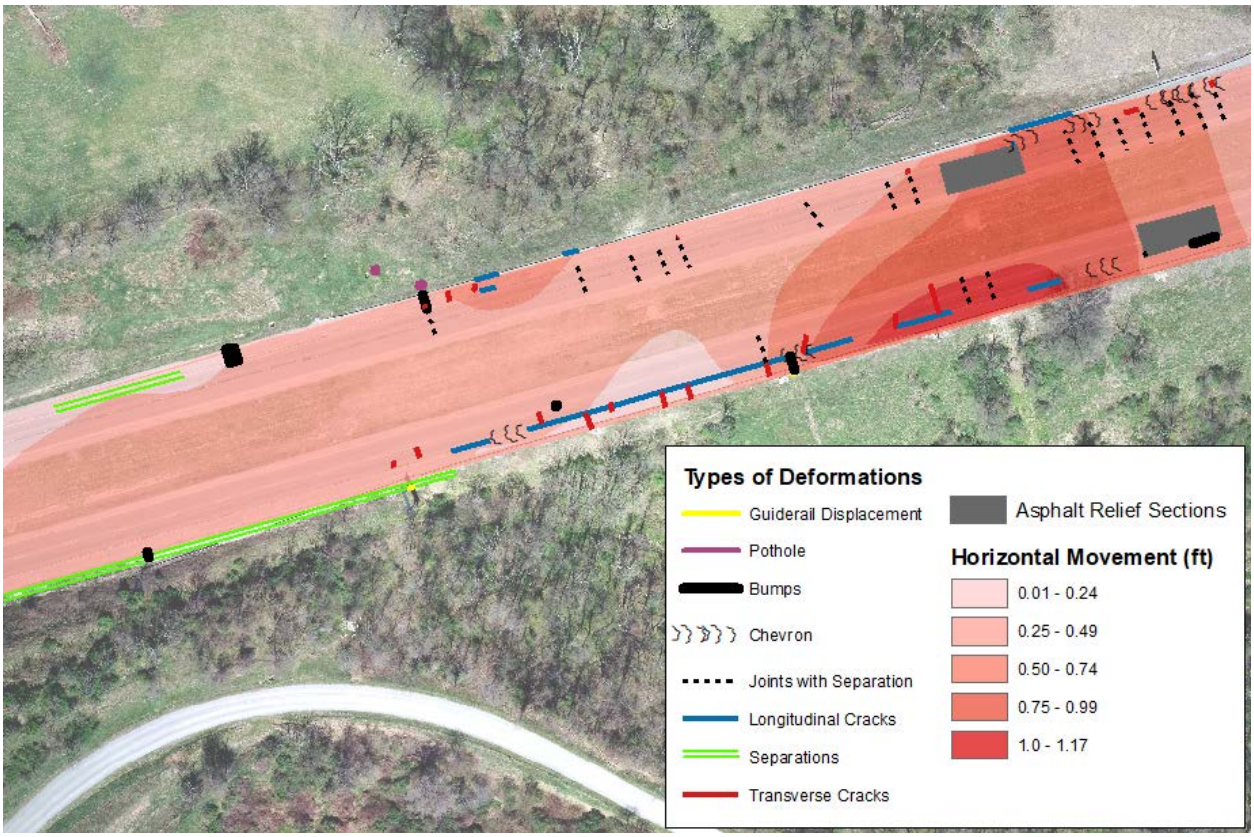

Figure 80 Highway observations in areas of large horizontal movements on February 14th

Figure 80 shows the distresses observed on the highway in the areas of high horizontal movement on February 14th. Damage observed in this region on this day included the formation of a large blow-up on top of an existing transverse crack, the widening of joints, transverse cracking, and the formation of longitudinal cracks in the rumble strip.

The horizontal movement between February 14th and February 19th was relatively consistent at a moderate magnitude along the entire extent of the highway within the study area, dissipating slightly to the west of the western asphalt relief sections. Despite the moderate magnitude of horizontal movement, most of the damage on the western side of the highway was observed at this time. Distress observed in this region can be seen in Figure 52 and included lane-to-shoulder separations, widened contraction joints, and transverse cracks.

Based on the review of the distress observed in relation to horizontal movements, it is evident that there is a relationship between the large horizontal movements and the occurrence of highway distress on the eastern side of the study area. This is demonstrated by the formation of large compression bumps and blow-ups, shear failures, and longitudinal cracks in areas that were subjected to horizontal movements greater than 1-foot.

However, on the western side of embankment #1, the highway surface did not experience incremental horizontal movements greater than 1-foot, meaning that the relationship between the horizontal movement and damage is less evident. This section of the study area experienced horizontal movement gradually and in smaller increments between February 14th and March 7th. It can also be observed that the western side of the highway experienced less damage than the eastern side. This indicates that the gradual movements may have given the pavement structure a chance to adapt to the movement rather than causing immediate failure, which further suggests that there is a relationship between the magnitude of horizontal movement and the amount of damage that occurs on the highway surface.

6.2 Pavement Behavior

As described previously, the highway surface experienced significant deformation as a result of the undermining event. The deformations occurred in both the vertical and horizontal planes with as much as 5-feet of vertical elevation drop in the center of the panel and as much as 2-feet of horizontal movement within the panel study area. By reviewing the horizontal movements displayed in Figure 36 and Figure 42 through Figure 46 it is evident that the highway twisted throughout the study area. As can be seen in Figure 37, there appears to be a pivot point

in the central embankment, with the eastern side of the highway moved towards the center of the panel, while the western side of the highway moved parallel towards the gateroads in the direction of the longwall face. Thus, while the vertical component of the subsidence basin performed according to the predictive models, the horizontal component of the subsidence basin was influenced by features within the highway alignment.

This twisting was likely caused by the structural system of connected concrete slabs. The pavement in the travel lanes was composed of 13-inch thick structural concrete slabs, 20-feet in length. The travel lanes were contained on each side by Type 1 concrete shoulders. Both the travel lanes and the shoulders were overlaid with asphalt prior to the undermining. The concrete slabs were connected to each other with dowel bars and were connected to the shoulders with rebar tie bars. Although the steel design was not specified in the plans received from PennDOT, based on similar roads constructed the transverse joints should have been reinforced with 1.5-inch diameter dowels placed 12 inches apart in both the travel lanes and the shoulders, with the first dowel bar 6 inches from the lane-shoulder joint. The longitudinal joints should have #5 deformed bars spaced 30 inches apart. As a result of these reinforcing bars, the pavement acted as a structural system, preventing individual slabs from experiencing large horizontal deformations without moving the adjacent slabs.

The movement of the road surface was likely further influenced by the material properties of the embankment and the pavement subbase. As the embankment appeared to act as a pivot point for the system, the granular fill material in the embankment may have absorbed movement and promoted rotation. Additionally, the pavement subbase consisted of an open graded granular material, which likely allowed the pavement surface to slide like it was on marbles and act independently from the material below. The presence of an open graded granular base was also

beneficial in reducing stress build-up within the surface layer as it was able to act as a slip plane between the highly mobilized support layers and the pavement surface. This combination of material properties would have encouraged movement, and when combined with the structural design of the pavement, could be responsible for the twisting observed.

The dowel bars and tie bars may also have mitigated the damage to the surface. The dowel bars restricted the slabs from shifting out of alignment, while the tied shoulders, that ran continuous through the asphalt relief sections in the mainline, also helped in keeping the mainline lanes from migrating out of alignment. A key benefit was that the dowel bars facilitated large increases in joint width without compromising joint performance. The tension and compression forces that occurred during subsidence caused these joints to widen and close and the functioning dowels were able to accommodate that. The tied shoulders and functioning dowels also may have prevented some of the more catastrophic failures of the pavement surface, such as large separations of the shoulder and the lanes, transverse offsets between slabs, and vertical misalignment between slabs. These types of failure would have been far more destructive and dangerous to drivers but were not observed during this undermining event.

6.2.1 Contraction Joints

The contraction joints located throughout the pavement sections opened and closed throughout the undermining process to accommodate the flexural movement within the pavement independent of the translational and vertical movements of the subbase. The joints opened significantly, as much as 0.75-inches in places, which was nearly three-times their original width. However, by the end of the undermining process, almost all the joints had returned to their initial widths. The full-depth asphalt sections constructed on each end of the section of undermined

highway made these large joint openings possible, while limiting the occurrence of blow-ups. The doweled joints allowed the pavement to expand and contract as the subsidence basin formed while restraining the slabs from becoming misaligned, thus limiting the damage that occurred.

Though the joints were only designed to withstand typical temperature variations, during the undermining event they acted as locations within the structural material for the pavement to expand, contract, and deform. The width of the crack at the contraction joint below the joint reservoir sawed into the surface can be estimated using Equation 6-1 (AASHTO, 1993). The values utilized in these equations were determined using typical properties for concrete and the AASHTO 1993 Pavement Design Manual.

$$\Delta L_{opening} = 12cL(\alpha * \Delta T + \varepsilon) = 0.16 \text{ in} \quad \textbf{[6-1]}$$

Where: c = 0.8 for an unstabilized subgrade
L = 20-feet slabs
α = thermal coefficient for limestone aggregate = $4.5x10^{-6}/°F$
ε = drying shrinkage = $4.5x10^{-4}\ in/in$
ΔT = temperature of concrete at time of set – temperature of concrete at time of interest
temperature = 85 – 0 = 85°F

Based on Equation 6-1, the joints were designed to withstand small amounts of expansion and contraction due to temperature variation. The sealant was installed in the joints to accommodate such movement. When subjected to greater strains during the undermining, the joints were able to open further than this design value but were not able to close more than the fractions of an inch allowable by the crack between the pavement slabs. Fortunately, the undermining occurred during the winter months, meaning that the joints were open due to the cold

and provided slightly more space for compression. Evidence of the joints opening far beyond the allowable limit can be seen in pictures that were taken of the highway during the undermining, some of which can be seen in Figure 81. These images show the joints opening far beyond what could be accommodated by the joint sealant, resulting in the separation of the sealant from the asphalt. From these pictures it can be determined that many of the joints opened two and three times their original widths.

Figure 81 Field images of open pavement joints during undermining

6.2.2 Asphalt Relief Sections

As described previously, four asphalt relief sections (2 per direction) were constructed in areas estimated to be in the compression regions just inside the inflection plane of the subsidence basin (Figure 61). These sections were constructed by removing 60 feet of concrete in both travel lanes, creating 24-foot by 60-foot sections, and replacing it with full depth asphalt. As asphalt is more compressible than concrete, it can better absorb the movement caused as the subsidence basin forms. The doweled concrete shoulders were maintained along both sides of the full-depth asphalt sections to provide stability in these regions by preventing lateral misalignment.

Much of the distress that was observed on the highway during the undermining was concentrated around these asphalt relief sections, indicating they performed as intended. As previously mentioned, on the eastern side of the undermined section, large compression bumps formed within the asphalt relief sections on both the eastbound and westbound lanes. These compression bumps were about 1-foot high and needed to be milled so that vehicles could safely pass through this region. The formation of this type of failure indicates that large amounts of compressive forces were concentrated in this location.

The LiDAR survey data was used to examine the compression in the asphalt relief sections. Though all of the sections showed some amount of compression, the asphalt relief section on the eastern side of the westbound lanes, depicted in Figure 82, demonstrates the largest change. This relief section compressed between 1-foot and 1.5-feet over the length of the section, corresponding to a strain of 1.7% to 2.5%. These values are only estimates though, as the damage on the highway surface obscures the ability to see the exact edges of the relief section in the LiDAR points; however, the magnitude of movement observed is well above the accuracy of the scans, indicating that the compression depicted is more than survey error.

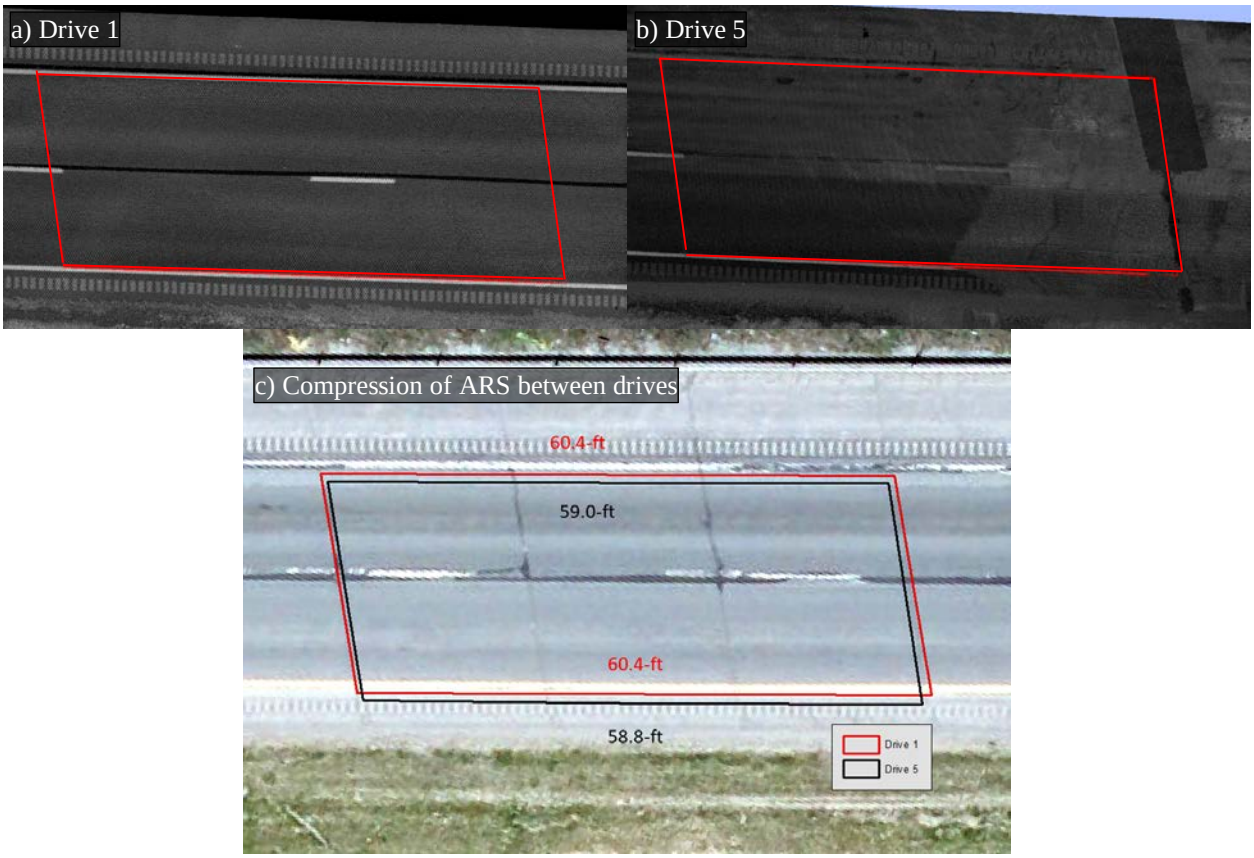

Figure 82 Movement of eastern asphalt relief section on westbound lanes showing compression of the roadway after the longwall face passed beneath the highway section in LiDAR scans (a and b) and digitized boundaries (c)

The formation of the shear failures also tended to concentrate in the areas around the asphalt relief sections. As previously mentioned, these shear failures resulted from opposing forces concentrating along an interface due to differential movement of the shoulder and travel lanes. As the concrete shoulder adjacent to the asphalt relief sections was not removed and replaced with full-depth asphalt, it was unable to compress to the same order of magnitude of the travel lanes. The shear failures occurring in these areas indicate that the travel lanes were able to accommodate larger compressive deformation across the asphalt relief sections than possible through the adjacent continuous concrete shoulder.

These shear failures occurred in the rumble strips as opposed to along the lane-shoulder joint. This indicates the tie bars connecting the shoulder to the travel lanes likely had to be sheared or deformed to accommodate the differential movement between the two lanes. Had these tie bars not been there, it is possible that the asphalt relief sections would have experienced and absorbed even more movement, as the concrete in the travel lanes adjacent to the full depth asphalt would not have been locked in place by the concrete in the shoulders.

6.3 Implication of Using Mitigation Techniques to Prevent Impacts to the Highway Pavement

Panel 15 will not be the last longwall panel that impacts a section of interstate in Pennsylvania. There are significant coal reserves that remain untouched in the Pittsburgh Coalbed that are conducive to longwall mining. Some of these coal reserves pass beneath existing Pennsylvania interstates I-70 and I-79. As such, it is very likely that sections of the interstates will be undermined again in the future and mitigation techniques will have to be employed based on things learned from previous longwall panels, including Panel 15.

Using the calibrated SDPS model created for Panel 15, the magnitude of subsidence and strain can be predicted for future longwall panels. Assuming that these panels will have a similar overburden type, width, extraction thickness, and gateroad design, the same parameters used to model Panel 15 can be used to model theoretical panels with higher and lower overburdens. The predicted vertical subsidence and horizontal strain, which can be used as a representation of damage, from these theoretical panels can be seen in Figure 83 and Figure 84.

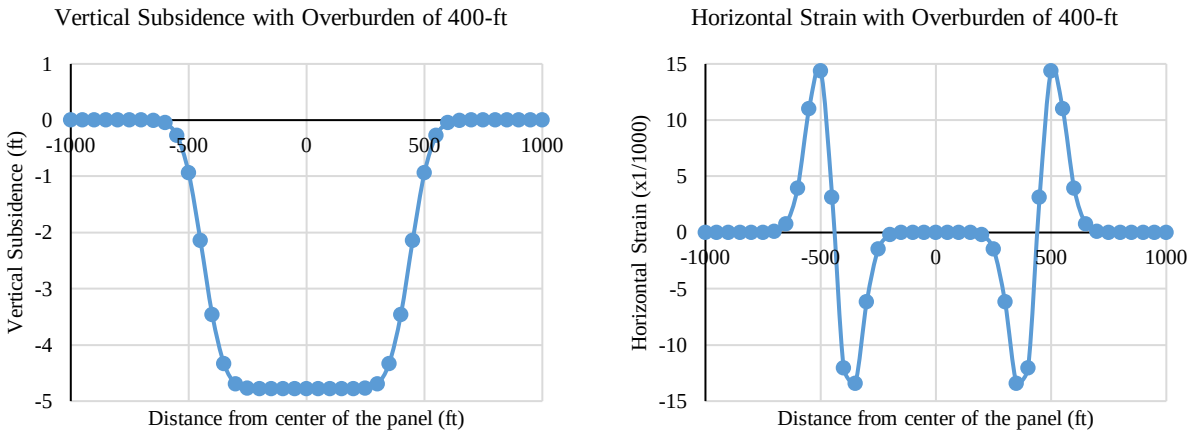

Figure 83 Vertical subsidence (left) and horizontal strain (right) predicted by SDPS for a panel with an overbuden of 400-feet

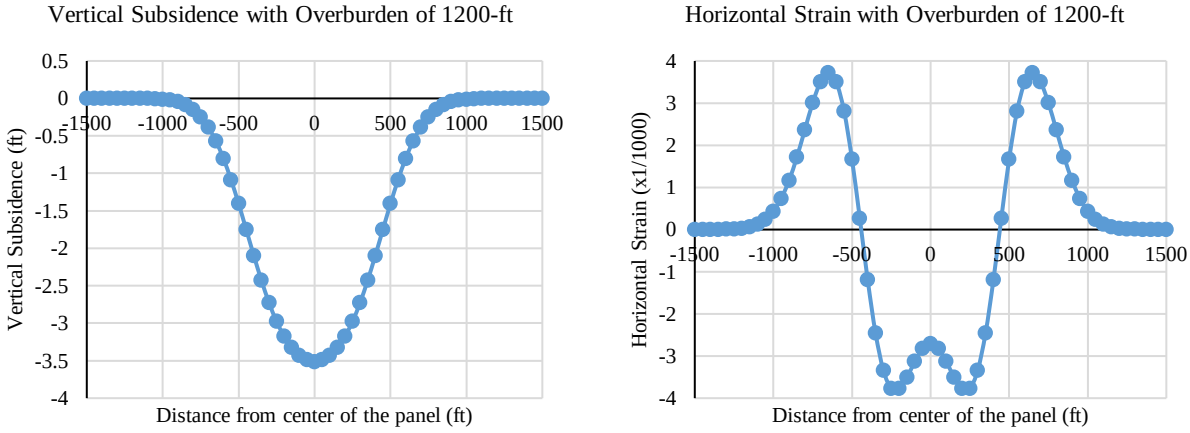

Figure 84 Vertical subsidence (left) and horizontal strain (right) predicted by SDPS for a panel with an overbuden of 1200-feet

Though the mitigation techniques used on Panel 15 worked well, there may be ways to improve them for future panels, especially those with a lower overburden. The proposed mitigation techniques include variations on the contraction joints and asphalt relief sections.

6.3.1 Contraction Joints

During the undermining of Panel 15, the contraction joints spaced 20-feet apart in the concrete beneath the asphalt overlay were also cut into the asphalt overlay and provided the roadway with locations to expand, contract, and deform. Through observation of Panel 15, it was determined that these contraction joints were critical to the behavior of the highway during undermining. As such, it can be theorized that additional contraction joints placed in both the concrete and asphalt overlay throughout a highway section being undermined could further improve the behavior of the pavement surface. Though Equation 6-1 dictates that no additional free space would be generated on the highway alignment by reducing the length of the concrete slabs, each additional joint would provide an additional location for expansion and deformation.

The theoretical models of future longwall panels at high and low overburdens in Figure 83 and Figure 84 show that the strains generated at low overburdens could be much higher than those experienced above Panel 15. If this is accurate, additional contraction joints would be necessary to help mitigate the damage caused by the additional strain. For a panel with an overburden of 400-feet that would generate twice as much strain on the surface (Figure 83), additional contraction joints would be necessary for them to have the same positive impact that the joints did above Panel 15.

6.3.2 Asphalt Relief Sections

Prior of the mining of Panel 15, the concrete was removed and replaced with full depth asphalt in four 60-foot sections of the travel lanes. These areas were intended to be placed in the areas of highest compressive strain to provide a more compressible material to accommodate the

large deformations. During the undermining, distress resulting from these compressive forces developed around these asphalt relief sections; compression bumps formed within these zones of relief and shear failures indicating differential movement between the travel lane and the shoulder formed on either side in the rumble strips.

As previously described, the differential movements indicate that the differences in stiffness between the full depth asphalt travel lanes and the shoulders with the concrete slabs may have inhibited the efficacy of the asphalt relief sections. To combat this concern, the concrete base could be removed from the shoulders in addition to the travel lanes. This would mean that the travel lanes would not be tied to a rigid structure and would allow the shoulder to compress at the same rate as the travel lanes. This change could permit additional movement in the asphalt relief sections and has been attempted outside of PennDOT's jurisdiction.

Though expanding the width of the asphalt relief sections into the shoulders would likely minimize the differential movement between the travel lanes and the shoulder, it could have adverse effects. By permitting additional movement in the asphalt relief sections, larger compression bumps could form in these areas, requiring more frequent milling of the features to maintain a passable road for drivers. In addition, removing all of the concrete base from a section of road would also remove all dowel and tie bars that held the road in place, meaning that the section could potentially slide out of alignment with the rest of the highway when subjected to undermining forces.

In addition to modifying the size of the asphalt relief sections, it may also be beneficial to modify the locations of these mitigation features. As can be seen in Figure 83, in panels with low overburdens, the areas of high compressive strain will be more concentrated towards the edges of the panel. As such, for these panels, it would be beneficial to move the relief sections closer to the

edges of the panels and make them longer to accommodate the increase in strain. Contrarily, in panels with high overburdens, the concentration of strain will be lower and more distributed throughout the panel, as can be seen in Figure 84. For these panels, placing additional asphalt relief sections in the center of the basin may be best to mitigate the damage caused by the strain. Even in the panels with medium overburden, an additional relief section could be beneficial. Smaller compression features occurred in the center of the Panel 15 study area, showing there was a buildup of compressive strain in this area as well that might have been mitigated by the flexibility of full depth asphalt.

7.0 Lessons Learned and Future Research

Though the analysis of Panel 15 was effective, and the panel's movements were able to be characterized, if the study was to be repeated a few changes should be considered. The following changes should be considered for future studies:

- Additional horizontal accuracy in all forms of surveys would also have been beneficial for analysis.
- Damage observations collected more frequently than once a week so that they could be better compared with the longwall face positions
- Implementation of redundancies to prevent the loss of tiltmeter data that occurred due to equipment malfunction and theft
- Additional tiltmeters positioned adjacent to westbound lanes to supplement the instruments placed next to the eastbound lanes. These additional instruments would have helped to characterize the far side of the road relative to the longwall face advancement
- Installation of clip gauges on the joints and strain gauges on the slabs to provide additional information as to the performance of the pavement

In addition to the modifications that should be considered for future studies listed above, the extraction of Panel 15 beneath I-70 inspired a number of additional areas of research. The following areas of study related to the undermining of I-70 could be pursued in future research endeavors:

- Consideration of the impact of an adjacent longwall panel being mined. Based on the study performed by Yancich of the Gateway panels mined in the 1980s, there is evidence that the mining of subsequent panels can affect areas over gateroads and previously mined panels.

As Panel 15 was the first panel in a district to be extracted and the behavior of the subsequent panel was not monitored, the opportunity to study this impact was missed.

- Consideration of the impact of weather and temperature on the pavement behavior when undermined. Panel 15 impacted I-70 during the winter months when the contraction joints were open, and the surface material was frozen due to the cold. Had the panel been mined in the spring or summer, the impacts on the highway and adjacent slopes could have been different.
- Consideration of the impact of the condition of road surface prior to undermining on its performance during a subsidence event. The section of I-70 considered in this study was newly paved, meaning that there was no damage to the highway surface prior to mining. Had the panel undermined a section of road with an older overlay, the impacts observed on the highway surface could have been different.
- Examination of the influence of the dowels and tie bars on the highway surface when undermined and how these bars deformed as the pavement surface moved.
- Examination of the influence of pavement materials on the performance of the road during undermining. Pavement properties such as the mix of asphalt and concrete and the type of subbase used should be considered. New variations on concrete or asphalt materials that would be more suitable to accommodate the longwall mining stresses and strains could also be considered as alternative designs.

8.0 Summary

The data collected during the PennDOT investigation has allowed for a thorough analysis of the behavior of an interstate pavement subjected to longwall mining subsidence. These observations have enhanced our understanding of how the formation of a subsidence basin caused by longwall mining, may impact highway alignments.

- The subsidence basin dropped the road surface as much as 4.3-feet in areas adjacent to the cut slopes. Additional vertical subsidence was observed on the highway adjacent to the center embankment.
- The subsidence basin caused as much as 1.5-feet of horizontal movement on the highway surface. More horizontal movement was observed on the eastern side of the study area than the western side. The eastern side of the highway section moved towards the center of the basin, while the western side moved towards the longwall face. This difference in direction of movement indicates twisting of the pavement structure, likely caused by the reinforced pavement structure.
- The central embankment experienced more than 2-feet of horizontal movement on the northern slope. Significantly less movement was observed on the southern slope. An additional 0.7-feet of vertical movement was in the center of the embankment. The additional horizontal and vertical movement observed on the central embankment indicated that the embankment experienced consolidation and lateral spreading during undermining. The data collected with the inclinometers supported the finding of lateral spreading.
- Pavement failures including transverse cracks, longitudinal cracks, compression bumps, blow-ups, shear failures, widened joints, separations between the edge of the slab and

adjacent soil, and guiderail deformations. The transverse cracks and widened joints occurred primarily in the travel lanes and resulted from tensile strain. The compression bumps and guiderail deformations resulted from compressive strain. The shear failures occurred primarily in the rumble strips between the outside travel lane and the outside shoulder as a result of differential movements.

- The empirical relationships and profile functions that were developed using panels previously mined in the Pittsburgh Coalbed show that the model can be used to effectively predict vertical subsidence. These relationships define a distance of about 165-feet between the edge of the longwall panel and the point where the surface subjected to longwall subsidence switches from tension to compression. Through an analysis of the observational data, it was confirmed that tensile features tended to occur within 165-feet of the longwall face, while compression features tended to occur once the longwall face was more than 165-feet away. This confirms that the empirical relationships were accurate in predicting the zones of compression and tension on the highway surface.
- The SDPS model matched the observed highway data very well in the vertical plane, except for the section of highway adjacent to the center embankment. The model did not match the observed highway data as well in the horizontal plane, except for eastern side of the highway before the asphalt relief section, indicating the impact of the asphalt relief sections on the pavement performance.
- Many of the critical failures that occurred on the pavement surface occurred in areas of high horizontal deformation.
- During the undermining event, the contraction joints opened as much as 0.75-inches in some places, which was nearly three-times the original width. These joints served as

locations within the structural pavement system to expand, contract, and deform during mining. Modifying the placement and frequency of these joints could mitigate subsidence damage from future undermining.

- The asphalt relief sections were areas of full depth asphalt that were constructed in the travel lanes in regions where the highest stresses and strains were expected to occur. As the asphalt is more compressible than the concrete, many of the compression bumps formed in these areas and the shear failures formed in the rumble strips due to differential movements between the outside lane and the shoulder. These sections proved to be an effective mitigation technique by concentrating the damage in one location for repair. Modifying the size, placement, and width of these relief sections could improve their ability to mitigate future subsidence damage.

9.0 Conclusion

The purpose of this study was to analyze and interpret the movement of the highway study area caused by the mining of longwall Panel 15. Panel 15 was approximately 1,200-feet wide and 14,500-feet long and crossed below the road at a 35-degree angle, causing about 3,300-feet of the highway alignment to be influenced by the mining. This mining activity formed a subsidence basin on the surface that caused the highway to move in horizontal and vertical directions.

During the undermining, data in the form of observations, surveys, and sensor measurements were collected to characterize the movement of the surface. Through a review of all this data, it was determined that the center of the road dropped about 4.3-feet adjacent to the cut slopes and nearly 5-feet over the central embankment. As it was constructed out of a granular fill, the embankment facilitated additional movement on the highway surface through its consolidation and spreading. Aside from the section of roadway directly over the embankment, the vertical subsidence basin formed on the highway surface behaved as expected. The horizontal movement, however, did not behave according to predictive models; during the subsidence event, the highway surface experienced twisting, facilitated by the connectivity of the reinforced pavement structure, with the eastern half of the study area moving towards the center of the basin and the western side of the study area moving towards the longwall face.

As a result of the significant horizontal movements, damage occurred to the highway primarily in the form of cracks, widened joints, and compression bumps. Throughout the study area cracks and contraction joints opened and then closed as the longwall face passed beneath the highway. Compression bumps formed in areas of large compressive stress; these features formed primarily in the areas adjacent to the asphalt relief sections, in which the concrete was removed

and replaced with full depth asphalt to accommodate large horizontal strains. Due to the concentration of damage, the contraction joints and the asphalt relief sections acted as the primary mitigation techniques to minimize damage on the pavement surface.

Longwall panels will likely pass beneath Pennsylvania interstates again in the future, just as they did in the past. Based on what was learned from the mining of Panel 15, a combination of mitigation techniques involving the asphalt relief sections, the contraction joints, and the pavement material properties should be considered for any future highway alignments being undermined by a longwall panel. As sections of highway continue to be undermined, more trends in the effects of longwall mining on interstates will be established, providing a greater understanding of impact of longwall mining subsidence on interstate alignments and pavement structures.

Appendix A Complete Record of Observed Features on Pavement

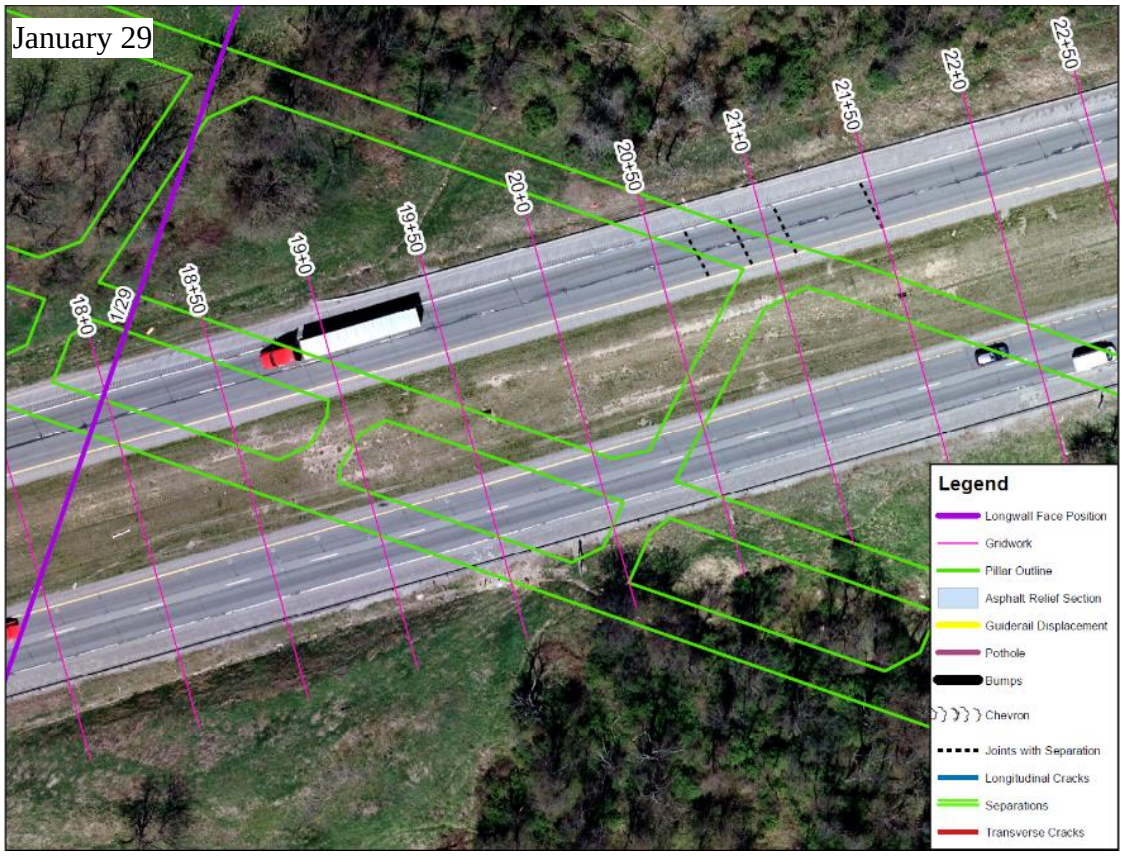

Appendix Figure 1 Damage observed on highway on January 29th

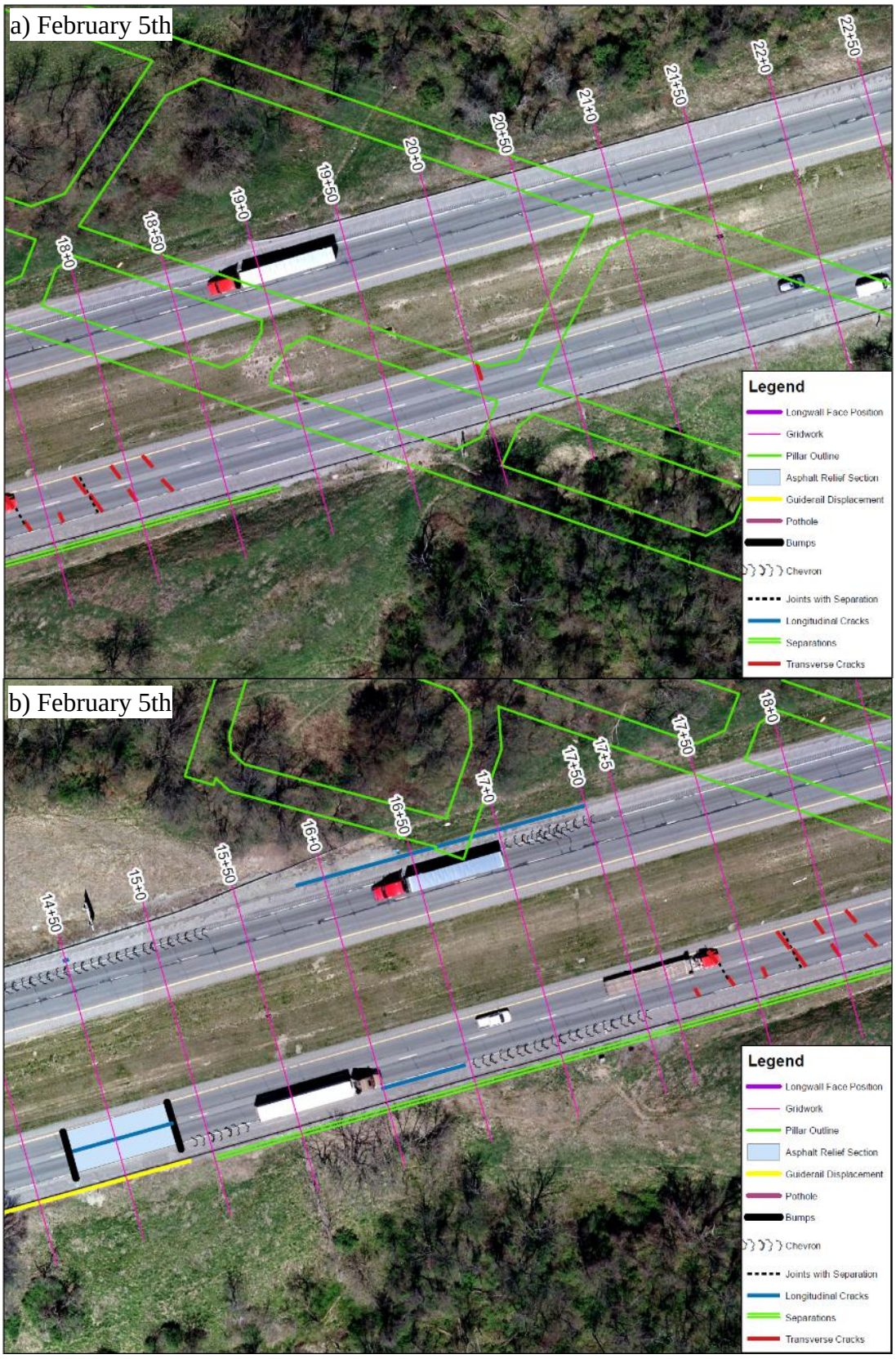
a) February 5th
18+0
18+50
19+0
19+50
20+0
20+50
21+0
21+50
22+0
22+50
Legend
Longwall Face Position
Gridwork
Pillar Outline
Asphalt Relief Section
Guiderail Displacement
Pothole
Bumps
Chevron
Joints with Separation
Longitudinal Cracks
Separations
Transverse Cracks
b) February 5th
14+50
15+0
15+50
16+0
16+50
17+0
17+50
17+5
17+50
18+0
Legend
Longwall Face Position
Gridwork
Pillar Outline
Asphalt Relief Section
Guiderail Displacement
Pothole
Bumps
Chevron
Joints with Separation
Longitudinal Cracks
Separations
Transverse Cracks

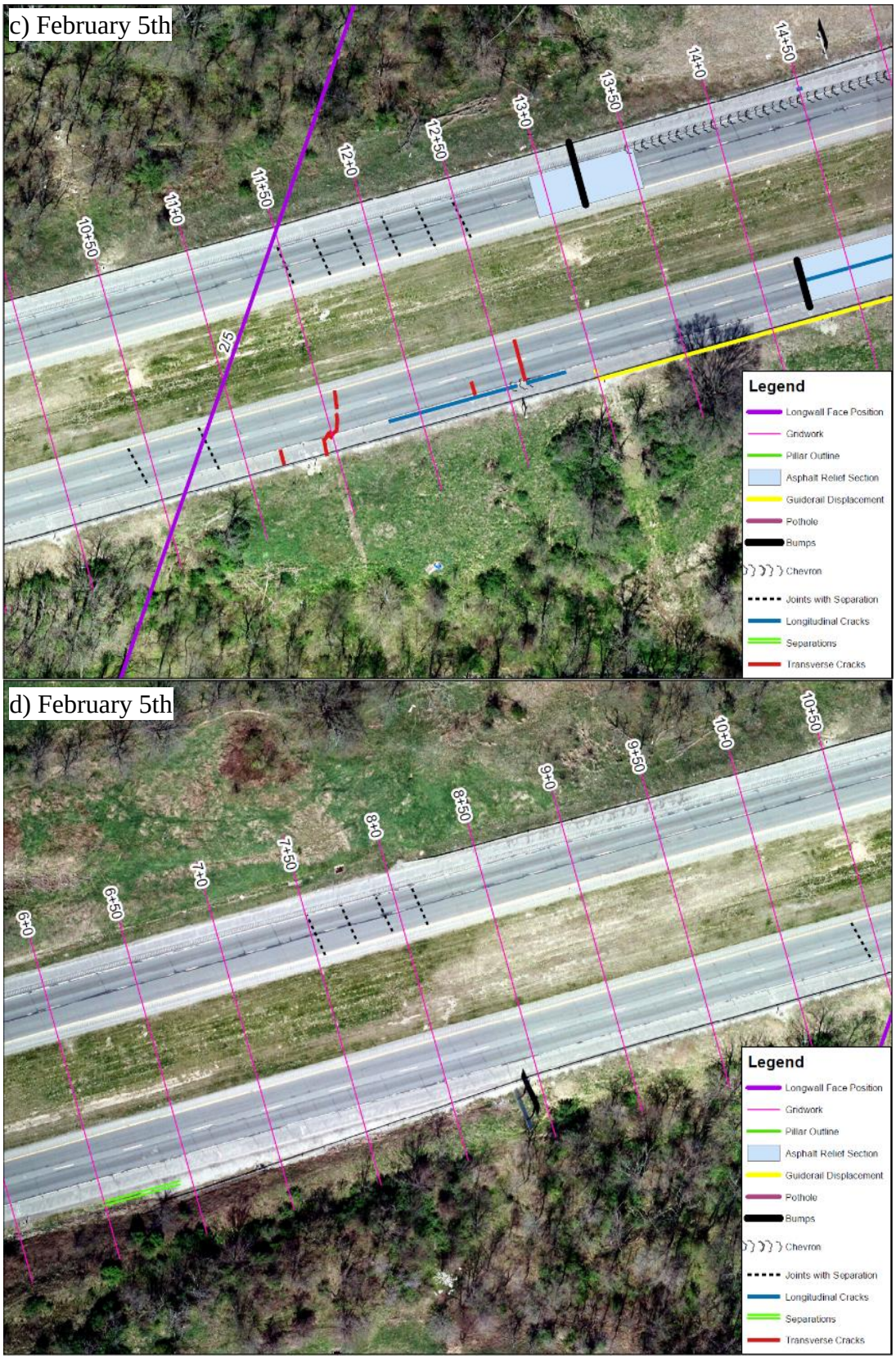

Appendix Figure 2 Damage observed on highway on February 5th

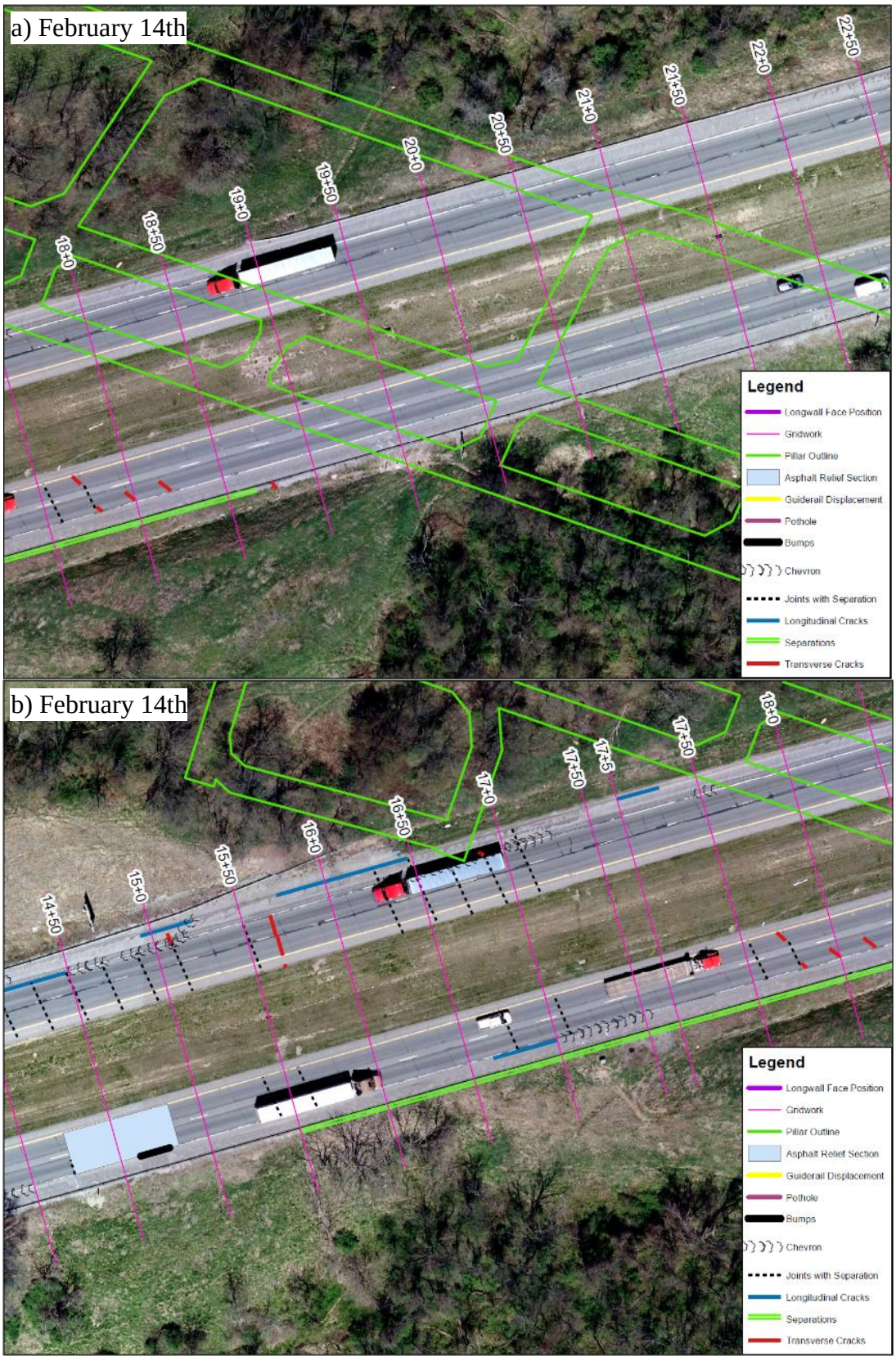
a) February 14th
18+0
18+50
19+0
19+50
20+0
20+50
21+0
21+50
22+0
22+50
Legend
Longwall Face Position
Gridwork
Pillar Outline
Asphalt Relief Section
Guiderail Displacement
Pothole
Bumps
Chevron
Joints with Separation
Longitudinal Cracks
Separations
Transverse Cracks
b) February 14th
14+50
15+0
15+50
16+0
16+50
17+0
17+50
17+5
17+50
18+0
Legend
Longwall Face Position
Gridwork
Pillar Outline
Asphalt Relief Section
Guiderail Displacement
Pothole
Bumps
Chevron
Joints with Separation
Longitudinal Cracks
Separations
Transverse Cracks

c) February 14th

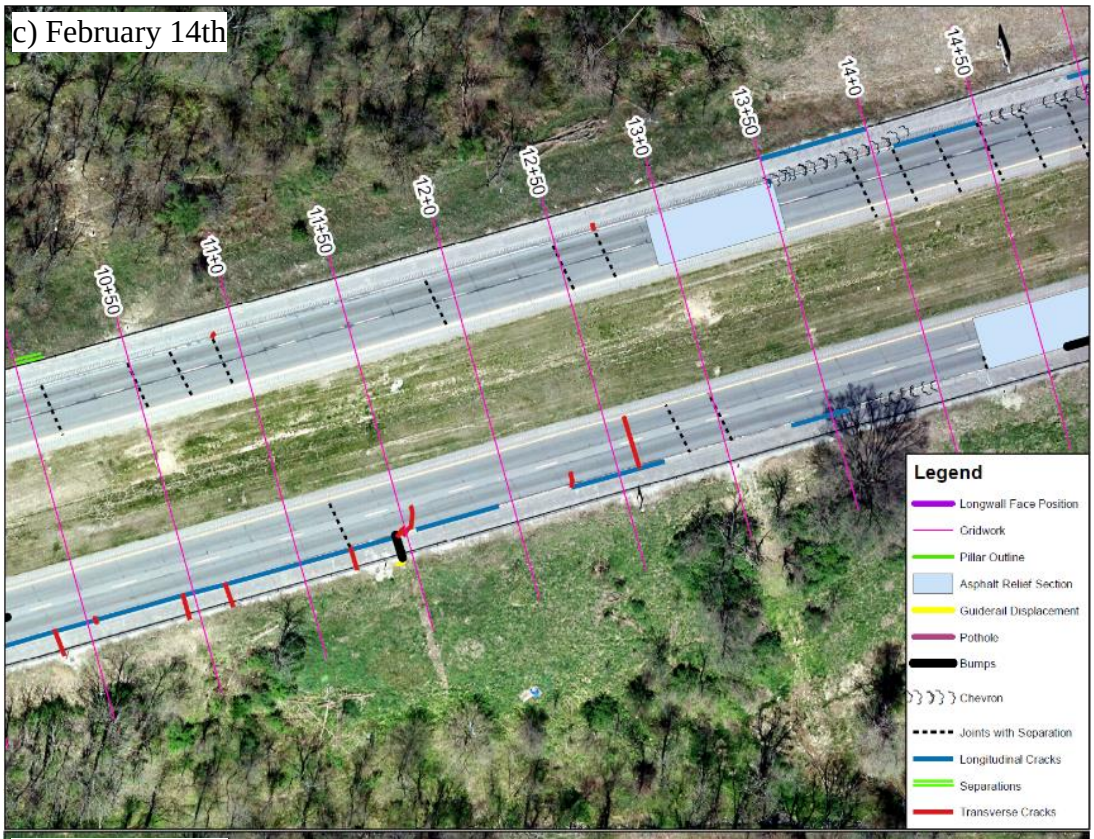

d) February 14th

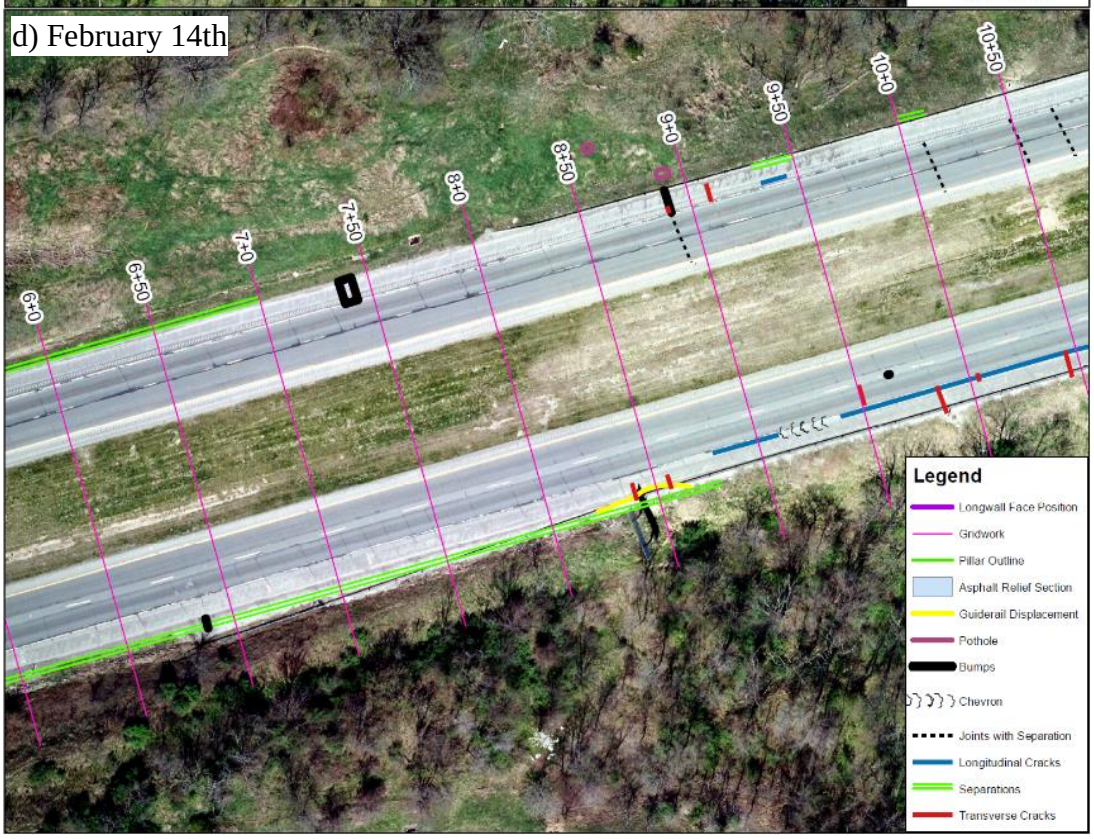

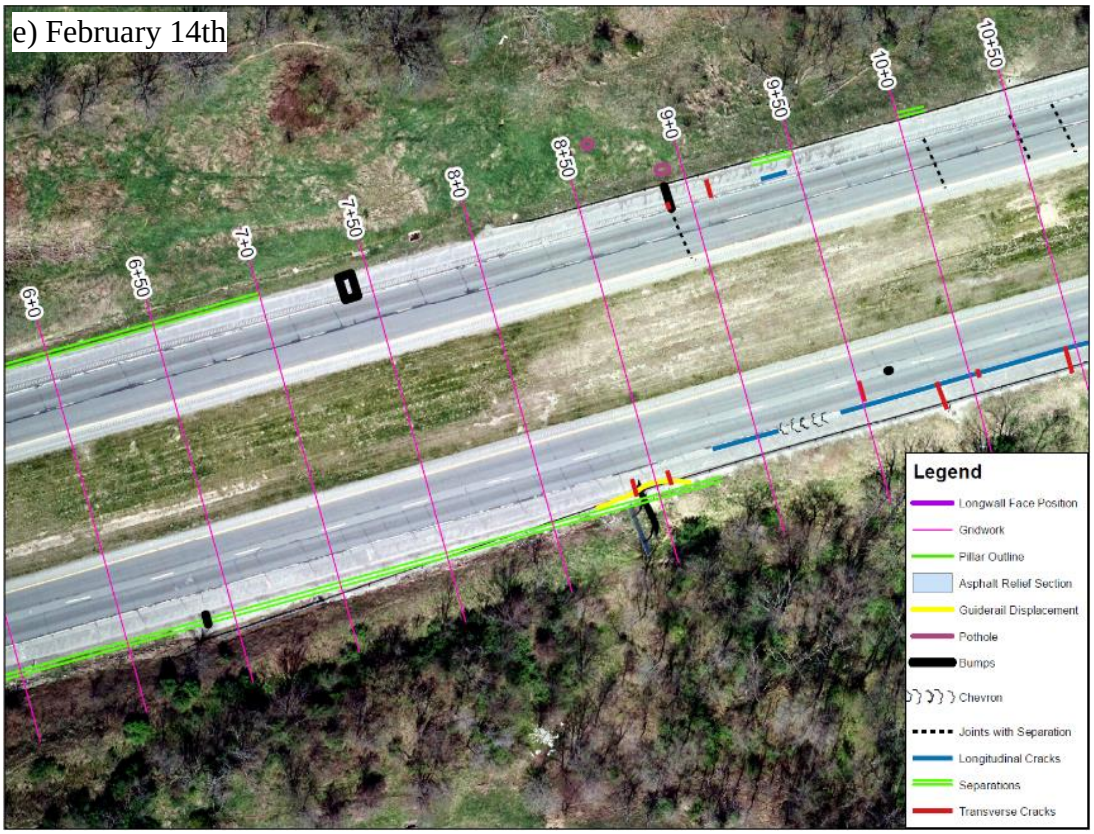

Appendix Figure 3 Damage observed on highway on February 14th

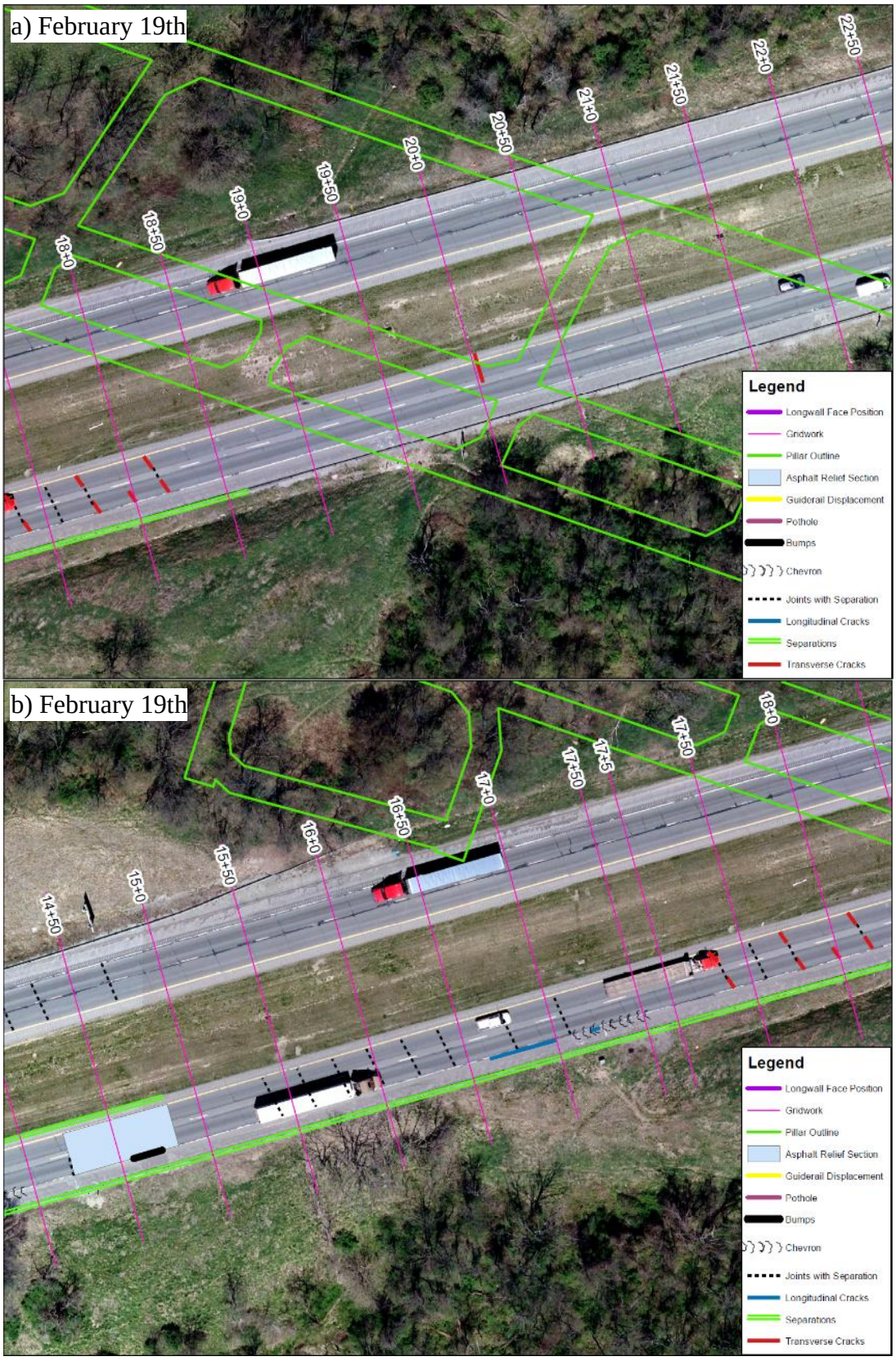
a) February 19th
18+0
18+50
19+0
19+50
20+0
20+50
21+0
21+50
22+0
22+50
Legend
Longwall Face Position
Gridwork
Pillar Outline
Asphalt Relief Section
Guiderail Displacement
Pothole
Bumps
Chevron
Joints with Separation
Longitudinal Cracks
Separations
Transverse Cracks
b) February 19th
14+50
15+0
15+50
16+0
16+50
17+0
17+50
17+5
17+50
18+0
Legend
Longwall Face Position
Gridwork
Pillar Outline
Asphalt Relief Section
Guiderail Displacement
Pothole
Bumps
Chevron
Joints with Separation
Longitudinal Cracks
Separations
Transverse Cracks

c) February 19th

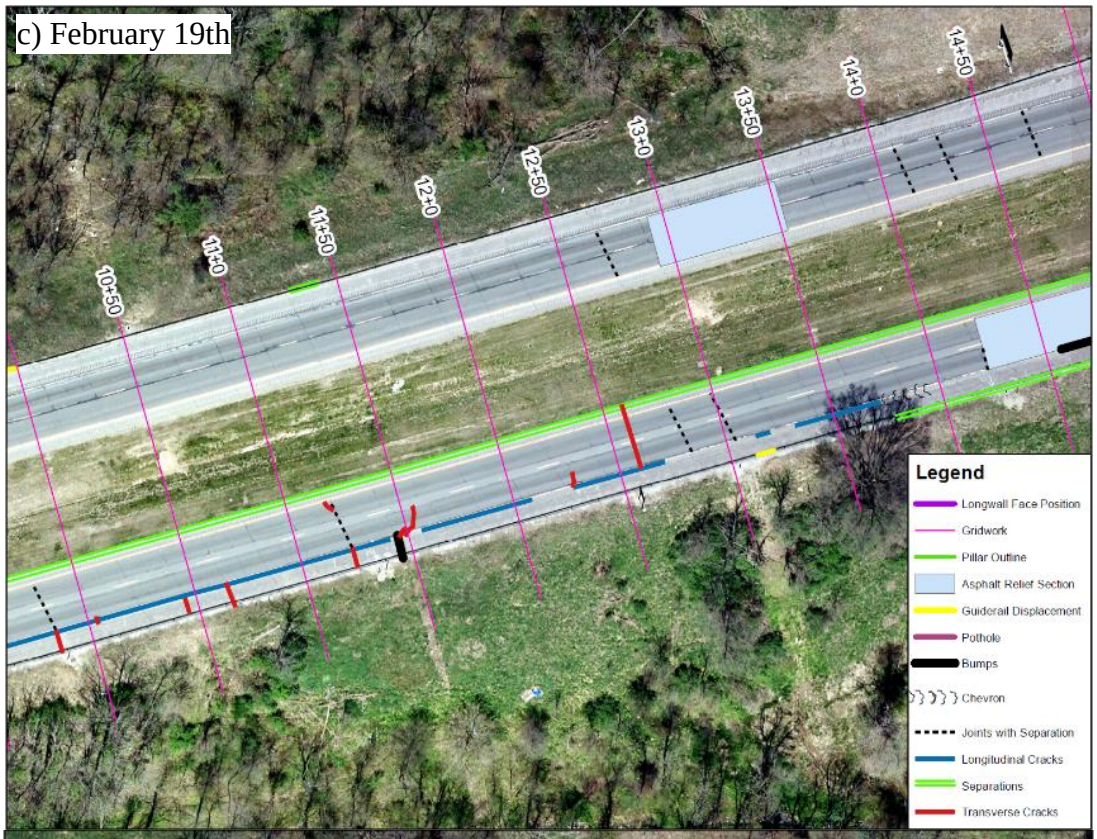

d) February 19th

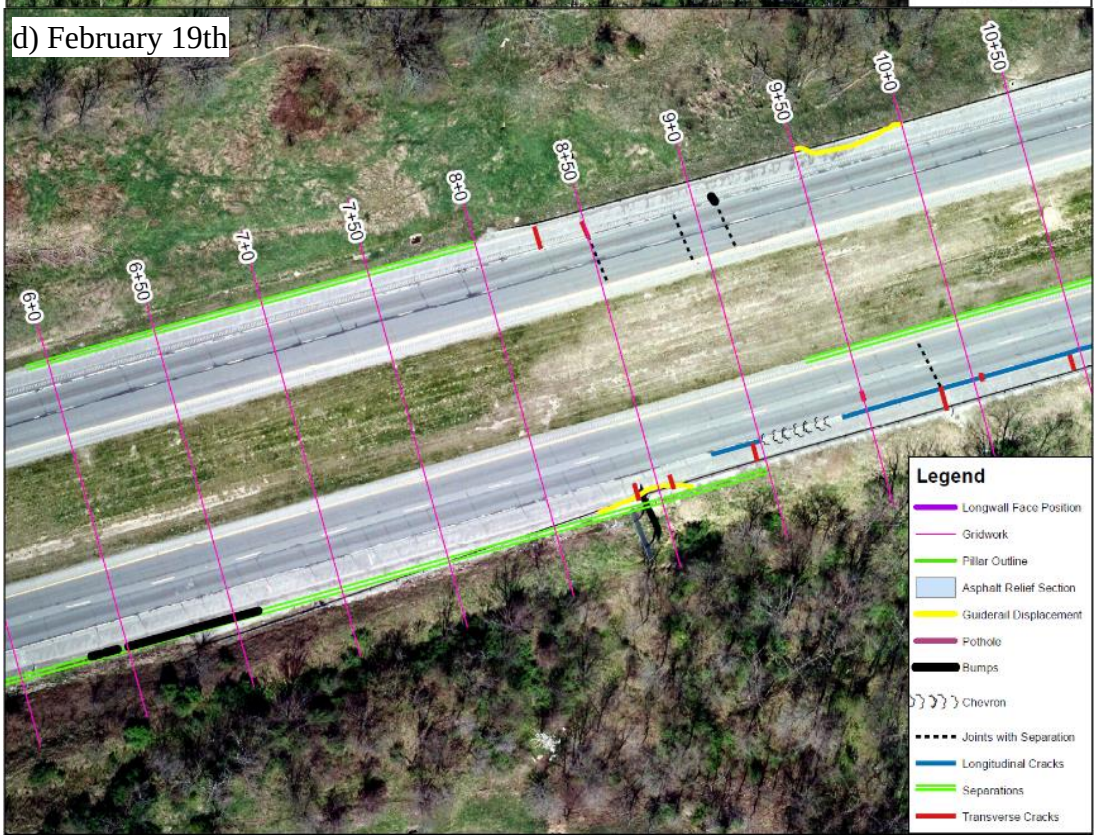

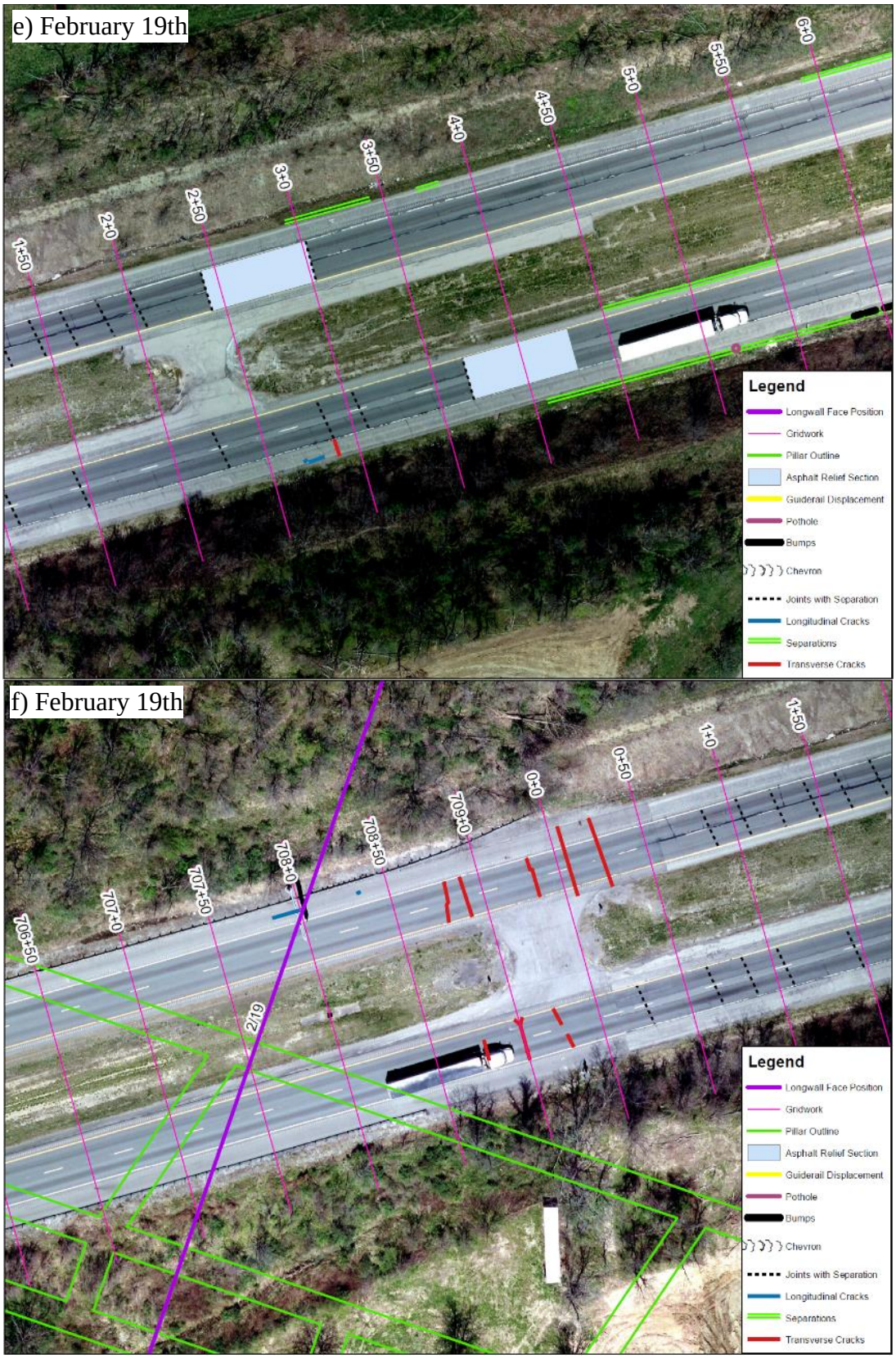

Appendix Figure 4 Damage observed on highway on February 19th

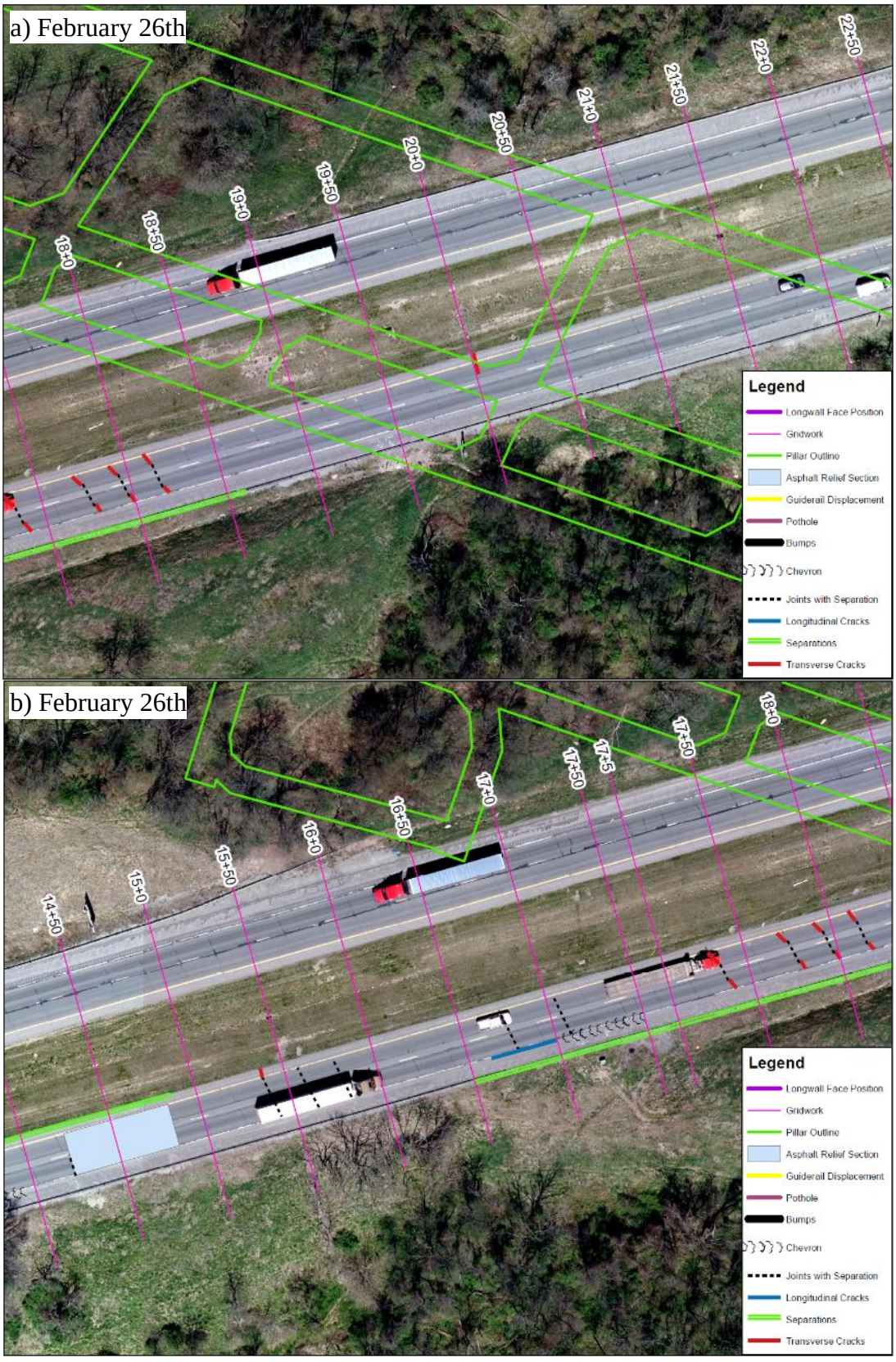
a) February 26th
22+50
22+0
21+50
21+0
20+50
20+0
19+50
19+0
18+50
18+0
Legend
Longwall Face Position
Gridwork
Pillar Outline
Asphalt Relief Section
Guiderail Displacement
Pothole
Bumps
Chevron
Joints with Separation
Longitudinal Cracks
Separations
Transverse Cracks
b) February 26th
18+0
17+50
17+5
17+50
17+0
16+50
16+0
15+50
15+0
14+50
Legend
Longwall Face Position
Gridwork
Pillar Outline
Asphalt Relief Section
Guiderail Displacement
Pothole
Bumps
Chevron
Joints with Separation
Longitudinal Cracks
Separations
Transverse Cracks

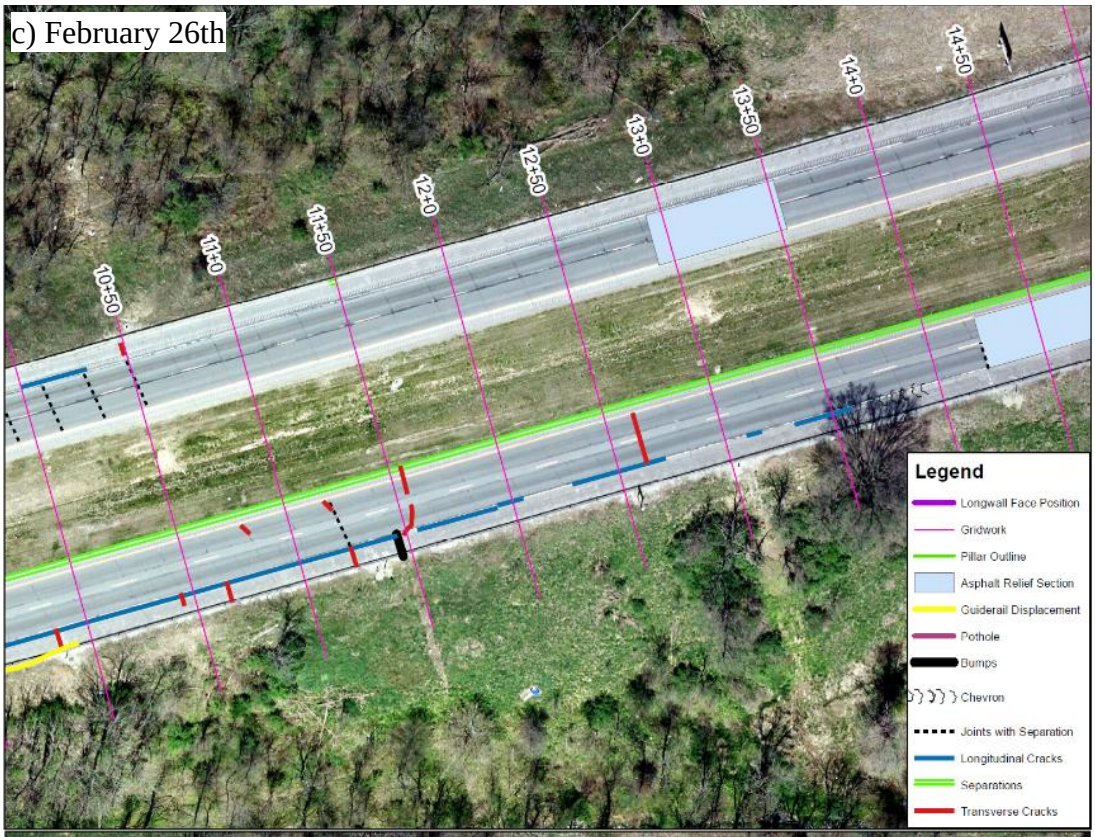
c) February 26th
10+50
11+0
11+50
12+0
12+50
13+0
13+50
14+0
14+50
Legend
Longwall Face Position
Gridwork
Pillar Outline
Asphalt Relief Section
Guiderail Displacement
Pothole
Bumps
Chevron
Joints with Separation
Longitudinal Cracks
Separations
Transverse Cracks

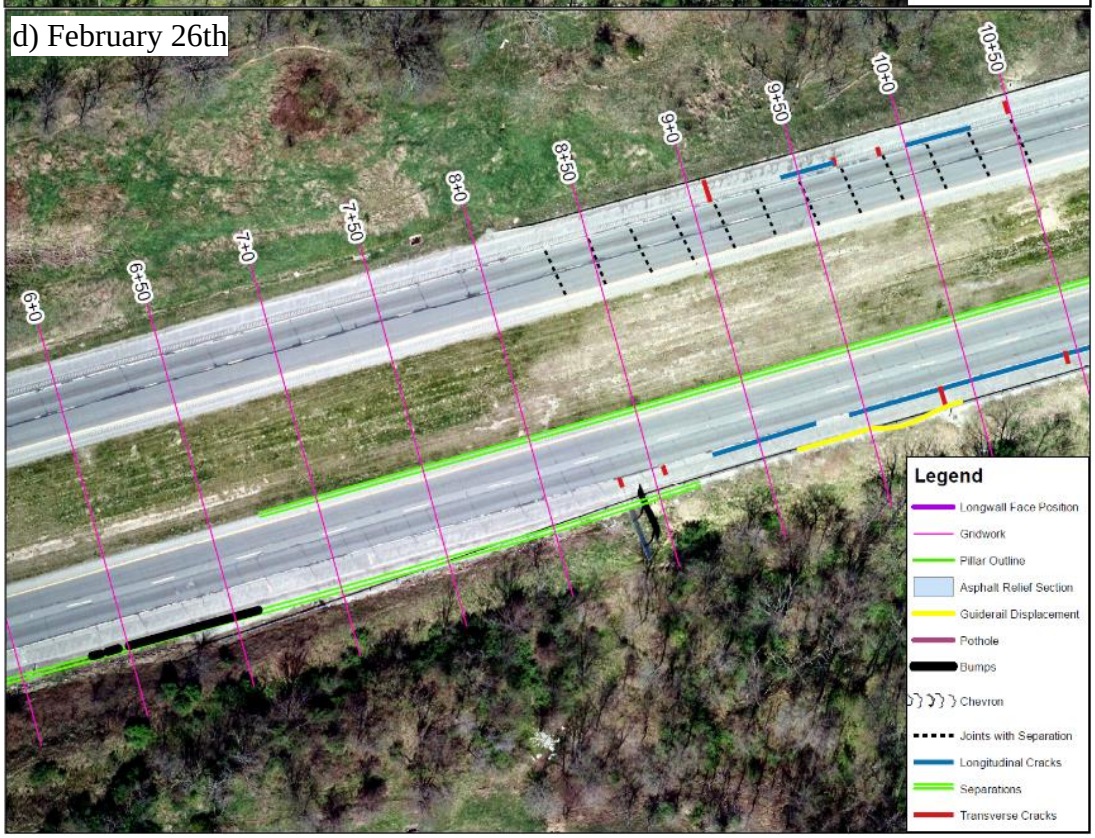
d) February 26th
6+0
6+50
7+0
7+50
8+0
8+50
9+0
9+50
10+0
10+50
Legend
Longwall Face Position
Gridwork
Pillar Outline
Asphalt Relief Section
Guiderail Displacement
Pothole
Bumps
Chevron
Joints with Separation
Longitudinal Cracks
Separations
Transverse Cracks

e) February 26th

f) February 26th

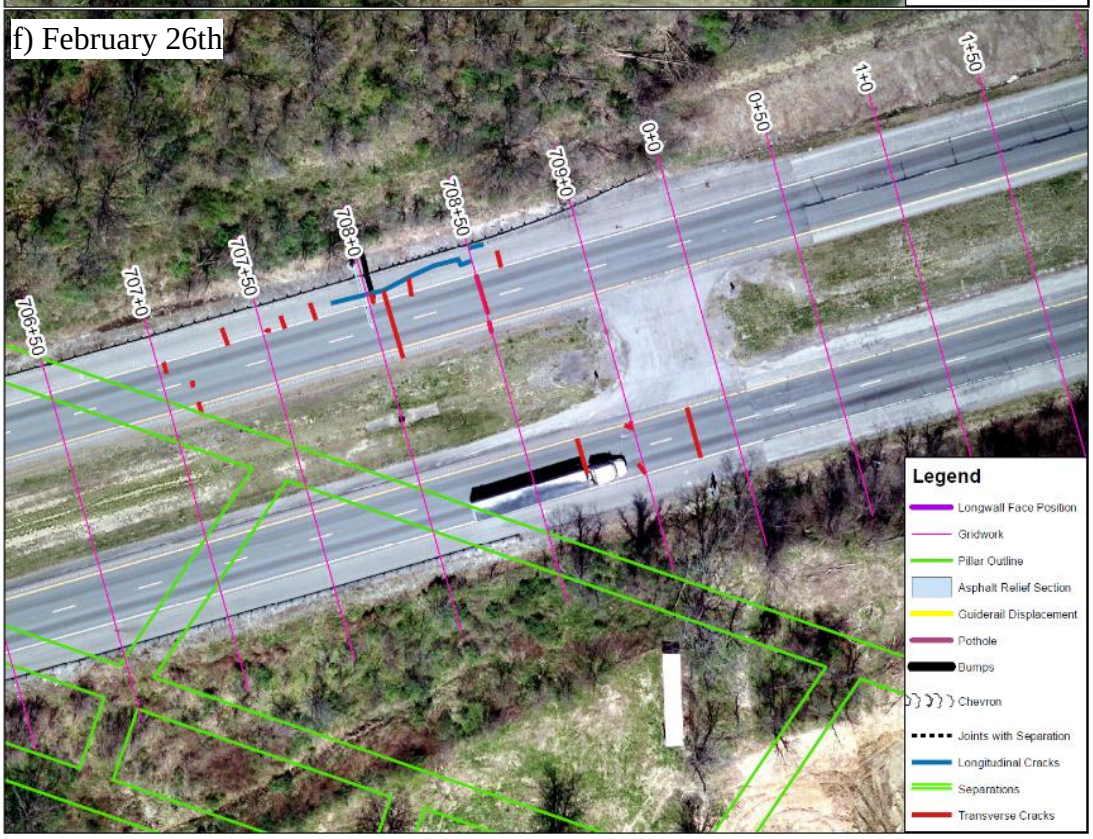

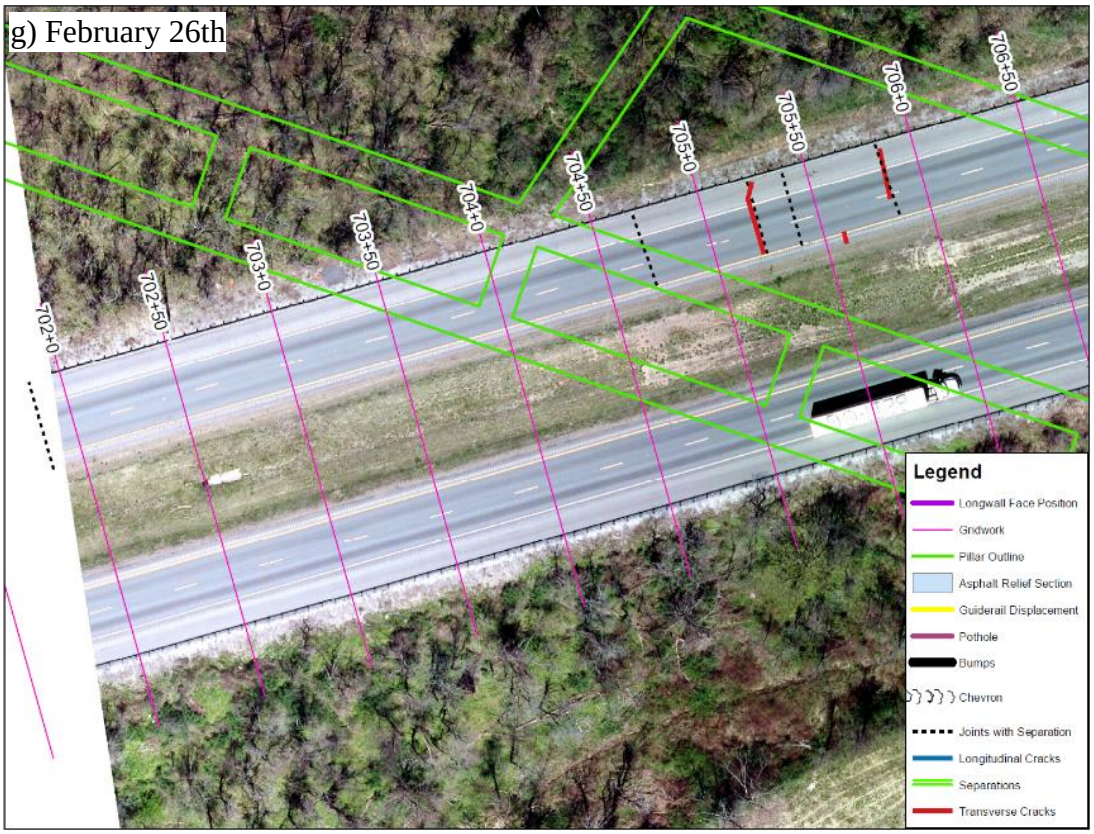

Appendix Figure 5 Damages observed on highway on February 26th

Note: on this date the longwall face was well beyond the study area

Appendix B SDPS Modeling Guide

The SDPS software was used to model the predicted subsidence caused by longwall Panel 15 when it undermined I-70 in the winter of 2019. The software requires inputs of prediction points and mine plans, which can be created in real space or around a fixed origin. These parameters can be generated in AutoCAD and then imported into the software for analysis.

A detailed mine plan was obtained from the Tunnel Ridge Mine. The panel outline was located in real space using the West Virginia State Plane Coordinate System and was created in AutoCAD. The drawing showed the location of the panel and all the associated pillars located in the gateroads. For analysis in SDPS, the mine plan was simplified; this was done by creating a single polyline inside of the gateroads to demonstrate the area of coal extracted. This polyline was then exported as an object from AutoCAD and saved as a .dxf file to be imported into SDPS.

Prediction points were also needed for the analysis of the panel in SDPS. In order to calculate all of the necessary parameters, the prediction points needed to be oriented on a grid and have the elevation of the surface topography. To generate this file, the Carlson software was downloaded to add additional capabilities to AutoCAD. The following steps were used to generate the file.

1. Import the elevation contours for the study area into the Carlson software. This should be in .dwg format
2. Click the **Make 3D Grid File** tool in the **Grids** tab. The **Grid File to Create – (grd)** menu opens up.
    a. Browse to the folder that you want to store the grid file in and name you grid. Click Save. The **Make 3D Grid File** menu opens.

b. In the “Make 3D Grid File” menu, ensure that the **Source Data** option is set to **Screen Entities**. The Source data is going to be the elevation contours.

c. Make sure the Range of Elevations/Values to Process encompasses the minimum and maximum elevation values in the elevation contours data file.

d. Leave the Modeling Method to Triangulation, the Triangulation Mode to Auto Detect, and make sure Use Inclusion/Exclusion Areas is unchecked.

e. Ensure Set Grid Position is set to **Screen Pick**

f. Ensure Specify Grid Resolution As is set to **Dimensions of Cell**

   i. **X = 50**

   ii. **Y= 50**

g. Press **OK**

3. The menu disappears and prompts the user to pick the features which will populate the elevation values of the Grid file. Drag the mouse to select the elevation contours and press **Enter**. The software may pause for a second, indicating that it is creating the Grid file.

4. Go to the Grid file in the folder you created it in and open the file with Notepad. The file may contain “N” values, i.e. “Null” values. These null values are of cells beyond the extent of the elevation contours and therefore should not have an effect on the prediction model. However, SDPS will not accept these values, so replace them with the value of the average elevation in your study area. To do this use the **Replace** tool in Notepad. Save your Grid. The Grid file is now complete.

Once the prediction points and the mine plan were generated, these parameters were input into SDPS for analysis. The SDPS software can be downloaded from Carlson and can analyze

openings using the profile function or the influence function. For this analysis, the influence function was utilized. The following steps were taken to create and run the SDPS model.

1. Open SDPS and click the influence function button to launch the software.
2. Go to the file drop down and save the project file. This will save all the subsequent components that are created.
3. Use the File drop down and click **Import SDPS Components**.
    a. Import the mine plan by clicking the **AutoCAD MinePlan [DXF]** tab.
        i. Browse for the .dxf file created for the mine plan
        ii. Ensure that the name of the Active Panel Layer matches the name of the layer used in the AutoCAD file generated previously.
        iii. Click on the **Longwall** option in the Extracted Area/Panel Type box.
        iv. Click on the **Average Elevation** option in the Elevation box and set the average elevation to 600-feet, which is the average elevation of the Pittsburgh Coalbed in the location of Panel 15
        v. Click on the **Use %Hardrock** option in the Subsidence Parameters box and set the average %Hardrock to 30%, which is the calibrated value for this area of overburden. The calculated supercritical subsidence factor for 30% Hardrock should be 59.5%.
        vi. Import the mine plan. One panel should be successfully imported.
    b. Import the prediction points by clicking the **Carlson Software Grid** tab. Browse for the txt file created. Click import and points throughout the study area should be imported.

4. Use the Edit drop down and click **Rectangular Mine Plan**. One panel should be detailed in the parcel management tab. Using the **Edge Effect Management** tab, define an edge effect of 175-feet around all sides of the panel. This value was determined to match with the collected survey data. If the Edge Effect Management tab is greyed out, check the box to enable edge effect management.
5. Use the Calculate drop down and click **Calculate Deformations**. Change the output path so ensure that the calculations are saved in the proper location. Check the output options desired; the options used for this analysis were calculate subsidence, calculate horizontal displacement, calculate horizontal strain, and calculate ground strain (grid). Change the Output Format to XYZ Data, which will allow the data to be analyzed in Excel or ArcGIS. Click Calculate and wait for model to run.

Once the model calculates, it is complete. The SDPS data can be previewed using the SDPS graph function or imported into Excel or ArcGIS. Ensure that the data from the model looks correct before manipulating it for analysis. Further analysis of the model can be performed in Excel or ArcGIS.

Bibliography

AASHTO Guide for Design of Pavement Structures. (1993). American Association of State Highway and Transporataion Officials.

Adelsohn, E., Iannacchione, A., & Winn, R. (2019). Investigations on Longwall Mining Subsidence Impacts on Pennsylvania Highway Alignments. *38th Conference on Ground Control in Mining*, 239–250.

Agioutantis, Z., Newman, C., Leon, G. B. J., & Karmis, M. (2016). Minimizing Impacts on Streams due to Underground Mining by Predicting Surface Ground Movements. *Mining Engineering*, 68–72.

Agioutantis, Z. & Karmis, M. (2013). Recent Developments on Surface Ground Strain Calculations Due to Underground Mining in Appalachia. *International Conference on Ground Control in Mining*, *32*, 214–219.

Agioutantis, Z. Karmis, M. & Jarosz, A. (n.d.). Prediction Of Surface Subsidence And Strain In The Appalachian Coalfields Using Numerical Methods. *International Conference on Ground Control in Mining*, *7*, 95–100.

Bartels, J., Gallagher, S., & Ambrose, D. (n.d.). Continuous Mining: A pilot study of the roole of visual attention locations and work position in underground coal mines. *NIOSH*. https://www.cdc.gov/niosh/mining/UserFiles/works/pdfs/cmaps.pdf

Bayer, A., & Nienhaus, K. (2000). *Capacity model for room & pillar operations with continuous miners.*

Continuous Miners. (n.d.). Retrieved February 15, 2020, from http://www.coaleducation.org/technology/Underground/continuous_miners.htm

DaCanal, T. (2019). *The Influence of Subsidence Laws and Regulations on the Underground Bituminous Coal Industry in the Commonwealth of Pennsylvania over the Last 25 Years*. University of Pittsburgh.

Daigle, L., & Mills, K. F. (2017). Experience of Monitoring Shear Movements in the Overburden Strata Around Longwall Panels. *17th Coal Operators' Conference*.

E. Fathi Salmi, M. Nazem, & M. Karakus. (2016). Numerical analysis of a large landslide induced by coal mining subsidence. *Engineering Geology*, 141–152. https://doi.org/10.1016/j.enggeo.2016.12.021

Gutierrez, J. J., Vallejo, L. E., & Lin, J. S. (2010). *A Study of Highway Subsidence due to Longwall Mining using data collected from I-79* (Final Contract Report Conctract #510601). University of Pittsburgh.

Hebblewhite, B., Waddington, A., & Wood, J. (2000). Regional Horizontal Surface Displacements Due to Mining Beneath Sever Surface Topography. *19th Conference on Ground Control in Mining*, 149–157.

Iannacchione, A. (2018). *Controlling Subsidence Imacts to Water Supplies*.

Iannacchione, A., Tonsor, S., Witkowski, M., Benner, J., Hale, A., & Shendge, M. (2008). *The Effects of Subsidence Resulting from Underground Bituminous Coal Mining on Surface Structures and Features and on Water Resources, 2003 to 2008: Vol. 3rd Five Year Report*. Pennsylvania Department of Environmental Protection. https://www.dep.pa.gov/Business/Land/Mining/BureauofDistrict Mining/Act54/Pages/default.aspx

Jarosz, A., Karmis, M., & Sroka, A. (1990). Subsidence development with time ? Experiences from longwall operations in the Appalachian coalfield. *International Journal of Mining and Geological Engineering*, *8*(3), 261–273. https://doi.org/10.1007/BF01554045

Karmis, M., Haycocks, C., Eitani, I., & Webb, B. (1981). A Study of Longwall Subsidence in the Appalachian Coal Region using Field Measurements and Computure Modeling Technigues. *1st Conference on Ground Control in Mining*, *1*, 220–229.

Karmis, M., Mastoris, J., & Agioutantis, Z. (1994). An Investigation into the Potential of the "Damage Angle" Concept for Assessing the Impacts of Underground Mining on the Surface. *SME Annual Meeting*.

Longwall Mining. (n.d.). Retrieved February 15, 2020, from http://www.coaleducation.org/technology/Underground/Longwall_Mining.htm

Luo, Y., Yang, J., & Jiang, H. (2019). Techniques for Assessing and Mitigating Longwall Subsidence Effects on Interstate Highways. *Society for Mining, Metallurgy, & Exploration*.

Mark, C., & Gauna, M. (2017). Preventing roof fall fatalities during pillar recovery: A ground control success story. *International Journal of Mining Science and Technology*, *27*(1), 107–113. https://doi.org/10.1016/j.ijmst.2016.09.030

McCulloch, C. M., Diamond, W. P., Bench, B. M., & Deul, M. (1975). *Selected geologic factors affecting mining of the Pittsburgh coalbed* (Report of Investigations No. 8093). Bureau of Mines. https://stacks.cdc.gov/view/cdc/9241

Miller, J. S., & Bellinger, W. Y. (2003). *Distress Identification Manual for Long-Term Pavement Performance* (FHWA-RD-03-031; p. 164). U.S. Department of Transportation, Federal Highway Administration.

Model 906 Little Dipper. (2015). Jewell Instruments LLC.

Newman, D., Agioutantis, Z., & Karmis, M. (2001). SDPS for Windows: An Integrated Approach to Ground Deformation Prediction. *International Conference on Ground Control in Mining*, *20*, 6.

O'Connor, K. (2001). *The Effect of Undermining Interstate Route 70, South Strabane Township, Washington County, Pennsylvania* (Service Purchase Contract No. 3500016513; p. 22). Pennsylvania Deparment of Environmental Protection.

PA Mining History. (n.d.). Department of Environmental Protection. Retrieved February 15, 2020, from https://www.dep.pa.gov:443/Business/Land/Mining/Pages/PA-Mining-History.aspx

Paul Jeran, & Vladimir Adamek. (1988). *Subsidence due to undermining of sloping terrain: A case study* (Report of Investigations No. 9205). Bureau of Mines. https://stacks.cdc.gov/view/cdc/10723

Peng, S. S., & Chen, D. W. (1981). *Analysis of Surface Subsidence Parameters Due to Underground Longwall Mining in the Northern Appalachian Coalfield* (p. 22). Department of Mining Engineering, West Virginia University.

Peng, S. S., & Cheng, S. L. (1981). Predicting Surface Subsidence for Damage Prevention. *Coal Mining and Processing*, 84–95.

Peng, S. S., & Chiang, H. S. (1984). *Longwall Mining*. 708.

Peng, S. S., Ma, W. M., & Zhong, W. L. (1992). *Surface Subsidence Engineering*. Society for Mining, Metellurgy, & Exploration.

Pennsylvania—State Energy Profile Overview—U.S. Energy Information Administration (EIA). (2019). Retrieved February 15, 2020, from https://www.eia.gov/state/?sid=PA

Puertas, J. J. G. (n.d.). *ESTIMATING HIGHWAY SUBSIDENCE DUE TO LONGWALL MINING*. 177.

RST MEMS Digital Inclinometer System Instruction Manual (No. ICM0083E). (2019). RST Instruments.

Saeidi, A., Deck, O., Al Heib, M., Verdel, T., & Rouleau, A. (2013). Adjusting the Influence Fuction Method for Subsidence Prediction. *Key Engineering Materials*, *553*, 59–66.

Yancich, R. D. (1986). *Surface Subsidence in Longwall Mining—A Case Study*. Department of Mining Engineering, West Virginia University.